Microbial electrosynthesis for acetate production from carbon dioxide: innovative biocatalysts leading to enhanced performance

Aryal, Nabin; Zhang, Tian; Tremblay, Pier-Luc

Publication date:
2017

Document Version
Publisher's PDF, also known as Version of record

Microbial electrosynthesis for acetate production from carbon dioxide: innovative biocatalysts leading to enhanced performance

PhD Thesis written by Nabin Aryal
Supervisor Tian Zhang
Co-supervisor Pier-Luc Tremblay

Novo Nordisk Foundation Center for Biosustainability
Technical University of Denmark
Kemitorvet 220, 2800 kgs. Lyngby
Denmark

Preface

The following PhD thesis is written as a partial fulfillment of the requirement from the Technical University of Denmark (DTU) to obtain a PhD degree. The research presented in this thesis was conducted from 15th February 2014 to 25th February 2017 under the supervision of Senior Researcher Tian Zhang and the co-supervision of Researcher Pier-Luc Tremblay at the Novo Nordisk Center for Biosustainability, DTU. The PhD was funded through external funding "FutureChem, Biosustainable Production of Chemicals from Thin Air" attributed by the Novo Nordisk Foundation. The thesis was evaluated by Professor Alex Toftgaard Nielsen from DTU, Federico Aulenta, Research Scientist from Water Research Institute, National Research Council (CNR-IRSA) Italy and Assistant Professor Amelia-Elena Rotaru from University of Southern Denmark.

Nabin Aryal
6th June 2017
Novo Nordisk Foundation Center for Biosustainability
Technical University of Denmark (DTU)

Acknowledgements and Thanks

First and Foremost I would like to express my gratitude to my supervisor Prof. Tian Zhang and co-supervisor Dr. Pier-Luc Tremblay. Thank you for all your scientific guidance, support, motivation, inspiration and for providing me the great opportunity to join the Novo Nordisk Center for Biosustainability on this PhD journey.

My PhD journey has been completed with many ups and downs, and nothing could have been done without the support of many people. Special thanks to Fariza Ammam, Dawid Mariusz Lizak Torbjørn Ølshøj Jensen and Isotta D'Arrigo for their priceless support that helped me understand molecular biology, microbial physiology, and experimental design. I feel lucky that I was surrounded by such nice lab colleagues. I am also thankful to Torbjørn for scientific support and for helping me to prepare an abstract for this thesis in Danish.

I would also like to give special thanks to Sailesh Malla for inspiration, motivation, and scientific guidance and for being a brother supporting my stay in Denmark. Furthermore, I am thankful to Professor Alex Toftgaard Nielsen for his strong support during my stay at DTU Lyngby campus. For the great scientific discussions, I want to thank Sheila Ingemann Jensen, Christian Bille

Jendresen, Elleke Fenna Bosma, Rosa Aragão Börner, Kristoffer Bach Falkenberg and Hemanshu Mundhada from Alex group.

Since this thesis is an interdisciplinary study combining bacterial physiology, analytical chemistry, electrochemistry and material sciences, without collaborations, it would have been impossible to finish this PhD project. I would like to express my gratitude to all our collaborators including Prof. Qijin Chi, Prof. Anders Egede Daugaard, Arnab Halder, Minwei Zhang, Marc Hvid Overgaard, Adam C. Stoot, and Michal Wagner for electrode materials development. I would like to acknowledge Mette Kristensen and Konstantin Schneider for the scientific advices on analytics and fermentation technology. I would also not be here without the support of Deepak Pant and Xochitl Dominguez Benetton, thank you for the scientific advices and motivation you provided in the early stage of my PhD.

Big thanks to my CfB colleagues Gossa, Javier, Daniel, Justyna Maria, Michael Jenny Marta, Yaojun, Pep, Sumesh Stephanie, Xinglin, Yasin, , GG, Ida, Maja, Alicia, Songyuan, Oliver, Jerome, Mathew, Suresh, Kasper, Abida, Alicia, Anna, Lejla, Mohammad, Lumeng, Christian, Fabienne, Helene, Ivan, Nusa, Rocio, Anaelle, Andreas, Patricia, David, Se Hyeuk, Svetlana, who made a nice

working environment and have truly made this period of my life one that I will fondly remember.

Special thanks go to my European family members Christa Haeuser, Dorte Jensen, Jette Jacobsen and Lenka Zuska who made my stay unforgettable in Denmark. Thank you Suman, Trishana, Arun, Puja, Sunil, Madhav, Govinda and Reema for being my family and friends in Europe. I am grateful to my flatmates, Saroj, Anjana, Manjana, Ramesh, Sujan, Bimala, Rakesh and Pramila for their company. I would also like to thank my best friends in Copenhagen especially, Rachana, Pawan, Mahesh, Sobit, Sarod, Sanu, Nima, Pradeep, Suraj, Ping, Ravi Chhetri and Sushil.

Finally, I would not have been able to complete my PhD without the selfless sacrifices made by my mother Ishowa Gyawali and my wife, Sunita Subedi. Thank you, my dear sweetheart, Sunita for your selfless love, kindness, and your endless support. I am always grateful to my father and all my family members specially Jhabindra Gyawali, Roma Kant Gyawali and Ambika Aryal who motivated me for further abroad studies.

Nabin Aryal
25th February 2017

Abbreviation

AR	Assessment Report
AF	Anaerobic Fermentation
BES	Bioelectrochemical System
CBB	Calvin-Benson-Bassham
CCU	Carbon Capture and Utilization
CLSM	Confocal Laser Scanning Microscopy
CO_2	Carbon dioxide
CO	Carbon monoxide
DSMZ	Deutsche Sammlung Mikroorganismen und Zellkulturen
EET	Extracellular electron transfer
EOR	Enhanced Oil Recovery
HER	Hydrogen evolution reaction
IPCC	Intergovernmental Panel on Climate Change
INDCs	Intended nationally determined contributions
MES	Microbial Electrosynthesis
MET	Mediated Electron Transfer
NASA	The National Aeronautics and Space Administration
PPM	Parts Per Million
rGO	Reduced graphene oxide

RuBisCO	Ribulose 1,5-bisphosphate carboxylase/ oxygenase
RVC	Reticulated vitreous carbon
SOFC	Solid oxide fuel cells
SHE	Standard Hydrogen Electrode
TCRE	Transient climate response to cumulative carbon emissions
TEPA	Tetraethylene pentamine
UNFCCC	United Nations Framework Convention on Climate Change
WL	Wood–Ljungdahl
3HP-4HB	3-hydroxypropionate-4-hydroxybutyrate
3D	Three dimensional

Abstract

Production of chemicals has significant influence on the emission of greenhouse gases (GHG) in particular carbon dioxide (CO_2), thereby contributing to the climate changes of our planet. There is a general acceptance that we need to reduce the emission of GHG on a global level to cope with these changes. Production of chemicals utilization of CO_2 as feedstock represents a sustainable alternative to many fossil derived products, which are non-renewable and have a strong negative impact on the environment. Microbial electrosynthesis (MES) is an emerging technique utilizing electrical energy for reduction of CO_2. In a MES reactor, microbial catalysts are acquiring electrons from an externally powered cathode to transform CO_2 into multi-carbon chemical commodities. The direct acquisition of electrons enables the use of multiple renewable electricity-sources including solar, wind, biochemical oxidation processes, or surpluses electricity from the power grid. Although MES is a promising approach, it is restricted by a low electron transfer rate from the cathode to a microbe as well as the CO_2 reduction rate is insufficient for scaling up. The main objective of the present study was to increase the overall productivity of MES by identifying more efficient electroautotrophic microbial catalysts and developing better cathode materials.

The genus *Sporomusa* is known for its abilities to convert CO_2 into acetate by MES. This study investigated the performance in MES of selected species of the *Sporomusa* genus including; *Sporomusa ovata* DSM-2662, *Sporomusa ovata* DSM-2663, *Sporomusa ovata* DSM-3300, *Sporomusa acidovorans*, *Sporomusa malonica*, and *Sporomusa aerivorans*. In which, *S. ovata* DSM-2663 was identified the most productive MES microbial catalyst among the tested group.

Furthermore, the study developed and tested novel cathode materials for application in MES including three-dimensional graphene functionalized carbon felt, freestanding and flexible graphene paper, and copper-reduced graphene oxide composite. When the copper-reduced graphene oxide composite electrode was used as the cathode for *S. ovata*-driven MES, acetate production rates as well as current density were significantly increased to1708.3 ± 333.3 mmol d^{-1} m-^{2} and -20.4 ± 1.0 A m^{-2} which is almost 21.5 fold higher acetate production compared to unmodified copper foam electrode. By identifying a better MES microbial catalyst and developing novel composite cathodes the electron transfer during MES as well as CO_2 reduction into acetate was significant improved.

Dansk Resume

Den nuværende produktion af kemikalier frigiver drivhusgasser, i særdeleshed CO_2, hvilket påvirker klimaet på jorden. Det er generelt accepteret, at udledningen af drivhusgasser skal reduceres for at modvirke disse klimaændringer. Kemikalieproduktion basseret på CO_2 repræsenterer et vedvarende alternativ til de produkter som produceres fra fossile resurser og har negativ indvirkning på miljøet. Mikrobiel ElektroSyntese (MES) er en teknik, under udvikling, med et stort potentiale. MES anvender elektroner til reduktion af CO_2. Omdannelsen katalyseres af mikroorganismer som erhverver elektronerne direkte fra en katode, som er forbundet en ekstern strømkilde, og omdanner CO_2 til molekyler med flere karbon atomer. Det direkte optag af elektroner muliggør udnyttelse af flere forskellige vedvarende elektricitets kilder så som sol, vind, biokemiske oxidationsprocesser eller overskydende elektricitet fra el-nettet. Til trods for potentialet er MES begrænset af en lav transfer rate af elektroner fra katoden til mikroorganismerne samt at CO_2 reduktions raten er for langsom til opskalering. Målet for dette studie var øge produktiviteten af MES ved at identificere mere effektive elektroautotrofe mikroorganismer samt at udvikle bedre materialer til katoden.

Slægten *Sporomusa* er kendt for dens evner til omdanne CO_2 til eddikesyre i MES. I dette studie er et udvalg af *Sporomusa* stammer blevet sammenholdt på basis i deres præstationer i MES. Stammerne inkluderer: *Sporomusa ovata* DSM-2662, *Sporomusa*

ovata DSM-2663, *Sporomusa ovata* DSM-3300, *Sporomusa acidovorans*, *Sporomusa malonica* og *Sporomusa aerivorans*. Foruden indentifikation af en bedre acetogen mikroorganisme til MES, ønskes der svar på hvorvidt evne til at omsætte CO_2 i MES er gennemgående for slægten *Sporomusa*. I blandt den testet gruppe stammer blev det fundet, at *S. ovata* DSM-2663 var den mest produktive i MES.

Derudover havde studiet også fokus på at udvikle og teste nye katodematerialer, herunder tredimensionelle graphenfunktionaliserede kulstof net, fritstående og fleksibel graphen papir samt kobberreduceret graphen oxid komposit. Anvendelse af det kobberreduceret graphen oxid komposit material som katode for MES med *S. ovata* resulterede i signifikant øget produktions rater samt øget strømdensitet. Den opnået produktivitet var 1708.3 ± 333.3 mmol d^{-1} m^{-2} og strømdensiteten var -20.4 ± 1.0 A m^{-2} (svarrende til en 21.5 fold stigning i eddike syre produktion sammenlignet med ikke modificeret kobberskums elektrode). Ved identifikation af en mikroorganisme med mere ønskelige egenskaber for MES samt udvikling af nye kompositmaterialer, lykkes det gennem dette studie at øge elektron tranfer raten og reduktions rate af CO_2 til eddiesyre i MES, signifikant.

List of publications

1. **Aryal, N.,** Halder, A., Tremblay, P. L., Chi, Q., & Zhang, T. (2016). Enhanced microbial electrosynthesis with three-dimensional graphene functionalized cathodes fabricated via solvothermal synthesis. *Electrochimica Acta*, *217*, 117-122
2. **Aryal, N.,** Tremblay P. L., Lizak D. M. & Zhang, T., (2017), Performance of Sporomusa species for the microbial electrosynthesis of acetate from CO_2. *Bioresource Technology* 233 (2017): 184-190.
3. **Aryal, N.,** Halder, A., Zhang M., Tremblay, P. L., Chi, Q., & Zhang, T., (2017), Freestanding and flexible graphene papers as bioelectrochemical cathode for selective and efficient CO_2 conversion. (Submitted)
4. **Aryal, N**., Tremblay, P. L., Overgaard M. H., Stoot A. C., & Zhang, T., (2017) Graphene-copper composite electrode for the high rate of acetate production from CO_2 in Microbial electrosynthesis. (Under Preparation)

Additional work during the PhD study but not included in this thesis

5. Lepage,G., Perrier, G., Merlin, G., **Aryal, N**., & Dominguez-Benetton, X. (2014). Multifactorial evaluation of the

electrochemical response of a microbial fuel cell. *RSC Advances*, 4(45), 23815-23825.

6. **Aryal, N.,** Tremblay, P. L, Daugaard, A. E., Wagner, M., & Zhang, T., (2017) A PEDOT: PSS polymerized electrode for the substantial improvement of acetate production by microbial electrosynthesis from carbon dioxide (Under Preparation)
7. Ammam, F., **Aryal, N.,** Tremblay, P. L., & Zhang, T., (2017). Conversion of fatty acids to their corresponding alcohols by *Sporomusa ovata* in microbial electrosynthesis. (Under Preparation)

Thesis outline

Microbial electrosynthesis (MES) is an emerging approach that uses electricity as an electron source for driving the production of chemicals including biofuels using electroautotrophic microorganisms as catalyst and carbon dioxide (CO_2) as an electron acceptor as well as carbon source. Currently, MES technology is under development and is still at lab scale. One of the major bottlenecks for the development of MES in an economically viable technology is the low production rate. To increase the productivity of MES technology, this PhD project identified a more efficient electroautotrophic microbial catalyst and developed better cathode materials. The PhD thesis is organized into the following chapters:

Chapter 1: Introduction

Chapter 1 provides an overview of global CO_2 emission, CO_2 reduction processes, principle, characteristics, possible applications, and challenges associated with MES.

Chapter 2: Performance of *Sporomusa* species for the MES of acetate from CO_2

Chapter 2 deals with the performance of *Sporomusa* species towards the synthesis of acetate from CO_2 in MES system. It involves the evaluation and comparison of acetate production and electron

transfer rates in MES system between six different species of *Sporomusa.*

Chapter 3: Substantial enhancement of MES for acetate production using novel composite cathodes

Chapter 3 describes the development of novel cathode materials with improved spatial arrangements with the objective of improving current density and acetate productivity during MES. Commercially-available cathode materials including carbon felt, graphite stick, carbon paper, and carbon cloth were tested in MES. Furthermore, novel composite cathodes including three-dimensional reduced graphene functionalized (3D-rGO) carbon felt, freestanding and flexible graphene paper were developed and tested in MES.

Chapter 4: Reduced graphene oxide-copper foam composite cathode for the microbial electrosynthesis of acetate from carbon dioxide

Chapter 4 describes the development of a reduced graphene oxide (rGO)-copper foam composite cathode for H_2-mediated high-rate acetate production. This project maximizes electrochemical H_2 generation with a novel cathode to provide a larger flux of reducing

equivalents to the microbial catalyst and thus accelerate acetate production during MES.

Chapter 5: - Conclusion and Perspective

Finally, Chapter 5 summarizes the outcome of this PhD project and describes the research needs for the development of MES into an economically viable technology.

Table of Contents

1 Introduction

1.1 Carbon dioxide emission

Due to human activities, atmospheric carbon dioxide (CO_2) concentration has rapidly increased and reaching 409.01 ppm in April 2017 as shown in figure 1[1]. Recent studies have identified a linear relationship between global mean temperatures and cumulative atmospheric CO_2 emission. The relationship, named the Transient Climate Response to cumulative carbon Emissions (TCRE), was highlighted in the fifth assessment report (AR5) of the Intergovernmental Panel on Climate Change (IPCC) [2,3].

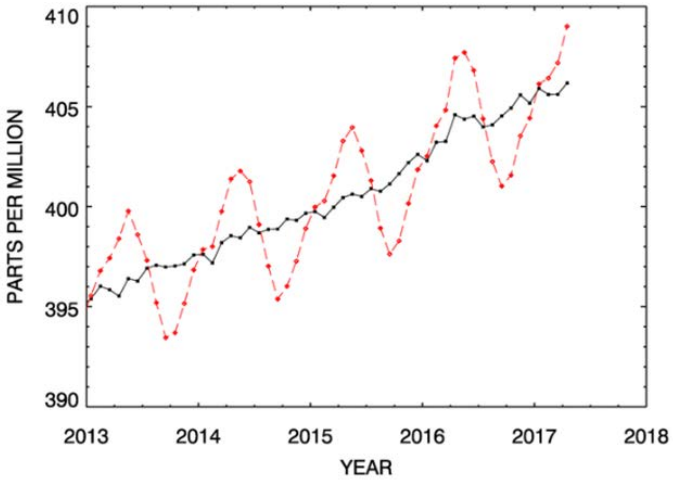

Figure 1. Recent global monthly mean CO_2 concentration graphs provided by the National Climatic Data Center, USA

Greenhouse gas emissions including CO_2 raise global temperature by trapping radiation from the sun into the atmosphere. Temperature increases caused by greenhouse gases alters the global carbon cycle, water cycle, weather patterns and threatens the equilibrium of multiple ecosystems. CO_2 emissions remain in the atmosphere for about 50 to 200 years, thus global warming effect will probably be a persistent problem for future generations [4–6]. The IPCC has concluded that if nothing is done, global carbon emissions will cause a significant raise of global temperature over the next century, which will result in devastating consequences for the planet[7].

In 2016, 195 countries at the United Nations Framework Convention on Climate Change (UNFCCC) in Paris agreed to limit the increase in global average temperature below 2°C above pre-industrial levels. Among all the proposed measures, the UNFCCC, IPCC and the International Energy Agency (IEA) have strongly recommended the intensive application of Capture and Utilization (CCU) strategies to curb global CO_2 emission.

1.2 Conversion and Utilization of CO_2

CO_2 can be utilized as an industrial feedstock for the production of chemicals. CO_2 utilization technologies are still in their infancy compared to more well-developed CO_2 storage approaches such as geological sequestration. However, CO_2 sequestration into

geological strata could be unsustainable due to concerns about possible release associated with earthquake and volcanic eruption. Hence, CO_2 utilization as an industrial feedstock could generate far more positive economic and environmental benefits.

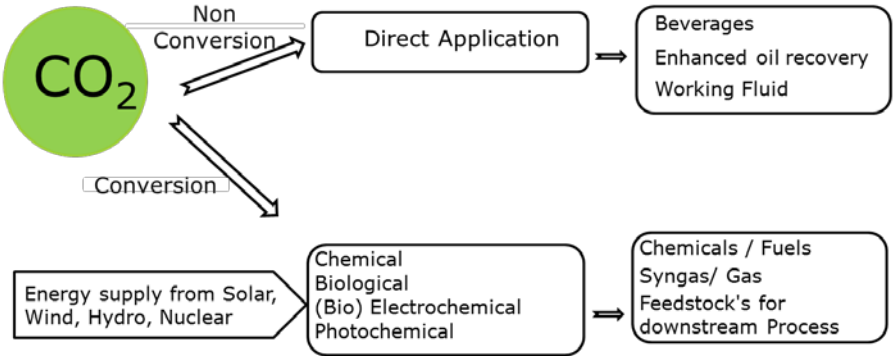

Figure 2. Possible strategies for CO_2 conversion and utilization.

So far, chemical, biological, photochemical as well as electrochemical CO_2 conversions are receiving attention for the production of fuels and chemicals.

1.2.1 Chemical conversion of CO_2

CO_2 can be converted into value-added products by employing abiotic catalysts. For instance, the direct synthesis of methanol has been successfully carried out from synthesis gas (syngas) in the presence of metallic catalysts [8–11]. Syngas is a mixture of gas

comprising CO, CO_2 and H_2, which can be obtained by the gasification of coal or biomass. Alternatively, syngas can come directly from industrial waste gases such as steel industries emissions. Likewise, heterogeneous catalysts have been used for the direct synthesis of methanol and dimethyl carbonate compounds from CO_2. [12–14] Recently, synthesis of methane has been carried out with monometallic, bimetallic and trimetallic catalysts from CO_2 and H_2 or syngas. Chemical conversion of CO_2 has already been scaled up with the construction in Germany of the Audi e-gas plant, which synthesizes methane from CO_2 and H_2[15,16]. CO_2 is the most oxidized and lowest energy compound of carbon,thus its chemical reduction requires significant quantities of energy. Because of thermodynamic constraints, low conversion efficiency, low product specificity and narrow product range, the chemical conversion of CO_2 has many limitations, and alternative strategies may become more productive.

1.2.2 Photochemical conversion of CO_2

Recently, photocatalytic technologies have been explored for CO_2 conversion. In the case of photocatalysis, transition-metal complexes catalysts have been employed to convert solar energy into chemical energy for the reduction of CO_2[17]. Transition-metal complexes can absorb a significant portion of the solar energy

spectrum and thus are good fit for photochemical applications.[18] Recently, photocatalysis had shown promising performance when semiconductors such as zinc oxide, cupric oxide or iron oxide were being used to produce CO, HCOOH, HCHO, CH_4 and CH_3OH, NH_3, and urea from CO_2 [19–21]. Until now, TiO_2 and composite materials comprising TiO_2 such as TiO_2/zeolite, $Pd/RuO_2/TiO_2$ are most performant catalysts for photochemical conversion processes due to their outstanding catalytic activity and high stability under solar irradiation. [22,23]. At the moment, the productivity and efficiency of CO_2 photochemical conversion have to be significantly optimized for large scale applications. Additionally, photocatalytic CO_2 reduction processes with high yield developed until now require sacrificial electron donors such as isopropanol and tertiary amines, which means that this technology is not completely sustainable and as useful as other for consuming the greenhouse gas CO_2 [22,23]

1.2.3 Electrochemical conversion of CO_2

CO_2 can also be converted into value-added compounds *via* electrochemical conversion approaches. Most of the experiments done for electrochemical CO_2 reduction have been carried out in bench-scale three electrode reactor systems, which contained a working electrode, a counter electrode and a reference electrode.

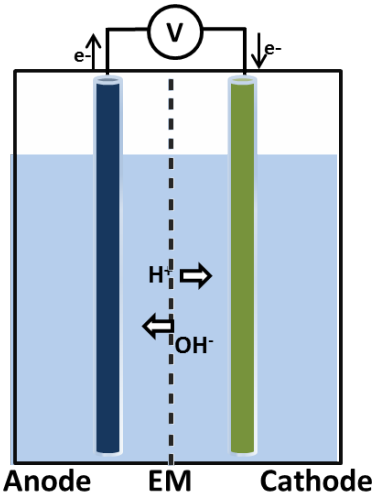

Figure 3. Electrochemical cell

Figure 5. Electrochemical cell with anodic oxidation reaction and cathodic reduction reaction and ions are migrating through exchange membrane (EM)

The electrochemical reduction of CO_2 has been investigated with different parameters including nature of the catalyst, electrode potential, pH, electrolyte composition as well as the temperature in both gas and liquid phases of the reactor[24]. The productivity of electrochemical CO_2 reduction and the nature of the product is strongly affected by experimental conditions [25–27]. In basic solution, formic acid, oxalic acid or oxalate, carbon monoxide, formaldehyde, and ethanol have all been produced electrochemically from CO_2. In acidic solution, acetate ethylenes

have been reported as primary product[28]. Recently, solid oxide fuel cells (SOFCs) have been shown to reduce CO_2 at higher temperature while transition metal-based electrodes can do the same thing at lower temperature. Even though it can lead to the generation of a large range of products, low-temperature CO_2 conversion in liquid phase required higher energy supply to overcome electrochemical overpotentials. Transition metals including titanium, molybdenum, chromium, tungsten, rhenium, manganese, iron, cobalt, nickel, ruthenium, palladium, platinum, copper, silver, and gold have all been used as a catalyst for electrochemical CO_2 reduction[29–35]. Other metals such as aluminum, indium, thallium, tin, lead, alkaline metals, and alkaline-earth metals have also been tested in lab-scale experiments [36–39]. Besides metallic catalysts, conductive polymers and carbon materials have been employed for electrochemical CO_2 reduction. Several critical challenges need to be addressed including high operation cost, low catalyst activity, insufficient catalyst durability and inability to control product specificity before large-scale application.[40,41]

1.2.4 Biological conversion of CO_2

Photosynthetic CO_2 utilization by plants is a relatively well understood phenomenon that converts light energy into chemical energy stored as carbohydrate molecules. Biological CO_2 reduction

is not restricted to photosynthetic organisms such as plants, cyanobacteria, and algae. Non-photosynthetic anaerobic bacteria also have the potential to reduce CO_2 into multicarbon compounds. Recently, non-photosynthetic autotrophic bacteria have attracted attention and are being developed for large scale production of biofuels and other chemicals from CO_2. The toolboxes of Synthetic Biology and Microbiology are currently employed to improve their metabolisms and expand the repertoire of chemicals they can produce.

Among autotrophic organisms, algae have one of the highest industrial potential for the establishment of large-scale bioreactor [42]. Algae fix CO_2 *via* photosynthesis through the Calvin-Benson-Bassham (CBB) cycle by using the ribulose 1,5-bisphosphate carboxylase/ oxygenase (RuBisCO) [43]. Their potential to fix CO_2 is attributed to high biomass production capability, fast CO_2 uptake and metabolization, and production of secondary products with high commercial value such as lipid, biofuels, lubricants, proteins, aquaculture nutrients, and fertilizers[44,45]. In recent years, substantial progress has been made in the synthetic biology for green algae and advanced genetic tools have been developed for model organisms such as *Chlamydomonas reinhardtii*, *Volvox carteri*, *Phaeodactylum tricornutum*, *Dunaliella salina*, and

Haematococcus pluvalis [46,47]. However, commercial application of algae as cell factories for CO_2 reduction could be problematic because of large surface area requirement, high operating cost, low biomass productivity, risk of contamination and low tolerance to stress such as flue gas toxicity[48]. Besides algae, photosynthetic cyanobacteria are also capable of fixing inorganic carbon from the atmosphere [49]. However, low efficiency and difficulty to maintain optimal growth temperature, pH, light intensity, nutrient supplies and aeration increase substantially operating cost for industrial application[48,50].

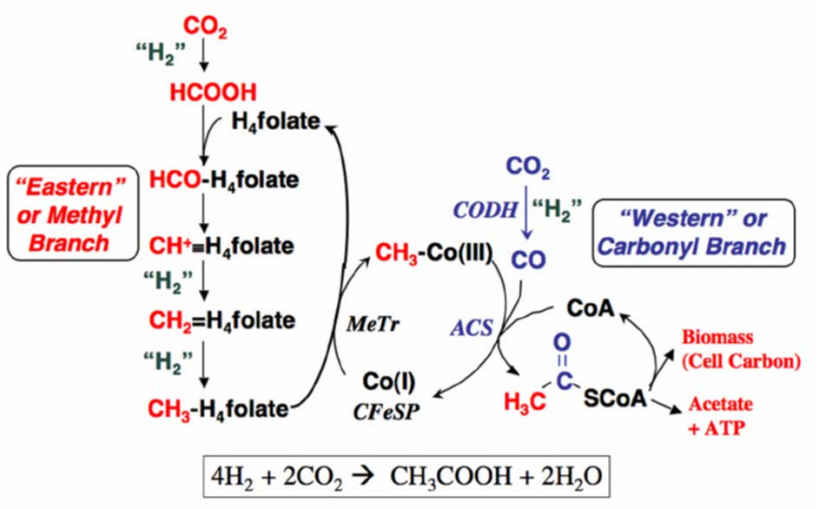

Figure 4. The Wood-Ljungdahl pathway from Ragsdale W.S et.al., 2008[51]

Non-photosynthetic anaerobic microbes are receiving a lot of attention for industrial applications. Many anaerobic autotrophic species designed as acetogens are capable of fixing CO_2 through the Wood–Ljungdahl (WL) pathway in which two molecules of CO_2 are combined to produce one molecule of acetyl-CoA as shown in figure [52]. Several industrially-relevant acetogenic strains have the ability to utilize CO_2 with CO and/or H_2 as electron donors to produce commodity chemicals such as ethanol, acetate, acetone, lactate, n-butanol, 2,3-butanediol, valerate, caproate and caprylate [53].

Autotrophic *archaea* including *Metallosphaera*, *Sulfolobus*, *Archaeoglobus*, and *Cenarchaeum* species can fix CO_2 via the 3-hydroxypropionate-4-hydroxybutyrate (3HP-4HB) cycle pathway[54–56]. Archaea can also reduce CO_2 into methane with H_2 as the electron donor. Methanogens such as *Methanobacterium thermoautotrophicum*, *Methanobacterium formicium* etc. are widely used in industrial processes for methane production as alternative fuel using H_2 as the electron donor[57,58].

Metabolic engineering tools have been employed to improve the production of chemicals from CO_2 in a wide range of species including *Clostridium autoethanogenum, Clostridium ljungdahlii*

and *Metallosphaera sedula*[59,60] [56,61]. However, genetic modification tools are not available for many anaerobic autotrophs, which complicates the development of bioindustrial processes. Synthetic biology is becoming a powerful tool for enhancing biological processes and its development for promising anaerobic autotrophs will be a major step toward industrial feasibility [62,63].

Recently, the company LanzaTech has established a large-scale plant in Beijing, China for ethanol production by acetogens from the fermentation of steel mill flue gas, which is composed of CO_2 CO, Nitrogen Oxides, and Sulfur Oxides. Other examples of pilot plants relying on acetogens for the conversion of CO_2 into biofuels or other chemicals include Taiwan Waste Gas to Fuel Demonstration Plant, Woody Biomass Syngas to Fuel & Chemicals Plant Georgia USA, Waste Gas to Fuel Industrial Pilot Plant-New Zealand, and Arcelor Mittal's integrated steel plant-Ghent Belgium for bioethanol production.

1.3 Microbial electrosynthesis

CO_2-rich gas wastes from industrial sources often does not contain any or enough reducing equivalents under the form of H_2 or CO to reduce all the CO_2 present [43,64]. In such case, approaches such as microbial electrosynthesis (MES) can be employed to supply

electrons to the microbial catalyst from electricity. During MES, electroautotrophic bacteria including acetogens reduce CO_2 by utilizing electrons from a cathode powered externally. MES systems can be powered with electricity generated from multiple renewable energy sources including wind turbine, solar and geothermal energy. MES can also be coupled with anodic processes performing chemical or biochemical oxidation processes. For example, MES could be partially powered by the oxidation of organic carbon molecules present in wastewater, effectively generating chemicals of interest while participating to the cleaning of wastewater. MES can also be used to store electricity surpluses from the power grid into the chemical bonds of biofuels. Due to the rapid increase of off-shore wind power station installation, 127 GWh of surplus electricity was reported in Germany in 2011[16].When powered by solar energy, MES become part of an artificial bioinorganic photosynthesis apparatus. The solar power conversion efficiency into biomass of natural photosynthesis is only between 2.9 and 4.3%[65]. It has been proposed that the combination of inorganic technologies for sun energy capture with MES could increase significantly solar-to-chemicals efficiency and thus outcompete bioproduction processes relying on natural photosynthesis.[65] Currently, the biggest obstacle for the development of MES as an

economically feasible technology is the low CO_2 reduction rate for the synthesis of chemicals.

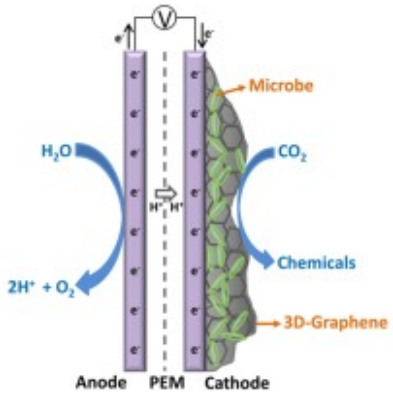

Figure 5. Microbial Electrosynthesis system with water oxidation as the anodic reaction. Microbes are reducing CO_2 into acetate with electrons from the cathode and protons migrating through a proton exchange membrane (PEM). From N. Aryal et al., 2016

1.3.1 Microbial electrosynthesis principle

Usually, MES reactors have a three-electrode configuration comprising a reference electrode, an anode, and a cathode and are partitioned into two chambers separated by an ion-exchange membrane (IEM). Oxidation processes generating protons and electrons occur at the anode. Then, electrons flow *via* an electric circuit from the anode to the cathode while protons pass through the IEM to reach the cathodic chamber. The microbial catalyst uses these protons and electrons to reduce CO_2 into multicarbon compounds. Electrons are either transferred directly or *via* a soluble

shuttle such as H_2 from the cathode to the microbes. Besides acetate, MES systems have been developed for the biocatalytic conversion of CO_2 into 2-oxobutyric acid, CH_4, formate, ethanol, butyrate, and propionate [66]87]. One of the first demonstrations of MES was done by Nevin et al., which showed the bioelectrochemical reduction of CO_2 mainly into acetate with the acetogenic bacterium *Sproromusa ovata* as microbial catalyst and a graphite cathode poised at -400 mV versus Standard Hydrogen Electrode (SHE) [66]. In this pioneering study, acetate production rate was 123 mM d^{-1} per square meter of the cathode surface. Since then, chemicals production rate in MES has been increased significantly by changing cathode materials and/or by applying lower cathode potential (Table 1). Both approaches augment electron transfer rate from the cathode to the microbial catalyst[68].[69]. For instance, certain cathode modifications such as coating 3D-rGO on carbon felt or carbon nanotubes on reticulated vitreous carbon (RVC), were shown to increase the surface area available for electron exchange with microbes as well as the electronic conductivity and the strength of electrostatic interactions between the cathode and microbes resulting in multifold increase in power densities and acetate production as shown in Table 1 [70–76].

Microbial catalysts are the other major component of MES reactor that can be optimized to augment productivity and efficiency. Both acetogenic pure cultures and enriched microbial mix culture communities have been tested in MES system for the high-rate production of commodity chemicals. Mixed cultures have been shown to perform better for acetate synthesis from CO_2 by MES, but pure cultures have other advantages that could be highly beneficial for the development of large-scale reactors[77].

1.3.2 Mixed culture microbial catalysts

Mixed culture-driven MES systems mainly produced acetate because acetogenic bacteria quickly become the dominating population if methanogenesis has been inhibited in the reactor. Mixed culture microbial catalysts have been shown to produce n-butanol, ethanol, acetate, propionate, and butyrate during MES [78–85]. Recently, Jourdin et al. 2016 have developed a mixed-culture driven MES process with a three-dimensional cathode made of RVC-modified with carbon nanotubes[86]. With this system, they reported the highest acetate production rate observed until now of 25.2 g d^{-1} per square meter of cathode polarized at -850 mV vs. SHE[86][77]. The good performance of mixed culture microbial catalysts in MES systems may be due in part to electron and nutrient transfers between the different species present[77]. This complex

interaction network may improve the transfer of electrons from the cathode to the acetate-producing bacterial cells present in the mixed population. Furthermore, mixed culture-driven MES does not require costly sterilization procedure, which is necessary for many pure culture bioproduction processes[70,72,86,87]. However, mixed culture microbial catalysts have two major disadvantages for MES: 1) costly methanogenesis inhibitors must be added to the reactor to ensure that only acetate and/or other multicarbon compounds are produced and that no methane will be generated, which would reduce product specificity as well as energetic efficiency; 2) multicarbon product range is very limited because it is impossible to use the toolbox of synthetic biology to engineer microbial catalysts for the synthesis of non-native products.

1.3.3 Pure culture microbial catalysts

The main advantages of using pure culture instead of mixed community are that product specificity is higher and that the metabolism of the microbial catalyst can be engineered. Genetic modifications can be used to both increase MES efficiency by streamlining the metabolism of the microbial catalysts and to expand the range of possible products. Several pure culture acetogens including *Sporomusa silvacetica*, *Sporomusa sphaeroides*, *Sporomusa ovata*, *Clostridium ljungdahlii*, *Clostridium aceticum*, and *Moorella thermoacetica* were shown to

be able to perform MES of acetate with a graphite cathode poised at -400 mV vs. SHE. [77][88][68,89][90] With pure culture acetogens, more than 80% of electrons supplied by the cathode usually end up in the multicarbon products[72,89,91,92]. Acetogenic bacteria performing MES show this high coulombic efficiency (CE) because contrary to other autotrophic bacteria, CO_2 is their carbon source as well as their final electron acceptor. Furthermore, the Wood–Ljungdahl pathway, which is used by acetogens to convert CO_2 into acetate, has been shown to be the most efficient non-photosynthetic carbon fixation pathway for the production of acetate and ethanol from CO_2. [82][48] Several studies have demonstrated over the years that *Sporomusa ovata* DSM-2662 is one of the best electroautotrophs for CO_2 reduction by MES[68,70,82,89,91–95]. For instance, acetate production rate was enhanced to 1052 mM d^{-1} per square meter of electrode by using a methanol-adapted *Sporomusa ovata* DSM-2662 strain with a carbon cloth cathode functionalized with rGO-tetraethylene pentamine (TEPA) poised at –690 mV vs SHE[96]. *C. ljungdahlii* is also a promising pure culture microbial catalyst for MES. This species is genetically tractable, which means that it can be engineered to synthesize a wide range of compounds from CO_2. Bajracharya et al. optimized the acetate production rate 325 mM d^{-1} per square meter of electrode with *C.*

ljungdahlii and a steel cathode at the applied potential of ‑695 mV vs. SHE[81].

1.3.4 Extracellular electron transfer (EET)

Extracellular electron transfer (EET) from the cathode to the electroautrophic microbial catalyst may occur via direct contact with outer membrane redox proteins or conductive extracellular proteins or indirectly via a soluble electron shuttle such as H_2, Fe^{2+}, formate or flavin as shown in figure 4[72]. At the moment, EET mechanisms in MES system are still mostly uncharacterized, and research efforts are underway to understand them better.

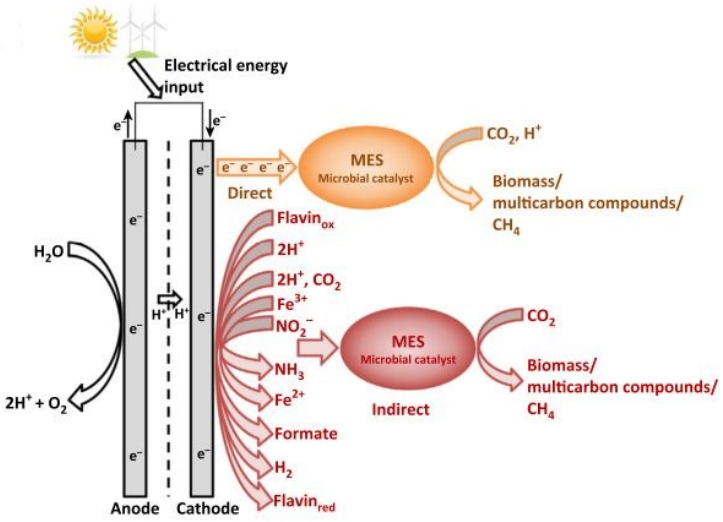

Figure 6. EET mechanisms from cathode to microbe. From Tremblay et al, , 2016

The hypothesis of direct electron transfer in MES is mainly based on the observation that acetate is produced by *S. ovata* from CO_2 in MES system with a cathode poised at a potential of -400 mV vs SHE[68]. It has been assumed that at this relatively high potential, no H_2 can be generated electrochemically and thus be used as an electron shuttle by acetogens[68,89]. However, a recent study has shown that H_2 and formate can both be produced at higher cathode potential than previously thought due to microbial activity, which calls into question the assumption that direct EET happens between the cathode and acetogens[97]. Still, if direct EET in MES system, it would probably require unique cell components such as *c*-type cytochromes or conductive pili that are capable of accepting and transporting electrons from a solid donor [98,99]. The clear advantage with direct EET is that the cathode can be poised at higher potential to drive MES, which means that less electrical energy would be required for the biological reduction of CO_2.

For indirect EET, H_2 is the most common shuttles transferring electrons from the cathode to acetogens during MES. The cathode potential must be relatively low to ensure that sufficient quantities of H_2 are generated to feed the metabolism of the microbial catalyst without becoming a restrain [67,97,99,100]. Interestingly, microbial activity has been shown recently to make H_2 evolution start at higher

cathode and to accelerate it significantly[101]. Fe^{2+}, formate and ammonia are also electrons shuttles shown to be responsible for electron transfer in different MES reactors[72].

1.3.5 Cathode materials and impact on MES performance

The optimal cathode for MES would have high electronic conductivity, low charge-transfer resistance, large surface area available for electron transfer to the microbial catalyst, exceptional mechanical strength, and high biocompatibility. Various approaches have been employed to optimize MES cathodes characteristics and improve electron transfer rates [75,88]. This includes electrode surface modifications with highly conductive and biocompatible materials forming three dimensional structures as illustrated in Figure 5.

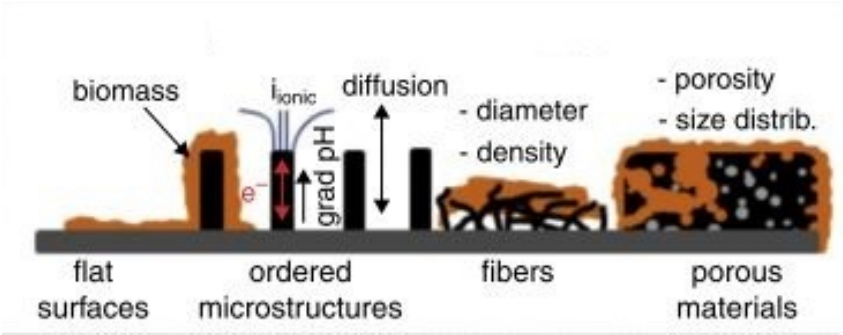

Figure 7. Biocathode surface and different examples of spatial modification. From Guo K., et. al., 2015

Carbon-based cathodes have been employed in multiples MES systems.[69]. These types of cathodes are relatively cheap, which is an important advantage for MES applications. Conventional carbon-based planar materials are graphite rod carbon cloth, carbon plate, carbon paper, activated carbon, gas diffusion activated carbon electrode, granules carbon, carbon fiber rod and carbon felt hybridized with stainless steel[70,86,90,95,103–107]. Recently, novel cathode materials have been developed such as graphene paper, carbon cloth-reduced graphene oxide tetraethylene pentamine (rGO-TEPA), 3D-rGO carbon felt, carbon nanotube on RVC for MES driven CO_2 reduction[93,94]. Overall, three-dimensional

Table 1:- Acetate production with modified electrode material using *Sporomusa ovata*

Electrode Materials	Production rate ($mMd^{-1}m^{-2}$)	Current density (mAm^{-2})	Applied Potential (mV vs SHE)	CE (%)	Reference
Carbon Cloth	88 ± 8	191 ± 10	-690	83 ± 3	[94]
Carbon Cloth- reduced graphene oxide tetraethylene pentamine	321 ± 53	686 ± 146			
Carbon Felt	136.5 ± 43.5	400 ± 10	-690	86 ± 3	[93]
Three dimensional -Graphene Carbon Felt electrode	925.5 ± 29.4	2450 ± 160			
Carbon cloth	30 ± 7	71 ± 11	-400	82 ± 12	[95]
Chitosan	229 ± 56	475 ± 18			
Cyanuric chloride	205 ± 50	451 ± 79			
3-Aminopropyltriethoxysilane	95 ± 20	206 ± 11			
Polyaniline	90 ± 22	189 ± 18			
Melamine	31 ± 8	69± 9			
Ammonia	28 ± 14	60 ± 21			
Au	181 ± 44	388 ± 43			
Pd	141 ± 35	320 ± 64			
Ni	136 ± 33	302 ± 48			
CNT-cotton	102 ± 25	220 ± 1			
CNT-polyster	96 ± 24	210 ± 13			
Graphite Stick	123	100	-400	82 ± 14	[85]
Graphite Stick -Ni Nano wire	282	890			

electrodes are recommended to enhance the productivity of MES because they offer high specific surface area, unable the formation of substantial biofilms, and provide better conductivity [81,83,108,109]. Besides carbon-based cathodes, metals, carbon-metal hybrid, and polymer-made cathodes have all been tested in MES systems such as Carbon cloth-Ni, Pd, Au, as shown in Table 1 [95]

The surface of carbon-based cathodes can be modified to improve MES. For instance, Zhang et al. coated a carbon cloth cathode with positively charged chitosan to promote better electronic interaction with negatively-charged *Sporomusa ovata* and the formation of a healthy electrocatalytic biofilm as shown in Table 1. In that study, acetate productivity was improved by 7.6 fold compared to unmodified carbon cloth[95]. Amore recent example is the deposition of rGO-TEPA on carbon cloth electrode.[94]. With this modification, spheres probably comprising bacteria and rGO-TEPA were formed at the surface of the cathode increasing the surface area available for electron transfer.[93,94].

Reference

[1] N. Climatic, NOVEMBER 2005 LOCAL CLIMATOLOGICAL DATA NOAA , National Climatic

Data Center EUREKA , CA, (2005).

[2] T.F. Stocker, Q. Dahe, G.-K. Plattner, L. V. Alexander, S.K. Allen, N.L. Bindoff, F.-M. Bréon, J.A. Church, U. Cubash, S. Emori, P. Forster, P. Friedlingstein, L.D. Talley, D.G. Vaughan, S.-P. Xie, Technical Summary, Clim. Chang. 2013 Phys. Sci. Basis. Contrib. Work. Gr. I to Fifth Assess. Rep. Intergov. Panel Clim. Chang. (2013) 33–115. doi:10.1017/ CBO9781107415324.005.

[3] P. Friedlingstein, R.M. Andrew, J. Rogelj, G.P. Peters, J.G. Canadell, R. Knutti, G. Luderer, M.R. Raupach, M. Schaeffer, D.P. van Vuuren, C. Le Quéré, Persistent growth of CO2 emissions and implications for reaching climate targets, Nat. Geosci. 7 (2014) 709–715. doi:10.1038/ngeo2248.

[4] D.J. Marcogliese, The impact of climate change on the parasites, 27 (2008) 467–484.

[5] J. Hansen, M. Sato, P. Hearty, R. Ruedy, M. Kelley, V. Masson-Delmotte, G. Russell, G. Tselioudis, J. Cao, E. Rignot, I. Velicogna, B. Tormey, B. Donovan, E. Kandiano, K. Von Schuckmann, P. Kharecha, A.N. Legrande, M. Bauer, Ice melt, sea level rise and superstorms: Evidence from paleoclimate data, climate modeling, and modern observations that 2^0c global warming could be dangerous,

Atmos. Chem. Phys. 16 (2016) 3761–3812. doi:10.5194/acp-16-3761-2016.

[6] R. Moss, J. Edmonds, K. Hibbard, M. Manning, S. Rose, D. van Vuuren, T. Carter, S. Emori, M. Kainuma, T. Kram, G. Meehl, J. Mitchell, N. Nakicenovic, K. Riahi, S. Smith, R. Stouffer, A. Thomson, J. Weyant, T. Wilbanks, The next generation of scenarios for climate change research and assessment., Nature. 463 (2010) 747–56. doi:10.1038/nature08823.

[7] K. (Kailai) Thambimuthu, M. Soltanieh, J.C. Abanades, R. Allam, O. Bolland, J. Davison, P. Feron, F. Goede, A. Herrera, M. Iijima, D. Jansen, I. Leites, P. Mathieu, E. Rubin, D. Simbeck, K. Warmuzinski, M. Wilkinson, R. Williams, M. Jaschik, A. Lyngfelt, R. Span, M. Tanczyk, Capture of CO2, IPCC Spec. Rep. Carbon Dioxide Capture Storage. (2005) 105–178.

[8] Y. Amenomiya, Methanol synthesis from CO2 + H2 II. Copper-based binary and ternary catalysts, Appl. Catal. 30 (1987) 57–68. doi:10.1016/S0166-9834(00)81011-8.

[9] M. Sahibzada, D. Chadwick, I.S. Metcalfe, Hydrogenation of carbon dioxide to methanol over palladium-promoted Cu/ZnO/A12O3 catalysts, Catal. Today. 29 (1996) 367–372. doi:10.1016/0920-5861(95)00306-1.

[10] J. Wambach, A. Baiker, A. Wokaun, CO2 hydrogenation over metal / zirconia catalysts, Phys. Chem. Chem. Phys. (1999) 5071–5080. doi:10.1039/a904923a.

[11] E.E. Ortelli, J. Wambach, A. Wokaun, Methanol synthesis reactions over a CuZr based catalyst investigated using periodic variations of reactant concentrations, Appl. Catal. A Gen. 216 (2001) 227–241. doi:10.1016/S0926-860X(01)00569-5.

[12] J. Słoczyński, R. Grabowski, A. Kozłowska, P. Olszewski, M. Lachowska, J. Skrzypek, J. Stoch, Effect of Mg and Mn oxide additions on structural and adsorptive properties of Cu/ZnO/ZrO2 catalysts for the methanol synthesis from CO2, Appl. Catal. A Gen. 249 (2003) 129–138. doi:10.1016/S0926-860X(03)00191-1.

[13] X.L. Wu, Y.Z. Meng, M. Xiao, Y.X. Lu, Direct synthesis of dimethyl carbonate (DMC) using Cu-Ni/VSO as catalyst, J. Mol. Catal. A Chem. 249 (2006) 93–97. doi:10.1016/j.molcata.2006.01.007.

[14] M. Aresta, A. Dibenedetto, M. Carone, T. Colonna, C. Fragale, Production of biodiesel from macroalgae by supercritical CO2 extraction and thermochemical liquefaction, Environ. Chem. Lett. 3 (2005) 136–139. doi:10.1007/s10311-005-0020-3.

[15] M. G??tz, J. Lefebvre, F. M??rs, A. McDaniel Koch, F. Graf, S. Bajohr, R. Reimert, T. Kolb, Renewable Power-to-Gas: A technological and economic review, Renew. Energy. 85 (2016) 1371–1390. doi:10.1016/j.renene.2015.07.066.

[16] L. J??rgensen, E.A. Ehimen, J. Born, J.B. Holm-Nielsen, Utilization of surplus electricity from wind power for dynamic biogas upgrading: Northern Germany case study, Biomass and Bioenergy. 66 (2014) 126–132. doi:10.1016/j.biombioe.2014.02.032.

[17] V. Balzani, A. Credi, M. Venturi, Photochemical conversion of solar energy, 2008. doi:10.1002/cssc.200700087.

[18] T.J. Meyer, Chemical approaches to artificial photosynthesis, Acc. Chem. Res. 22 (1989) 163–170. doi:10.1021/ar00161a001.

[19] P. Usubharatana, D. McMartin, A. Veawab, P. Tontiwachwuthikul, F. Engineering, V. Uni, S.S. Canada, Photocatalytic Process for CO 2 Emission Reduction from Industrial Flue Gas Streams, Ind. Eng. Chem. Res. 45 (2006) 2558–2568. doi:10.1021/ie0505763.

[20] G.M. Woodwell, The carbon dioxide problem, Role Terr. Veg. Glob. Carbon Cycle Meas. by Remote Sens. (1984) 3–17. doi:10.1007/978-94-009-3923-3_1.

[21] B. Liu, T. Torimoto, H. Yoneyama, Photocatalytic reduction

of carbon dioxide in the presence of nitrate using TiO2 nanocrystal photocatalyst embedded in SiO2 matrices, 0 (1998) 19–22.

[22] Slamet, H.W. Nasution, E. Purnama, S. Kosela, J. Gunlazuardi, Photocatalytic reduction of CO2 on copper-doped Titania catalysts prepared by improved-impregnation method, Catal. Commun. 6 (2005) 313–319. doi:10.1016/j.catcom.2005.01.011.

[23] G.R. Dey, A.D. Belapurkar, K. Kishore, Photo-catalytic reduction of carbon dioxide to methane using TiO2 as suspension in water, J. Photochem. Photobiol. A Chem. 163 (2004) 503–508. doi:10.1016/j.jphotochem.2004.01.022.

[24] T. V Magdesieva, I. V Zhukov, D.N. Kravchuk, O. a Semenikhin, L.G. Tomilova, K.P. Butin, Electrocatalytic CO2 reduction in methanol catalyzed by mono-, di-, and electropolymerized phthalocyanine complexes, Russ. Chem. Bull. 51 (2002) 805–812. doi:10.1023/A:1016076515710.

[25] B.A. Rosen, A. Salehi-Khojin, M.R. Thorson, W. Zhu, D.T. Whipple, P.J. Kenis, R.I. Masel, Ionic liquid-mediated selective conversion of CO(2) to CO at low overpotentials, Science (80-.). 334 (2011) 643–644. doi:10.1126/science.1209786.

[26] W. Tang, A.A. Peterson, A.S. Varela, Z.P. Jovanov, L. Bech,

W.J. Durand, S. Dahl, J.K. Norskov, I. Chorkendorff, The importance of surface morphology in controlling the selectivity of polycrystalline copper for CO2 electroreduction, Phys. Chem. Chem. Phys. 14 (2012) 76–81. doi:10.1039/C1CP22700A.

[27] H. Shibata, J.A. Moulijn, G. Mul, Enabling electrocatalytic Fischer-Tropsch synthesis from carbon dioxide over copper-based electrodes, Catal. Letters. 123 (2008) 186–192. doi:10.1007/s10562-008-9488-3.

[28] N.S. Spinner, J.A. Vega, W.E. Mustain, Recent progress in the electrochemical conversion and utilization of CO 2, Catal. Sci. Technol. Catal. Sci. Technol. (2012) 19–28. doi:10.1039/c1cy00314c.

[29] A. Fujishima, X. Zhang, D.A. Tryk, TiO2 photocatalysis and related surface phenomena, Surf. Sci. Rep. 63 (2008) 515–582. doi:10.1016/j.surfrep.2008.10.001.

[30] D.P. Summers, S. Leach, K.W. Frese, The electrochemical reduction of aqueous carbon dioxide to methanol at molybdenum electrodes with low overpotentials, J. Electroanal. Chem. 205 (1986) 219–232. doi:10.1016/0022-0728(86)90233-0.

[31] M. Asadi, B. Kumar, A. Behranginia, B. a Rosen, A. Baskin, N. Repnin, D. Pisasale, P. Phillips, W. Zhu, R. Haasch, R.F.

Klie, P. Král, J. Abiade, A. Salehi-Khojin, Robust carbon dioxide reduction on molybdenum disulphide edges., Nat. Com. 5 (2014) 4470. doi:10.1038/ncomms5470.

[32] K.C. Cheung, P. Guo, M.H. So, L.Y.S. Lee, K.P. Ho, W.L. Wong, K.H. Lee, W.T. Wong, Z.Y. Zhou, K.Y. Wong, Electrocatalytic reduction of carbon dioxide by a polymeric film of rhenium tricarbonyl dipyridylamine, J. Organomet. Chem. 694 (2009) 2842–2845. doi:10.1016/j.jorganchem.2009.04.034.

[33] Y. Hori, I. Takahashi, O. Koga, N. Hoshi, Electrochemical reduction of carbon dioxide at various series of copper single crystal electrodes, J. Mol. Catal. a-Chemical. 199 (2003) 39–47. doi:10.1016/S1381-1169(03)00016-5.

[34] T. V. Magdesieva, T. Yamamoto, D. a. Tryk, a. Fujishima, Electrochemical Reduction of CO[sub 2] with Transition Metal Phthalocyanine and Porphyrin Complexes Supported on Activated Carbon Fibers, J. Electrochem. Soc. 149 (2002) D89. doi:10.1149/1.1475690.

[35] M. Bourrez, F. Molton, S. Chardon-Noblat, A. Deronzier, [Mn(bipyridyl)(CO)3Br]: An abundant metal carbonyl complex as efficient electrocatalyst for CO2 reduction, Angew. Chemie - Int. Ed. 50 (2011) 9903–9906. doi:10.1002/anie.201103616.

[36] M. Jitaru, D. a. Lowy, M. Toma, B.C. Toma, L. Oniciu, Electrochemical reduction of carbon dioxide on flat metallic cathodes, J. Appl. Electrochem. 27 (1997) 875–889. doi:10.1023/1018441316386.

[37] G.K.S. Prakash, F.A. Viva, G.A. Olah, Electrochemical reduction of CO 2 over Sn-Nafion ?? coated electrode for a fuel-cell-like device, J. Power Sources. 223 (2013) 68–73. doi:10.1016/j.jpowsour.2012.09.036.

[38] K. Subramanian, K. Asokan, D. Jeevarathinam, M. Chandrasekaran, Electrochemical membrane reactor for the reduction of carbondioxide to formate, J. Appl. Electrochem. 37 (2007) 255–260. doi:10.1007/s10800-006-9252-6.

[39] A. Schizodimou, G. Kyriacou, Acceleration of the reduction of carbon dioxide in the presence of multivalent cations, Electrochim. Acta. 78 (2012) 171–176. doi:10.1016/j.electacta.2012.05.118.

[40] J. Schneider, H. Jia, J.T. Muckerman, E. Fujita, Thermodynamics and kinetics of CO2, CO, and H+ binding to the metal centre of CO2 reduction catalysts, Chem. Soc. Rev. 41 (2012) 2036. doi:10.1039/c1cs15278e.

[41] A.J. Morris, G.J. Meyer, E. Fujita, Molecular approaches to the photocatalytic reduction of carbon dioxide for solar fuels., Acc. Chem. Res. 42 (2009) 1983–94.

doi:10.1021/ar9001679.

[42] et al. S. Gregory, Evidence for wavelike energy transfer through quantum coherence in photosynthetic systems, Nature. 446 (2007) 782–786. doi:10.1038/nature05678.

[43] B. Zhao, Y. Su, Process effect of microalgal-carbon dioxide fixation and biomass production: A review, Renew. Sustain. Energy Rev. 31 (2014) 121–132. doi:10.1016/j.rser.2013.11.054.

[44] A.J. Cole, L. Mata, N.A. Paul, R. de Nys, Using CO2 to enhance carbon capture and biomass applications of freshwater macroalgae, GCB Bioenergy. 6 (2014) 637–645. doi:10.1111/gcbb.12097.

[45] P. Chen, M. Min, Y. Chen, L. Wang, Y. Li, Q. Chen, C. Wang, Y. Wan, X. Wang, Y. Cheng, S. Deng, K. Hennessy, X. Lin, Y. Liu, Y. Wang, B. Martinez, R. Ruan, Review of the biological and engineering aspects of algae to fuels approach, Int. J. Agric. Biol. Eng. 2 (2009) 1–30. doi:10.3965/j.issn.1934-6344.2009.04.001-030.

[46] Z. Dou, S. Heinhorst, E.B. Williams, C.D. Murin, J.M. Shively, G.C. Cannon, CO2 fixation kinetics of Halothiobacillus neapolitanus mutant carboxysomes lacking carbonic anhydrase suggest the shell acts as a diffusional barrier for CO2, J. Biol. Chem. 283 (2008) 10377–10384.

doi:10.1074/jbc.M709285200.

[47] J. Lu, C. Sheahan, P. Fu, Metabolic engineering of algae for fourth generation biofuels production, Energy Environ. Sci. 4 (2011) 2451–2466. doi:10.1039/C0EE00593B.

[48] M. Mikkelsen, M. Jørgensen, F.C. Krebs, The Teraton Challenge. A Review of Fixation and Transformation of Carbon Dioxide, Energy Environ. Sci. 3 (2010) 43–81. doi:10.1039/B912904A.

[49] G. Stephanopoulos, Synthetic Biology and Metabolic Engineering, {ACS} Synth. Biol. 1 (2012) 514–525. doi:10.1021/sb300094q.

[50] I.M.P. Machado, S. Atsumi, Cyanobacterial biofuel production, J. Biotechnol. 162 (2012) 50–56. doi:10.1016/j.jbiotec.2012.03.005.

[51] S.W. Ragsdale, E. Pierce, Acetogenesis and the Wood-Ljungdahl pathway of CO2 fixation, Biochim. Biophys. Acta - Proteins Proteomics. 1784 (2008) 1873–1898. doi:10.1016/j.bbapap.2008.08.012.

[52] H.A. Barker, M.D. Kamen, Carbon Dioxide Utilization in the Synthesis of Acetic Acid by Clostridium Thermoaceticum., Proc. Natl. Acad. Sci. U. S. A. 31 (1945) 219–25. doi:10.1073/pnas.31.8.219.

[53] M.W. Keller, G.J. Schut, G.L. Lipscomb, A.L. Menon, I.J.

Iwuchukwu, T.T. Leuko, M.P. Thorgersen, W.J. Nixon, A.S. Hawkins, R.M. Kelly, M.W.W. Adams, Exploiting microbial hyperthermophilicity to produce an industrial chemical, using hydrogen and carbon dioxide., Proc. Natl. Acad. Sci. U. S. A. 110 (2013) 5840–5. doi:10.1073/pnas.1222607110.

[54] C.M. Cooksley, Y. Zhang, H. Wang, S. Redl, K. Winzer, N.P. Minton, Targeted mutagenesis of the Clostridium acetobutylicum acetone-butanol-ethanol fermentation pathway, Metab. Eng. 14 (2012) 630–641. doi:10.1016/j.ymben.2012.09.001.

[55] M. Basen, J. Sun, M.W.W. Adams, Engineering a Hyperthermophilic Archaeon for Temperature-, 3 (2012) 1–8. doi:10.1128/mBio.00053-12.Editor.

[56] C. Leang, T. Ueki, K.P. Nevin, D.R. Lovley, A Genetic system for Clostridium ljungdahlii: A chassis for autotrophic production of biocommodities and a model homoacetogen, Appl. Environ. Microbiol. 79 (2013) 1102–1109. doi:10.1128/AEM.02891-12.

[57] F. Geppert, D. Liu, M. van Eerten-Jansen, E. Weidner, C. Buisman, A. ter Heijne, Bioelectrochemical Power-to-Gas: State of the Art and Future Perspectives, Trends Biotechnol. 34 (2016) 879–894. doi:10.1016/j.tibtech.2016.08.010.

[58] R.K. Thauer, A.-K. Kaster, H. Seedorf, W. Buckel, R.

Hedderich, Methanogenic archaea: ecologically relevant differences in energy conservation, Nat. Rev. Microbiol. 6 (2008) 579–591. doi:10.1038/nrmicro1931.

[59] S. Nagaraju, N.K. et al, Genome editing of Clostridium autoethanogenum using CRISPR/Cas9, Biotechnol. Biofuels. 9 (2016) 219. doi:10.1186/s13068-016-0638-3.

[60] Z. Ye, X. Li, Y. Cheng, Z. Liu, G. Tan, F. Zhu, S. Fu, Z. Deng, T. Liu, Evaluation of 3-hydroxypropionate biosynthesis in vitro by partial introduction of the 3-hydroxypropionate/4-hydroxybutyrate cycle from Metallosphaera sedula, J. Ind. Microbiol. Biotechnol. 43 (2016) 1313–1321. doi:10.1007/s10295-016-1793-z.

[61] B.P. Tracy, S.W. Jones, A.G. Fast, D.C. Indurthi, E.T. Papoutsakis, Clostridia: The importance of their exceptional substrate and metabolite diversity for biofuel and biorefinery applications, Curr. Opin. Biotechnol. 23 (2012) 364–381. doi:10.1016/j.copbio.2011.10.008.

[62] J.W. Lee, D. Na, J.M. Park, J. Lee, S. Choi, S.Y. Lee, Systems metabolic engineering of microorganisms for natural and non-natural chemicals, Nat. Chem. Biol. 8 (2012) 536–546. doi:10.1038/nchembio.970.

[63] R.M. Zelle, E. De Hulster, W.A. Van Winden, P. De Waard, C. Dijkema, A.A. Winkler, J.M.A. Geertman, J.P. Van

Dijken, J.T. Pronk, A.J.A. Van Maris, Malic acid production by Saccharomyces cerevisiae: Engineering of pyruvate carboxylation, oxaloacetate reduction, and malate export, Appl. Environ. Microbiol. 74 (2008) 2766–2777. doi:10.1128/AEM.02591-07.

[64] H. Atomi, Microbial enzymes involved in carbon dioxide fixation, J. Biosci. Bioeng. 94 (2002) 497–505. doi:10.1016/S1389-1723(02)80186-4.

[65] T. Zhang, More efficient together, Science (80-.). 350 (2015) 738–739. doi:10.1126/science.aad6452.

[66] K.P. Nevin, T.L. Woodard, A.E. Franks, Z.M. Summers, D.R. Lovley, Microbial electrosynthesis: Feeding microbes electricity to convert carbon dioxide and water to multicarbon extracellular organic compounds, MBio. 1 (2010). doi:10.1128/mBio.00103-10.

[67] R. Ganigué, S. Puig, P. Batlle-vilanova, M.D. Balaguer, Microbial electrosynthesis of butyrate from carbon dioxide, (2015) 1–4.

[68] K.P. Nevin, T.L. Woodard, A.E. Franks, Microbial Electrosynthesis: Feeding Microbes Electricity To Convert Carbon Dioxide and Water to Multicarbon Extracellular Organic Compounds, MBio. 1 (2010) e00103-10. doi:10.1128/mBio.00103-10.Editor.

[69] K. Guo, A. Prévoteau, S. a Patil, K. Rabaey, Engineering electrodes for microbial electrocatalysis, Curr. Opin. Biotechnol. 33 (2015) 149–156. doi:10.1016/j.copbio.2015.02.014.

[70] S. Bajracharya, A. ter Heijne, X. Dominguez Benetton, K. Vanbroekhoven, C.J.N. Buisman, D.P.B.T.B. Strik, D. Pant, Carbon dioxide reduction by mixed and pure cultures in microbial electrosynthesis using an assembly of graphite felt and stainless steel as a cathode, Bioresour. Technol. (2015). doi:10.1016/j.biortech.2015.05.081.

[71] M. Younas, L. Loong Kong, M.J.K. Bashir, H. Nadeem, A. Shehzad, S. Sethupathi, Recent Advancements, Fundamental Challenges, and Opportunities in Catalytic Methanation of CO2, Energy and Fuels. 30 (2016) 8815–8831. doi:10.1021/acs.energyfuels.6b01723.

[72] P.-L. Tremblay, L.T. Angenent, T. Zhang, Extracellular Electron Uptake: Among Autotrophs and Mediated by Surfaces, Trends Biotechnol. xx (2016) 1–12. doi:10.1016/j.tibtech.2016.10.004.

[73] P. Batlle-Vilanova, S. Puig, R. Gonzalez-Olmos, M.D. Balaguer, J. Colprim, Continuous acetate production through microbial electrosynthesis from CO 2 with microbial mixed culture, J. Chem. Technol. Biotechnol.

(2015) n/a-n/a. doi:10.1002/jctb.4657.

[74] C.G.S. Giddings, K.P. Nevin, T. Woodward, Simplifying microbial electrosynthesis reactor design, Front. Microbiol. 6 (2015) 1–6. doi:10.3389/fmicb.2015.00468.

[75] L.T. Angenent, M. a Rosenbaum, Microbial electrocatalysis to guide biofuel and biochemical bioprocessing, Biofuels. 4 (2013) 131–134. doi:10.4155/bfs.12.93.

[76] T. Zhang, H. Nie, T.S. Bain, H. Lu, M. Cui, O.L. Snoeyenbos-West, A.E. Franks, K. Nevin, T.P. Russell, D. Lovley, Improved cathode materials for microbial electrosynthesis, Energy Environ. Sci. (2012) 217–224. doi:10.1039/c2ee23350a.

[77] H.D. May, P.J. Evans, E. V. LaBelle, The bioelectrosynthesis of acetate, Curr. Opin. Biotechnol. 42 (2016) 225–233. doi:10.1016/j.copbio.2016.09.004.

[78] K. Rabaey, R. a Rozendal, Microbial electrosynthesis - revisiting the electrical route for microbial production., Nat. Rev. Microbiol. 8 (2010) 706–716. doi:10.1038/nrmicro2422.

[79] G. Mohanakrishna, J.S. Seelam, K. Vanbroekhoven, An enriched electroactive homoacetogenic biocathode for the microbial electrosynthesis of acetate through carbon dioxide reduction, Faraday Discuss. 0 (2015) 1–18.

doi:10.1039/C5FD00041F.

[80] S. Bajracharya, K. Vanbroekhoven, C.J.N. Buisman, D. Pant, D.P.B.T.B. Strik, Application of gas diffusion biocathode in microbial electrosynthesis from carbon dioxide, Environ. Sci. Pollut. Res. 23 (2016) 22292–22308. doi:10.1007/s11356-016-7196-x.

[81] S. Bajracharya, A. Ter Heijne, X. Dominguez Benetton, K. Vanbroekhoven, C.J.N. Buisman, D.P.B.T.B. Strik, D. Pant, Carbon dioxide reduction by mixed and pure cultures in microbial electrosynthesis using an assembly of graphite felt and stainless steel as a cathode, Bioresour. Technol. 195 (2015) 14–24. doi:10.1016/j.biortech.2015.05.081.

[82] F. Ammam, P.-L. Tremblay, D.M. Lizak, T. Zhang, Effect of tungstate on acetate and ethanol production by the electrosynthetic bacterium Sporomusa ovata, Biotechnol. Biofuels. 9 (2016) 163. doi:10.1186/s13068-016-0576-0.

[83] L. Jourdin, S. Freguia, B.C. Donose, J. Keller, Autotrophic hydrogen-producing biofilm growth sustained by a cathode as the sole electron and energy source, Bioelectrochemistry. 102 (2015) 56–63. doi:10.1016/j.bioelechem.2014.12.001.

[84] Z. Zaybak, J.M. Pisciotta, J.C. Tokash, B.E. Logan, Enhanced start-up of anaerobic facultatively autotrophic biocathodes in bioelectrochemical systems, J. Biotechnol.

168 (2013) 478–485. doi:10.1016/j.jbiotec.2013.10.001.

[85] H. Nie, T. Zhang, M. Cui, H. Lu, D.R. Lovley, T.P. Russell, Improved cathode for high efficient microbial-catalyzed reduction in microbial electrosynthesis cells., Phys. Chem. Chem. Phys. 15 (2013) 14290–4. doi:10.1039/c3cp52697f.

[86] L. Jourdin, T. Grieger, J. Monetti, V. Flexer, S. Freguia, Y. Lu, J. Chen, M. Romano, G.G. Wallace, J. Keller, High Acetic Acid Production Rate Obtained by Microbial Electrosynthesis from Carbon Dioxide, Environ. Sci. Technol. (2015) acs.est.5b03821. doi:10.1021/acs.est.5b03821.

[87] L. Jourdin, S. Freguia, B.C. Donose, J. Chen, G.G. Wallace, J. Keller, V. Flexer, A novel carbon nanotube modified scaffold as an efficient biocathode material for improved microbial electrosynthesis, J. Mater. Chem. A. 2 (2014) 13093. doi:10.1039/C4TA03101F.

[88] N. Faraghiparapari, K. Zengler, Production of organics from CO2 by microbial electrosynthesis (MES) at high temperature, J. Chem. Technol. Biotechnol. (2016). doi:10.1002/jctb.5015.

[89] D.R. Lovley, K.P. Nevin, Electrobiocommodities: Powering microbial production of fuels and commodity chemicals from carbon dioxide with electricity, Curr. Opin. Biotechnol. 24

(2013) 385–390. doi:10.1016/j.copbio.2013.02.012.

[90] S. a. Patil, J.B. a. Arends, I. Vanwonterghem, J. van Meerbergen, K. Guo, G.W. Tyson, K. Rabaey, Selective Enrichment Establishes a Stable Performing Community for Microbial Electrosynthesis of Acetate from CO $_2$, Environ. Sci. Technol. (2015) 150701101446004. doi:10.1021/es506149d.

[91] P.-L. Tremblay, T. Zhang, Electrifying microbes for the production of chemicals, Microb. Physiol. Metab. (2015) 201. doi:10.3389/fmicb.2015.00201.

[92] P.-L. Tremblay, D. Höglund, A. Koza, I. Bonde, T. Zhang, Adaptation of the autotrophic acetogen Sporomusa ovata to methanol accelerates the conversion of CO2 to organic products, Sci. Rep. 5 (2015) 16168. doi:10.1038/srep16168.

[93] N. Aryal, A. Halder, P.L. Tremblay, Q. Chi, T. Zhang, Enhanced microbial electrosynthesis with three-dimensional graphene functionalized cathodes fabricated via solvothermal synthesis, Electrochim. Acta. 217 (2016) 117–122. doi:10.1016/j.electacta.2016.09.063.

[94] L. Chen, P.-L. Tremblay, S. Mohanty, K. Xu, T. Zhang, Electrosynthesis of acetate from CO2 by a highly structured biofilm assembled with reduced graphene oxide–tetraethylene pentamine, J. Mater. Chem. A. 4 (2016) 8395–

8401. doi:10.1039/C6TA02036D.

[95] T. Zhang, H. Nie, T.S. Bain, H. Lu, M. Cui, O.L. Snoeyenbos-West, A.E. Franks, K. Nevin, T.P. Russell, D. Lovley, Improved cathode materials for microbial electrosynthesis, Energy Environ. Sci. 6 (2013) 217–224. doi:10.1039/c2ee23350a.

[96] L. Chen, P. Tremblay, S. Mohanty, K. Xu, T. Zhang, Electrosynthesis of acetate from CO 2 by a highly structured bio fi lm assembled with reduced, J. Mater. Chem. A Mater. Energy Sustain. 4 (2016) 8395–8401. doi:10.1039/C6TA02036D.

[97] J.S. Deutzmann, M. Sahin, A.M. Spormann, Extracellular enzymes facilitate electron uptake in biocorrosion and bioelectrosynthesis, MBio. 6 (2015) 1–8. doi:10.1128/mBio.00496-15.

[98] F. Harnisch, L.F.M. Rosa, F. Kracke, B. Virdis, J.O. Kr??mer, Electrifying white biotechnology: Engineering and economic potential of electricity-driven bio-production, ChemSusChem. 8 (2015) 758–766. doi:10.1002/cssc.201402736.

[99] D.R. Lovley, K.P. Nevin, Electrobiocommodities: Powering microbial production of fuels and commodity chemicals from carbon dioxide with electricity, Curr. Opin. Biotechnol. 24

(2013) 385–390. doi:10.1016/j.copbio.2013.02.012.

[100] D.R. Lovley, Powering microbes with electricity: Direct electron transfer from electrodes to microbes, Environ. Microbiol. Rep. 3 (2011) 27–35. doi:10.1111/j.1758-2229.2010.00211.x.

[101] E. Blanchet, F. Duquenne, Y. Rafrafi, L. Etcheverry, B. Erable, A. Bergel, Importance of the hydrogen route in up-scaling electrosynthesis for microbial CO 2 reduction, Energy Environ. Sci. Energy Environ. Sci. 8 (2015) 3731–3744. doi:10.1039/c5ee03088a.

[102] B.E.. Logan, K. Rabaey, Conversion of wastes into bioelectricity and chemicals by using microbial electrochemical technologies., Science (80-.). 337 (2012) 686−690. doi:10.1126/science.1217412.

[103] C.W. Marshall, D.E. Ross, E.B. Fichot, R.S. Norman, H.D. May, Electrosynthesis of Commodity Chemicals by an Autotrophic Microbial Community, Appl. Environ. Microbiol. 78 (2012) 8412–8420. doi:10.1128/AEM.02401-12.

[104] K.P. Nevin, T.L. Woodard, A.E. Franks, Microbial Electrosynthesis : Feeding Microbial Electrosynthesis : Feeding Microbes Electricity To Convert Carbon Dioxide and Water to Multicarbon Extracellular Organic, (2010).

doi:10.1128/mBio.00103-10.Editor.

[105] K.P. Nevin, S. a. Hensley, A.E. Franks, Z.M. Summers, J. Ou, T.L. Woodard, O.L. Snoeyenbos-West, D.R. Lovley, Electrosynthesis of organic compounds from carbon dioxide is catalyzed by a diversity of acetogenic microorganisms, Appl. Environ. Microbiol. 77 (2011) 2882–2886. doi:10.1128/AEM.02642-10.

[106] M.A. Rosenbaum, A.W. Henrich, Engineering microbial electrocatalysis for chemical and fuel production, Curr. Opin. Biotechnol. 29 (2014) 93–98. doi:10.1016/j.copbio.2014.03.003.

[107] M. a. Rosenbaum, A.E. Franks, Microbial catalysis in bioelectrochemical technologies: Status quo, challenges and perspectives, Appl. Microbiol. Biotechnol. 98 (2014) 509–518. doi:10.1007/s00253-013-5396-6.

[108] F. Kracke, I. Vassilev, J.O. Krömer, Microbial electron transport and energy conservation - The foundation for optimizing bioelectrochemical systems, Front. Microbiol. 6 (2015) 1–18. doi:10.3389/fmicb.2015.00575.

[109] H. Wang, Z.J. Ren, A comprehensive review of microbial electrochemical systems as a platform technology, Biotechnol. Adv. 31 (2013) 1796–1807. doi:10.1016/j.biotechadv.2013.10.001.

2 Performance of Sporomusa species for the microbial electrosynthesis of acetate from CO_2

Authors:

Nabin Aryal[1], Pier-Luc Tremblay[2], Dawid M. Lizak[1], Tian Zhang[1,2]*

Affiliation:-

[1]The Novo Nordisk Foundation Center for Biosustainability, Technical University of Denmark, Hørsholm, Denmark

[2]School of Chemistry, Chemical Engineering and Life Science, Wuhan University of Technology, Wuhan 430070, PR China

*Corresponding author: zhang@biosustain.dtu.dk

Keywords:

Microbial electrosynthesis; *Sporomusa*; microbial catalyst; H_2 oxidation; acetate

Bioresource Technology 233 (2017) 184–190

Contents lists available at ScienceDirect

Bioresource Technology

journal homepage: www.elsevier.com/locate/biortech

Performance of different *Sporomusa* species for the microbial electrosynthesis of acetate from carbon dioxide

Nabin Aryal [a], Pier-Luc Tremblay [b], Dawid M. Lizak [a], Tian Zhang [a,b,*]

[a] The Novo Nordisk Foundation Center for Biosustainability, Technical University of Denmark, Kgs. Lyngby, Denmark
[b] School of Chemistry, Chemical Engineering and Life Science, Wuhan University of Technology, Wuhan 430070, PR China

HIGHLIGHTS

- Six *Sporomusa* species were evaluated for microbial electrosynthesis activity.
- *S. ovata* DSM-2663 was the best microbial catalyst for MES among the tested species.
- MES performance varies greatly among the six *Sporomusa* species.
- *Sporomusa* oxidizing H_2 efficiently are not necessarily good MES microbial catalysts.

GRAPHICAL ABSTRACT

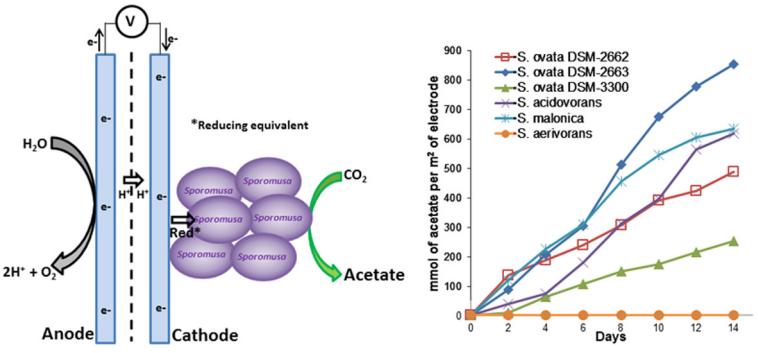

ARTICLE INFO

Article history:
Received 1 January 2017
Received in revised form 24 February 2017
Accepted 25 February 2017
Available online 28 February 2017

Keywords:
Microbial electrosynthesis
Sporomusa
Microbial catalyst
H_2 oxidation
Acetate

ABSTRACT

Sporomusa ovata DSM-2662 produces high rate of acetate during microbial electrosynthesis (MES) by reducing CO_2 with electrons coming from a cathode. Here, we investigated other *Sporomusa* for MES with cathode potential set at −690 mV vs SHE to establish if this capacity is conserved among this genus and to identify more performant strains. *S. ovata* DSM-2663 produced acetate 1.8-fold faster than *S. ovata* DSM-2662. On the contrary, *S. ovata* DSM-3300 was 2.7-fold slower whereas *Sporomusa aerivorans* had no MES activity. These results indicate that MES performance varies among *Sporomusa*. During MES, electron transfer from cathode to microbes often occurs *via* H_2. To establish if efficient coupling between H_2 oxidation and CO_2 reduction may explain why specific acetogens are more productive MES catalysts, the metabolisms of the investigated *Sporomusa* were characterized under H_2:CO_2. Results suggest that other phenotypic traits besides the capacity to oxidize H_2 efficiently are involved.

1. Introduction

Microbial electrosynthesis (MES) technology is being developed for the production of multicarbon commodities such as acetate and biofuels from the greenhouse gas CO_2 and from electrons coming from the cathode of a bioelectrochemical system (BES) (Lovley and Nevin, 2013 and Rabaey and Rozendal, 2010). One of the main features of MES is that electrical energy powers directly the biological synthesis of specific chemicals (Tremblay and Zhang, 2015). For instance, MES can be driven with electricity surplus from the power grid to store electrical energy into the chemical bonds of products of interest (Jürgensen et al., 2014 and Tremblay and Zhang, 2015). MES can also be coupled with photoelectrodes or photovoltaics to carry out artificial bioinorganic photosynthesis, a

* Corresponding author at: School of Chemistry, Chemical Engineering and Life Science, Wuhan University of Technology, Wuhan 430070, PR China.
E-mail address: zhang@biosustain.dtu.dk (T. Zhang).

http://dx.doi.org/10.1016/j.biortech.2017.02.128
0960-8524/

bioproduction process that has the potential to be significantly more efficient than natural photosynthesis (Liu et al., 2015, 2016; Lovley and Nevin, 2013; Nichols et al., 2015 and Zhang, 2015).

BES reactors employed for MES often consist of an anodic chamber and a cathodic chamber separated by an ion-exchange membrane (IEM) (Jourdin et al., 2014; LaBelle et al., 2014; Nevin et al., 2010 and Nevin et al., 2011). Protons and electrons required for CO_2 reduction are generated at the anode *via* oxidation reactions that can be abiotic or biologically-driven (Rabaey and Rozendal, 2010 and Villano et al., 2010). The microbial catalyst grown in the cathodic chamber reduces CO_2 to chemicals with electrons from the cathode and protons that passed through the IEM. The whole process requires an external source of power to drive both the anodic and cathodic reactions.

Compared to other autotrophic microbes, acetogens are microbial catalysts of choice for MES or for other autotrophic bioprocess such as gas fermentation because CO_2 is their final electron acceptor (Drake et al., 1997, 2008 and Ragsdale and Pierce, 2008). This means that most electrons coming from a cathode or other electron donors end up in the reduced products resulting in high coulombic efficiency (Tremblay and Zhang, 2015). Acetogens reduce CO_2 via the Wood-Ljungdahl pathway mainly into acetate but also into ethanol, butyrate, 2,3-butanediol, and 1-butanol (Schiel-Bengelsdorf and Dürre, 2012). In MES reactors inoculated with environmental samples and treated to inhibit methanogenesis, acetogens such as *Acetobacterium* sp. usually become predominant and produce primarily acetate from CO_2 and electricity (Bajracharya et al., 2015, 2016, 2017; Jourdin et al., 2014, 2015; LaBelle et al., 2014; Marshall et al., 2012, 2013; Mohanakrishna et al., 2015). Furthermore, pure culture-driven MES system has been demonstrated with different acetogenic species including *Sporomusa ovata*, *Sporomusa sphaeroides*, *Sporomusa silvacetica*, *Acetobacterium woodii*, *Clostridium ljungdahlii*, *Clostridium aceticum*, and *Moorella thermoacetica* (Arends, 2013; Gong et al., 2013; Nevin et al., 2010, 2011; Nie et al., 2013 and Zhang et al., 2013).

Sporomusa ovata DSM-2662 and strains derived from it are some of the most productive and efficient acetogenic bacteria capable of driving MES (Aryal et al., 2016; Chen et al., 2016 and Tremblay et al., 2015). The affinity of the *Sporomusa* genus for the cathode as a source of electrons is also highlighted by the fact that a microbial community enriched in a MES system from an environmental inoculum has been shown to contain a large population of *Sporomusa* spp. (Zhu et al., 2015). It has been proposed that one of the major routes for electron transfer from the cathode of a MES reactor to acetogens is *via* molecular H_2 (May et al., 2016 and Tremblay et al., 2016). Besides MES, *S. ovata* DSM-2662 is also an efficient strain for H_2:CO_2 gas fermentation for which it has been shown to have a high acetate production rate compared to other acetogens (Groher and Weuster-Botz, 2016). The performance of *S. ovata* DSM-2662 in MES reactor as well as during H_2:CO_2 fermentation could be explained in part by a high metabolic capacity for the usage of H_2 as an electron donor.

The main purpose of the study presented here was to determine if the capacity of reducing CO_2 *via* MES is conserved throughout the *Sporomusa* genus and if *S. ovata* DSM-2662 is really the most productive *Sporomusa* wild type strain. Thus, different *Sporomusa* never evaluated before with a cathode as the electron source were screened for MES performance and compared with *S. ovata* DSM-2662. This includes *S. ovata* DSM-2663, *S. ovata* DSM-3300, *Sporomusa acidovorans*, *Sporomusa malonica* and *Sporomusa aerivorans*. Additionally, in order to establish if acetogens efficient at reducing CO_2 to acetate with H_2 as the electron donor are automatically good microbial catalyst for MES, the growth and acetate production rate of *Sporomusa* spp. were studied under a H_2:CO_2 atmosphere.

2. Materials and methods

2.1. Strains and culture conditions

S. ovata DSM-2662, *S. ovata* DSM-2663, *S. ovata* DSM-3300, *S. acidovorans* DSM-3132, *S. malonica* DSM-5090 and *S. aerivorans* DSM-13326 were obtained from the Deutsche Sammlung Mikroorganismen und Zellkulturen (DSMZ) (Table 1). Under a N_2:CO_2 (80:20) atmosphere, *S. ovata* strains, *S. acidovorans* and *S. malonica* were routinely maintained in the DSM 311 medium of the Deutsche Sammlung Mikroorganismen (DSM) with 40 mM betaine as substrate, whereas *S. aerivorans* was maintained in the DSM 503a medium in the presence of 5 g l^{-1} Na-DL-lactate. Each culture was transferred at least three times under autotrophic conditions with a H_2:CO_2 (80:20) atmosphere (1.7 atm) before subsequent experiments. Casitone, sodium sulfide, and resazurin were omitted for all experiments with DSM-311 medium. Yeast extract was also omitted for experiments with *S. ovata* strains whereas 0.3 g l^{-1} yeast extract was added for experiments with *S. acidovorans* or *S. malonica*. Casamino acids, resazurin and dithiothreitol were omitted and 0.3 g l^{-1} yeast extract was added for experiments with *S. aerivorans* in DSM 503a medium. *S. acidovorans*, *S. malonica* and *S. aerivorans* cannot grow without yeast extract addition. For MES experiments, cysteine was also omitted from all cultivation media. For all the different *Sporomusa* species tested in this study and for every media employed here, no growth or acetate production was observed in the absence of either H_2 or the poised cathode of a MES reactor as electron donor, indicating that small amount of yeast extract or other components of the culture media were not used as growth substrates.

2.2. Microbial electrosynthesis of acetate from CO_2

H-cell type three-electrode MES reactors were operated at 25 °C with different *Sporomusa* grown in the cathode chamber as described previously (Tremblay et al., 2015). Briefly, the graphite stick cathode (36 cm^2) and anode (36 cm^2) were suspended in 250 ml of cultivation medium in two chambers separated by a Nafion 115 ion-exchange membrane (Ion Power, Inc., New Castle, DE, USA). All experiments repeated in triplicate were carried out with a CH Instrument potentiostat (CH Instruments, Inc, USA) and the cathode potential was set at −690 mV versus Standard Hydrogen Electrode (SHE). 100 ml of *Sporomusa* cultures grown on H_2:CO_2 at an optical density (545 nm) of ca. 0.1 were used to inoculate the cathode chamber. *Sporomusa* cultures were further established in the cathode chamber by bubbling with a hydrogen-containing gas mix N_2:CO_2:H_2 (83:10:7) and by swapping the medium three times. Each medium swap was performed after the *Sporomusa* cultures reached an OD_{545} of ca. 0.1. After the third medium swap, the gas mix was switched to N_2:CO_2 (80:20) for few hours before data start being collected for the MES experiments. During the whole experiment, the anode chamber was continuously bubbled with N_2:CO_2. Electrochemical data were collected for a period of two weeks with the potentiostat and analyzed with EC-Lab v.10.2 software (BioLogic, France).

2.3. Acetate concentration measurement

Acetate was quantified by High Performance Liquid Chromatography (HPLC) as previously described (Tremblay et al., 2015). Briefly, a HPX-87 H anion exchange column (Bio-Red Laboratories Inc., California, USA) at 30 °C was used with 5 mM H_2SO_4 as the mobile phase at a flow rate of 0.6 ml min^{-1}. A refractive index detector was used for detection and the results were analyzed with the Chromeleon 7 software (ThermoFisher Scientific, Denmark).

Table 1
Important characteristics of *Sporomusa* strains investigated in this study.

Strain	Other designation	Isolation source	Autotrophic growth mode	Other characteristic	Reference
S. ovata DSM-2662	Type strain, H1	Sugar beet leaf silage	MES, H_2:CO_2, formate, methanol	Gram−, Spore-forming	Möller et al. (1984) and Nevin et al. (2010)
S. ovata DSM-2663	H6	Mud, Leine river	MES, H_2:CO_2, formate, methanol	Gram−, Spore never observed	Möller et al. (1984) This study
S. ovata DSM-3300	Nile	Mud, Nile river	MES, H_2:CO_2, formate, methanol	Gram -, Spore-forming	Möller et al. (1984) This study
S. acidovorans DSM-3132	Type strain, Mol	Alcohol distillation wastewater fermenter	MES, H_2:CO_2, formate, methanol	Gram−, Spore-forming, yeast extract required for growth	Ollivier et al. (1985) This study
S. malonica DSM-5090	Type strain, Wo	Mud of polluted freshwater Gl2	MES, H_2:CO_2, formate, methanol	Gram−, Spore-forming, yeast extract required for growth	Dehning et al. (1989) This study
S. aerivorans DSM-13326	Type strain, TmAO3	Gut of soil-feeding termite	H_2:CO_2, formate, methanol	Gram−, Spore-forming, High capacity for oxygen scavenging, yeast extract required for growth	Boga et al. (2003) This study

Unpaired *t*-test was used to evaluate the statistical significance of difference observed between *Sporomusa* in acetate production rate as well as in current density and doubling time.

2.4. Confocal Laser Scanning Microscopy

For Confocal Laser Scanning Microscopy (CLSM) image, cathodes were removed from MES reactors after two weeks of operation and treated with LIVE/DEAD® BacLight™ Bacterial Viability Kit (ThermoFisher Scientific) to stain *Sporomusa* cells as described previously (Aryal et al., 2016). CLSM images were taken with a LSM5 Pascal laser scanning microscope (Zeiss) and the images were further analyzed with the ZEN imaging software (Zeiss, Germany). Z-stack composite images formed with multiple images taken at different focal distances are presented here to render the many layers of bacterial cells present at the surface of the cathode.

2.5. Whole-genome sequencing

Genomes of *S. ovata* DSM-2663 and *S. ovata* DSM-3300 were sequenced as described previously (Tremblay et al., 2015). Briefly, Genomic DNA of both strains was extracted with Easy-DNA gDNA purification Kit (Life Technologies, Carlsbad, CA). Genomic libraries were generated with the TruSeq Nano DNA LT Sample Preparation Kit (Illumina Inc., San Diego CA). Average size of dsDNA fragments in the libraries was determined with an Agilent 2100 Bioanalyzer. Sequencing was carried out with a MiSeq Reagent kit v2 (300 cycles) on a MiSeq (Illumina) platform with a paired-end protocol and read lengths of 151 nucleotides. The sequencing reads were trimmed with Trimmomatic (Bolger et al., 2014) and variant calling was done with breseq (Deatherage and Barrick, 2014). The reference genome was *S. ovata* DSM 2662 (NCBI accession ASXP00000000.1) (Poehlein et al., 2013). All the samples had an average coverage of at least 30X.

3. Results and discussion

3.1. MES with Sporomusa ovata strains

Until now, three different strains of *S. ovata* have been isolated and deposited into culture collections (Table 1). Of those three strains, only *S. ovata* DSM-2662 (ATCC 35899) has been tested and shown to drive MES with cathodes made of different materials and poised at potentials ranging from −400 to −690 mV vs SHE (Aryal et al., 2016; Chen et al., 2016; Nevin et al., 2010; Nie et al., 2013; Tremblay et al., 2015 and Zhang et al., 2013). In an effort to identify better microbial catalysts for pure culture-driven MES and to establish if the capacity to drive MES is conserved in all *S. ovata* strains, the three strains were tested in a H-cell MES reactor (Fig. 1). The acetate production rate was increased 1.8-fold (p-value of 0.07) and the current density was enhanced 1.7-fold (p-value of 0.07) with *S. ovata* DSM-2663 compared to that of *S. ovata* DSM-2662 during MES (Fig. 1A and B; Table 2). On the contrary, *S. ovata* DSM-3300 was significantly less performant for MES with a current density 2.4 times lower (p-value of 0.03) and an acetate production rate 2.6 times lower (p-value of 0.03) than *S. ovata* DSM-2662 (Fig. 1A and C; Table 2). Compared to *S. ovata* DSM-2662 and *S. ovata* DSM-3300, *S. ovata* DSM-2663 had lower coulombic efficiency (Table 2). These results showed that although *S. ovata* DSM-2663 generated acetate faster than the two other strains, it was less efficient at converting electrons from the cathode specifically into acetate molecules.

Images of confocal laser scanning microscopy (CLSM) showed substantial cell attachment by *S. ovata* DSM-2662 and *S. ovata*

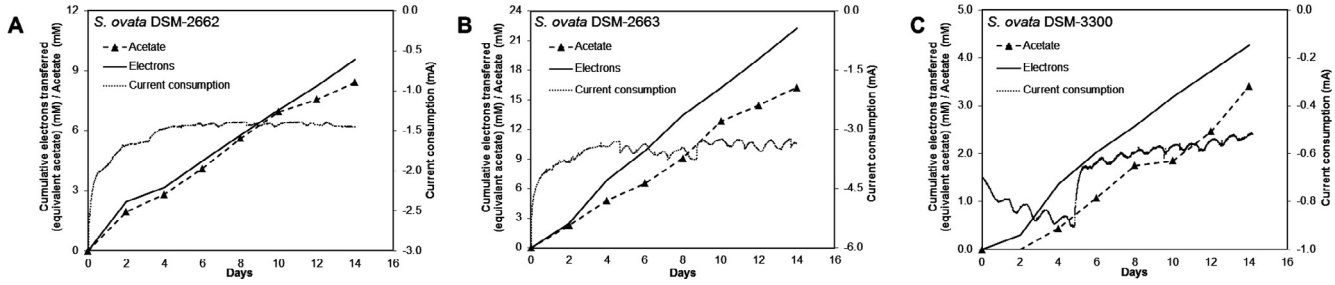

Fig. 1. Acetate production, current consumption and electron transferred during MES with (A) *S. ovata* DSM-2662, (B) *S. ovata* DSM-2663 and (C) *S. ovata* DSM-3300. Electron transferred curves correspond to the acetate concentration in mM if all the electrons transferred were converted to acetate. Acetate production curves in mM correspond to the real progression of acetate concentration in the MES reactor detected by high-pressure liquid chromatography. Results shown are from a representative example of three replicate MES reactors.

Table 2
The average acetate production and current consumption density of MES with different *Sporomusa*.

Strain	Acetate production rate[a]		Current density[a] (mA m^{-2})	Coulombic efficiency[a] (%)
	mmol m^{-2} day^{-1}[b]	mM day^{-1}		
S. ovata DSM-2662	34.3 ± 7.0	0.49 ± 0.10	454.2 ± 150.4	91.8 ± 5.3
S. ovata DSM-2663	61.1 ± 18.1	0.88 ± 0.26	782.5 ± 187.1	61.1 ± 12.6
S. ovata DSM-3300	12.9 ± 5.6	0.19 ± 0.08	191.2 ± 5.2	84.9 ± 4.0
S. acidovorans	44.1 ± 14.2	0.63 ± 0.20	572.1 ± 210.6	69.9 ± 0.9
S. malonica	45.4 ± 4.9	0.65 ± 0.07	703.2 ± 168.4	90.8 ± 13.9
S. aerivorans	N.D.[c]	N.D.	25.6 ± 2.1	N.A.[d]
Sterile control	N.D.	N.D.	16.4 ± 3.0	N.A.

[a] Each value is the mean and standard deviation of three replicates.
[b] Values normalized with respect to the graphite stick cathode projected surface area.
[c] Not detected.
[d] Not applicable.

DSM-2663 at the surface of the graphite cathode. In the case of *S. ovata* DSM-3300, less cell attachment was observed at the surface of the electrode correlating well with its lower MES performance. The observations made here with the three tested *S. ovata* strains indicate that different "wild type" strains of the same acetogenic species do not have similar performance for MES.

3.2. Genome variations between the S. ovata strains

The three *S. ovata* strains tested here were isolated by the same research group from three different sources (Möller et al., 1984). In Möller et al. study, *S. ovata* DSM-2662, *S. ovata* DSM-2663 and *S. ovata* DSM-3300 were shown to have similar growth conditions and physiological characteristics. To ensure that the *S. ovata* cultures used here are really three distinct strains and to evaluate the level of difference between them, the genomes of *S. ovata* DSM-2663 and *S. ovata* DSM-3300 were sequenced and compared to the genome sequence of *S. ovata* DSM-2662 (Poehlein et al., 2013). *S. ovata* DSM-2663 had 69 genome variations including a base substitution in a subunit of a NADP-reducing dehydrogenase (*hndD2*) coupling the reduction of NADP to NADPH with the oxidation of molecular H_2 (Dermoun et al., 2002). This enzyme may be involved in energy conservation during autotrophic growth by *S. ovata*. Additionally, genes coding for regulatory proteins (*baeS*, SOV_1c09220) presented variations with possible effects on the expression of other genes in *S. ovata* DSM-2663, which could be related to the better MES performance of this strain. *S. ovata* DSM-3300 was significantly more distant from both *S. ovata* DSM-2662 and *S. ovata* DSM-2663 with ca. 36800 genome variations in genes coding for proteins with multiple functions such as regulation, H_2 metabolism, transport, energy conservation and CO_2 reduction via the Wood-Ljungdahl pathway. Genome sequencing results presented here confirmed that the studied strains were different genetically, which is probably related to the observed variation in MES performance.

3.3. Growth of S. ovata strains with H_2:CO_2

Below a potential of −590 mV vs SHE, carbonaceous cathodes evolve H_2 abiotically (Aulenta et al., 2008). Furthermore, the presence of microbial cells at the surface of the cathode has been shown to accelerate H_2 evolution (Deutzmann et al., 2015; Jourdin et al., 2016 and May et al., 2016). Therefore, in the MES system employed here with a graphite cathode set at potential of −690 mV vs SHE, it could be hypothesized that any acetogenic species has the potential to be a good candidate for the electrosynthesis of acetate if they are capable of growing efficiently with H_2 as the electron donor and CO_2 as the electron acceptor. To verify this hypothesis, the growth and acetate production of *S. ovata* DSM-2662, DSM-3300, and DSM-2663 was evaluated in batch mode under a H_2:CO_2 atmosphere (Fig. 2 and Table 3). The three strains had similar doubling times and acetate production rates, and thus, no relation could be established between their metabolism efficiency under a H_2:CO_2 atmosphere in batch mode and their MES performance. More specifically, results obtained with *S. ovata* DSM-3300 demonstrate that good fitness with H_2:CO_2 does not translate into good performance in the MES system (Figs. 1C and 2C).

3.4. MES and H_2:CO_2 growth with other Sporomusa species

Until now, all the *Sporomusa* species tested in the MES system were shown to be capable of reducing CO_2 with electrons coming from a cathode (Tremblay and Zhang, 2015). This also includes both *S. silvacetica* and *S. sphaeroides*, which are known to electrosynthesize acetate but significantly slower than *S. ovata* DSM-2662 (Nevin et al., 2010 and Nevin et al., 2011). To establish if

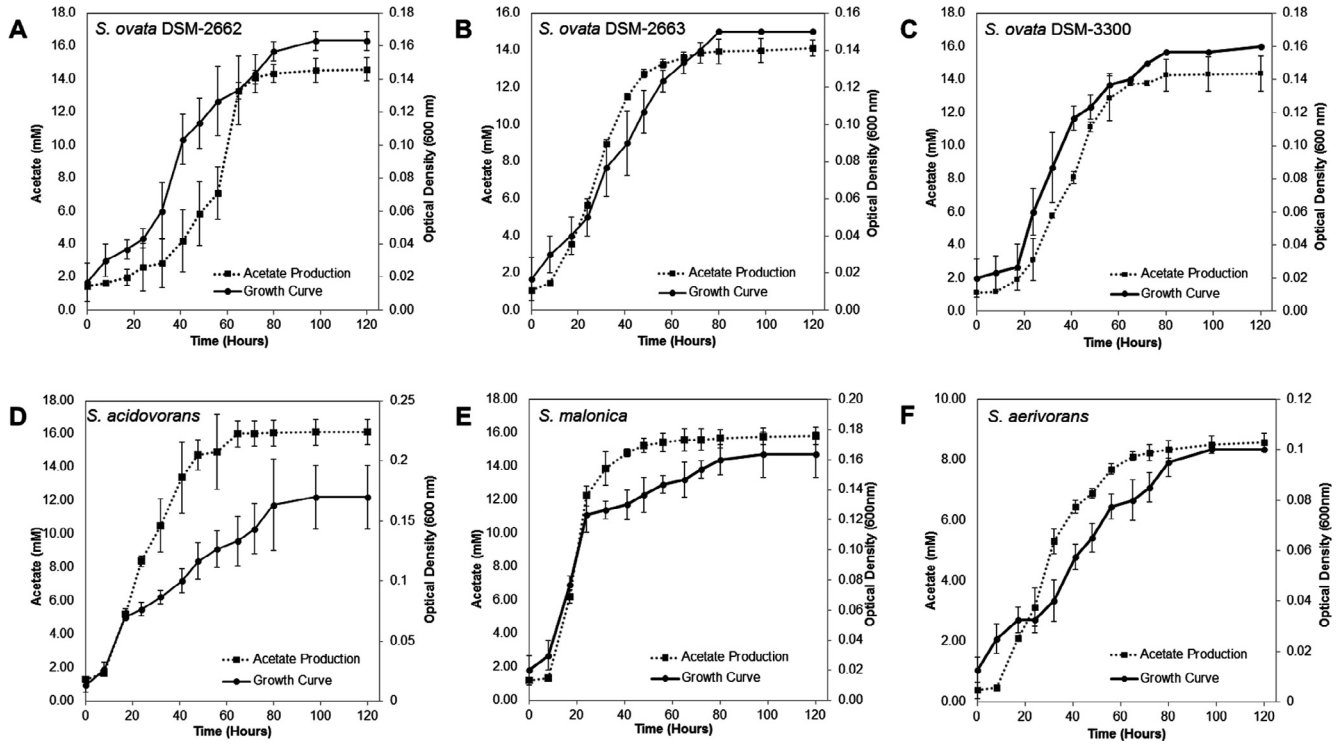

Fig. 2. Growth on H_2:CO_2 of (A) *S. ovata* DSM-2662, (B) *S. ovata* DSM-2663, (C) *S. ovata* DSM-3300, (D) *S. acidovorans*, (E) *S. malonica* and (F) *S. aerivorans*. Each curve is the mean and standard deviation of three replicates.

Table 3
Growth on H_2:CO_2 of different *Sporomusa*.

Strain	Doubling time[a] (Hour)	Acetate production[a] rate (mM day^{-1})
S. ovata DSM-2662	24.8 ± 4.0	6.7 ± 1.3
S. ovata DSM-2663	25.7 ± 2.9	7.2 ± 0.1
S. ovata DSM-3300	25.4 ± 0.7	6.5 ± 0.3
S. acidovorans	27.0 ± 4.4	7.9 ± 1.0
S. malonica	9.7 ± 1.9	10.2 ± 0.3
S. aerivorans	30.2 ± 3.1	3.2 ± 0.1

[a] Each value is the mean and standard deviation of three replicates.

the capacity to perform MES is a widespread characteristic within the *Sporomusa* genus, three other *Sporomusa* species including *S. acidovorans*, *S. malonica*, and *S. aerivorans* were tested in the MES reactor (Fig 3 and Table 2). *S. acidovorans* and *S. malonica* were drawing current and producing acetate from CO_2 at levels comparable to what has been observed with *S. ovata* DSM-2662 and *S. ovata* DSM-2663 (Fig. 3A and B). However, *S. acidovorans* had significantly lower coulombic efficiency than *S. malonica* and *S. ovata* DSM-2662. *S. aerivorans* did not electrosynthesize acetate from CO_2 and the observed current density was of the same order of magnitude as the abiotic control MES system (Fig. 3C). CLSM images showed substantial cell attachment of both *S. acidovorans* and *S. malonica* on the graphite cathode during MES.

Growth and acetate production of *S. acidovorans*, *S. malonica*, and *S. aerivorans* were also evaluated in batch mode under a H_2:CO_2 atmosphere (Fig. 2 and Table 3). *S. acidovorans* had a doubling time and an acetate production rate comparable to the three strains of *S. ovata*, whereas *S. malonica* exhibited the best growth performance among all the tested strains (Fig. 2 and Table 3). Compared to *S. ovata* DSM-2663, *S. malonica* was slightly less performant for MES but it grew 2.6 times faster (p-value of 0.001) and had an acetate production rate 1.4 times higher (p-value of 0.0001) under a H_2:CO_2 atmosphere (Fig. 2E and Table 3). This indicates that a more efficient metabolism with H_2:CO_2 does not necessarily translate into better MES performance. On the other hand, *S. aerivorans* was unable to perform MES but it was still

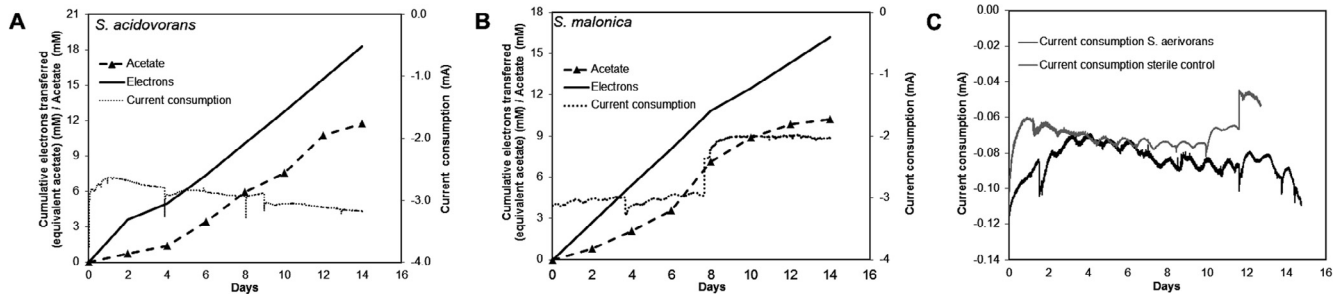

Fig. 3. Acetate production, current consumption and electron transferred during MES with (A) *S. acidovorans* and (B) *S. malonica*. (C) Current with *S. aerivorans* and the sterile medium control. No acetate was produced with *S. aerivorans* or the sterile medium control. Electron transferred curves correspond to the acetate concentration in mM if all the electrons transferred were converted to acetate. Acetate production curves in mM correspond to the real progression of acetate concentration in the MES reactor detected by high-pressure liquid chromatography. Results shown are from a representative example of three replicate MES reactors.

metabolically active under a H_2:CO_2 atmosphere and capable of generating biomass despite its significantly slower growth and acetate production than the other tested *Sporomusa* species (Fig. 2F and Table 3). These observations showed that the capacity of oxidizing H_2 for the reduction of CO_2 *via* the Wood-Ljungdahl pathway is not sufficient for an acetogenic species to be able to drive MES.

This study strongly suggested that acetogens performing well in MES reactors must have other characteristics than the ability to oxidize H_2 efficiently for the biological reduction of CO_2. For example, performant acetogenic MES microbial catalyst may 1) be more efficient at forming biofilm on electrode surface to increase the volume of electrons exchange, 2) have the capacity to accelerate the cathode-mediated H_2 evolution, 3) have uptake hydrogenases more suitable for H_2 oxidation in closed proximity to a cathode, or 4) be capable of acquiring electrons either directly or *via* alternative electron shuttles (Deutzmann et al., 2015; Jourdin et al., 2016; Patil et al., 2015; Tremblay et al., 2016).

In this work, MES acetate production rates for *Sporomusa* strains including *S. ovata* DSM-2663 were at least one order of magnitude slower than for H_2:CO_2 grown cultures (Tables 2 and 3). Previous studies have shown that using graphene-modified cathodes instead of the graphite cathode is sufficient to increase acetate production by *Sporomusa*-driven MES by one order of magnitude (Aryal et al., 2016; Chen et al., 2016). Further research is required to establish if employing *S. ovata* DSM-2663 in combination with graphene-modified cathodes or with other bioelectrochemical reactor improvements could have a synergistic effect on MES performance.

4. Conclusion

Among the tested *Sporomusa*, only *S. aerivorans* could not perform MES. This result demonstrates that the capacity of catalyzing MES is not conserved among the *Sporomusa* genus. *S. ovata* DSM-3300 catalyzed MES, but not as efficiently as other *Sporomusa*. Under a H_2:CO_2 atmosphere, *S. ovata* DSM-3300 reduced CO_2 similarly to the better MES microbial catalysts indicating that there is no correlation between fitness on H_2:CO_2 and MES performance. *S. ovata* DSM-2663 was the best MES microbial catalyst in this study. Although it had lower coulombic efficiency, *S. ovata* DSM-2663 could be a promising microbial catalyst for MES applications.

Acknowledgements

This work was funded by the Novo Nordisk Foundation.

Appendix A. Supplementary data

Supplementary data associated with this article can be found, in the online version, at http://dx.doi.org/10.1016/j.biortech.2017.02.128.

References

Arends, J., 2013. Optimizing the Plant Microbial Fuel Cell: Diversifying Applications and Product Outputs (dissertation). Ghent University.
Aryal, N., Halder, A., Tremblay, P.-L., Chi, Q., Zhang, T., 2016. Enhanced microbial electrosynthesis with three-dimensional graphene functionalized cathodes fabricated via solvothermal synthesis. Electrochim. Acta 217, 117–122.
Aulenta, F., Reale, P., Catervi, A., Panero, S., Majone, M., 2008. Kinetics of trichloroethene dechlorination and methane formation by a mixed anaerobic culture in a bio-electrochemical system. Electrochim. Acta 53, 5300–5305.
Bajracharya, S., ter Heijne, A., Dominguez Benetton, X., Vanbroekhoven, K., Buisman, C.J.N., Strik, D.P.B.T.B., Pant, D., 2015. Carbon dioxide reduction by mixed and pure cultures in microbial electrosynthesis using an assembly of graphite felt and stainless steel as a cathode. Bioresour. Technol. 195, 14–24.
Bajracharya, S., Vanbroekhoven, K., Buisman, C.J.N., Pant, D., Strik, D.P.B.T.B., 2016. Application of gas diffusion biocathode in microbial electrosynthesis from carbon dioxide. Environ. Sci. Pollut. Res. 23, 22292–22308.
Bajracharya, S., Yuliasni, R., Vanbroekhoven, K., Buisman, C.J.N., Strik, D.P.B.T.B., Pant, D., 2017. Long-term operation of microbial electrosynthesis cell reducing CO_2 to multi-carbon chemicals with a mixed culture avoiding methanogenesis. Bioelectrochemistry 113, 26–34.
Boga, H.I., Ludwig, W., Brune, A., 2003. *Sporomusa aerivorans* sp. nov., an oxygen-reducing homoacetogenic bacterium from the gut of a soil-feeding termite. Int. J. Syst. Evol. Microbiol. 53, 1397–1404.
Bolger, A.M., Lohse, M., Usadel, B., 2014. Trimmomatic: a flexible trimmer for Illumina sequence data. Bioinformatics 30, 2114–2120.
Chen, L., Tremblay, P.-L., Mohanty, S., Xu, K., Zhang, T., 2016. Electrosynthesis of acetate from CO_2 by a highly structured biofilm assembled with reduced graphene oxide–tetraethylene pentamine. J. Mater. Chem. A 4, 8395–8401.
Deatherage, D.E., Barrick, J.E., 2014. Identification of mutations in laboratory-evolved microbes from next-generation sequencing data using breseq. Methods Mol. Biol. 1151, 165–188.
Dehning, I., Stieb, M., Schink, B., 1989. *Sporomusa malonica* sp. nov., a homoacetogenic bacterium growing by decarboxylation of malonate or succinate. Arch. Microbiol. 151, 421–426.
Dermoun, Z., De Luca, G., Asso, M., Bertrand, P., Guerlesquin, F., Guigliarelli, B., 2002. The NADP-reducing hydrogenase from *Desulfovibrio fructosovorans*: functional interaction between the C-terminal region of HndA and the N-terminal region of HndD subunits. Biochim. Biophys. Acta 1556, 217–225.
Deutzmann, J.S., Sahin, M., Spormann, A.M., 2015. Extracellular enzymes facilitate electron uptake in biocorrosion and bioelectrosynthesis. mBio 6. e00496-15.
Drake, H.L., Daniel, S.L., Küsel, K., Matthies, C., Kuhner, C., Braus-Stromeyer, S., 1997. Acetogenic bacteria: what are the in situ consequences of their diverse metabolic versatilities? BioFactors 6, 13–24.
Drake, H.L., Gößner, A.S., Daniel, S.L., 2008. Old Acetogens, New Light. Ann. N. Y. Acad. Sci. 1125, 100–128.
Gong, Y., Ebrahim, A., Feist, A.M., Embree, M., Zhang, T., Lovley, D., Zengler, K., 2013. Sulfide-driven microbial electrosynthesis. Environ. Sci. Technol. 47, 568–573.
Groher, A., Weuster-Botz, D., 2016. Comparative reaction engineering analysis of different acetogenic bacteria for gas fermentation. J. Biotechnol. 228, 82–94.
Jourdin, L., Freguia, S., Donose, B.C., Chen, J., Wallace, G.G., Keller, J., Flexer, V., 2014. A novel carbon nanotube modified scaffold as an efficient biocathode material for improved microbial electrosynthesis. J. Mater. Chem. A 2, 13093–13102.
Jourdin, L., Grieger, T., Monetti, J., Flexer, V., Freguia, S., Lu, Y., Chen, J., Romano, M., Wallace, G.G., Keller, J., 2015. High acetic acid production rate obtained by microbial electrosynthesis from carbon dioxide. Environ. Sci. Technol. 49, 13566–13574.
Jourdin, L., Lu, Y., Flexer, V., Keller, J., Freguia, S., 2016. Biologically induced hydrogen production drives high rate/high efficiency microbial electrosynthesis of acetate from carbon dioxide. ChemElectroChem 3, 581–591.
Jürgensen, L., Ehimen, E.A., Born, J., Holm-Nielsen, J.B., 2014. Utilization of surplus electricity from wind power for dynamic biogas upgrading: Northern Germany case study. Biomass Bioenergy 66, 126–132.
LaBelle, E.V., Marshall, C.W., Gilbert, J.A., May, H.D., 2014. Influence of acidic pH on hydrogen and acetate production by an electrosynthetic microbiome. PLoS One 9, e109935.
Liu, C., Gallagher, J.J., Sakimoto, K.K., Nichols, E.M., Chang, C.J., Chang, M.C.Y., Yang, P., 2015. Nanowire-bacteria hybrids for unassisted solar carbon dioxide fixation to value-added chemicals. Nano Lett. 15, 3634–3639.
Liu, C., Colón, B.C., Ziesack, M., Silver, P.A., Nocera, D.G., 2016. Water splitting–biosynthetic system with CO_2 reduction efficiencies exceeding photosynthesis. Science 352, 1210–1213.
Lovley, D.R., Nevin, K.P., 2013. Electrobiocommodities: powering microbial production of fuels and commodity chemicals from carbon dioxide with electricity. Curr. Opin. Biotechnol. 24, 385–390.
Marshall, C.W., Ross, D.E., Fichot, E.B., Norman, R.S., May, H.D., 2012. Electrosynthesis of commodity chemicals by an autotrophic microbial community. Appl. Environ. Microbiol. 78, 8412–8420.
Marshall, C.W., Ross, D.E., Fichot, E.B., Norman, R.S., May, H.D., 2013. Long-term operation of microbial electrosynthesis systems improves acetate production by autotrophic microbiomes. Environ. Sci. Technol. 47, 6023–6029.
May, H.D., Evans, P.J., LaBelle, E.V., 2016. The bioelectrosynthesis of acetate. Curr. Opin. Biotechnol. 42, 225–233.
Mohanakrishna, G., Seelam, J.S., Vanbroekhoven, K., Pant, D., 2015. An enriched electroactive homoacetogenic biocathode for the microbial electrosynthesis of acetate through carbon dioxide reduction. Faraday Discuss. 183, 445–462.
Möller, B., Oßmer, R., Howard, B.H., Gottschalk, G., Hippe, H., 1984. *Sporomusa*, a new genus of gram-negative anaerobic bacteria including *Sporomusa sphaeroides* spec. nov. and *Sporomusa ovata* spec. nov. Arch. Microbiol. 139, 388–396.
Nevin, K.P., Woodard, T.L., Franks, A.E., Summers, Z.M., Lovley, D.R., 2010. Microbial electrosynthesis: feeding microbes electricity to convert carbon dioxide and water to multicarbon extracellular organic compounds. In: mBio 1. e00103-10.
Nevin, K.P., Hensley, S.A., Franks, A.E., Summers, Z.M., Ou, J., Woodard, T.L., Snoeyenbos-West, O.L., Lovley, D.R., 2011. Electrosynthesis of organic compounds from carbon dioxide is catalyzed by a diversity of acetogenic microorganisms. Appl. Environ. Microbiol. 77, 2882–2886.
Nichols, E.M., Gallagher, J.J., Liu, C., Su, Y., Resasco, J., Yu, Y., Sun, Y., Yang, P., Chang, M.C.Y., Chang, C.J., 2015. Hybrid bioinorganic approach to solar-to-chemical conversion. Proc. Natl. Acad. Sci. USA 112, 11461–11466.

Nie, H., Zhang, T., Cui, M., Lu, H., Lovley, D.R., Russell, T.P., 2013. Improved cathode for high efficient microbial-catalyzed reduction in microbial electrosynthesis cells. Phys. Chem. Chem. Phys. 15, 14290–14294.

Ollivier, B., Cordruwisch, R., Lombardo, A., Garcia, J.-L., 1985. Isolation and characterization of *Sporomusa acidovorans* sp. nov., a methylotrophic homoacetogenic bacterium. Arch. Microbiol. 142, 307–310.

Patil, S.A., Arends, J.B.A., Vanwonterghem, I., van Meerbergen, J., Guo, K., Tyson, G. W., Rabaey, K., 2015. Selective enrichment establishes a stable performing community for microbial electrosynthesis of acetate from CO_2. Environ. Sci. Technol. 49, 8833–8843.

Poehlein, A., Gottschalk, G., Daniel, R., 2013. First insights into the genome of the gram-negative, endospore-forming organism *Sporomusa ovata* strain H1 DSM 2662. Genome Announc. 1. e00734-13.

Rabaey, K., Rozendal, R.A., 2010. Microbial electrosynthesis — revisiting the electrical route for microbial production. Nat. Rev. Microbiol. 8, 706–716.

Ragsdale, S.W., Pierce, E., 2008. Acetogenesis and the Wood-Ljungdahl pathway of CO2 fixation. Biochim. Biophys. Acta 1784, 1873–1898.

Schiel-Bengelsdorf, B., Dürre, P., 2012. Pathway engineering and synthetic biology using acetogens. FEBS Lett. 586, 2191–2198.

Tremblay, P.-L., Zhang, T., 2015. Electrifying microbes for the production of chemicals. Front. Microbiol. 6, 201.

Tremblay, P.-L., Höglund, D., Koza, A., Bonde, I., Zhang, T., 2015. Adaptation of the autotrophic acetogen Sporomusa ovata to methanol accelerates the conversion of CO_2 to organic products. Sci. Rep. 5, 16168.

Tremblay, P.-L., Angenent, L.T., Zhang, T., 2016. Extracellular electron uptake: among autotrophs and mediated by surfaces. Trends Biotechnol. http://dx.doi.org/10.1016/j.tibtech.2016.10.004.

Villano, M., Aulenta, F., Ciucci, C., Ferri, T., Giuliano, A., Majone, M., 2010. Bioelectrochemical reduction of CO_2 to CH_4 via direct and indirect extracellular electron transfer by a hydrogenophilic methanogenic culture. Bioresour. Technol. 101, 3085–3090.

Zhang, T., 2015. More efficient together. Science 350, 738–739.

Zhang, T., Nie, H., Bain, T.S., Lu, H., Cui, M., Snoeyenbos-West, O.L., Franks, A.E., Nevin, K.P., Russell, T.P., Lovley, D.R., 2013. Improved cathode materials for microbial electrosynthesis. Energy Environ. Sci. 6, 217–224.

Zhu, X., Siegert, M., Yates, M.D., Logan, B.E., 2015. Alamethicin suppresses methanogenesis and promotes acetogenesis in bioelectrochemical systems. Appl. Environ. Microbiol. 81, 3863–3868.

Appendix A. Supplementary figures

Performance of different *Sporomusa* species for the microbial electrosynthesis of acetate from carbon dioxide

Nabin Aryal[1], Pier-Luc Tremblay[2], Dawid M. Lizak[1], Tian Zhang[1,2]*

[1]The Novo Nordisk Foundation Center for Biosustainablity, Technical University of Denmark, Hørsholm, Denmark

[2]School of Chemistry, Chemical Engineering and Life Science, Wuhan University of Technology, Wuhan 430070, PR China

*Corresponding author

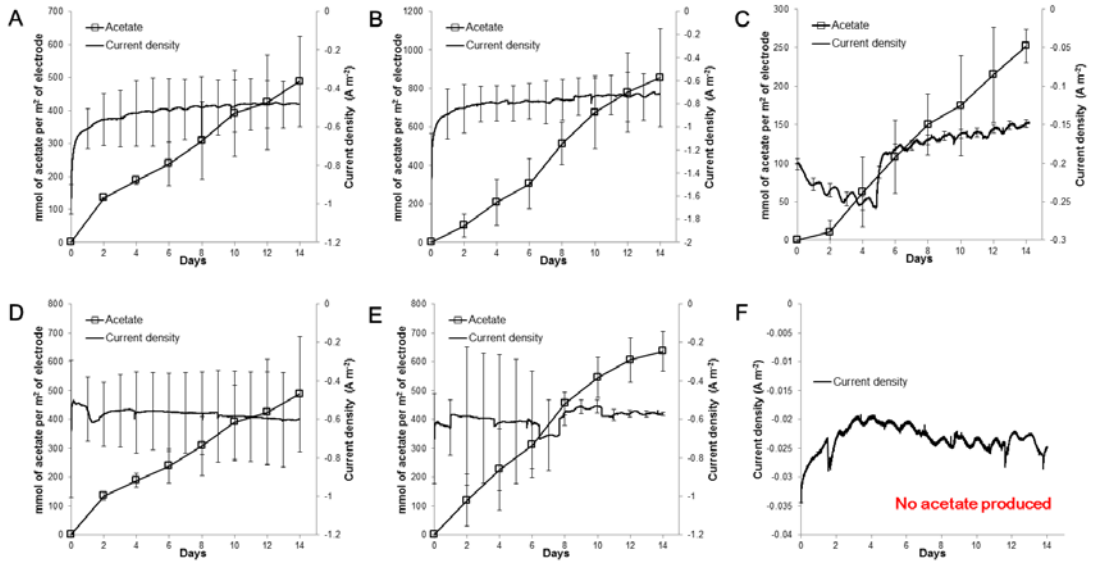

Figure S1. Acetate production per m^2 of electrode surface and current density. (A) *S. ovata* DSM-2662, (B) *S. ovata* DSM-2663, (C) *S. ovata* DSM-3300, (D) *S. acidovorans*, (E) *S. malonica* and (F) *S. aerivorans*. No acetate was produced by MES with *S. aerivorans*. Each curve is the mean and standard deviation of three replicates.

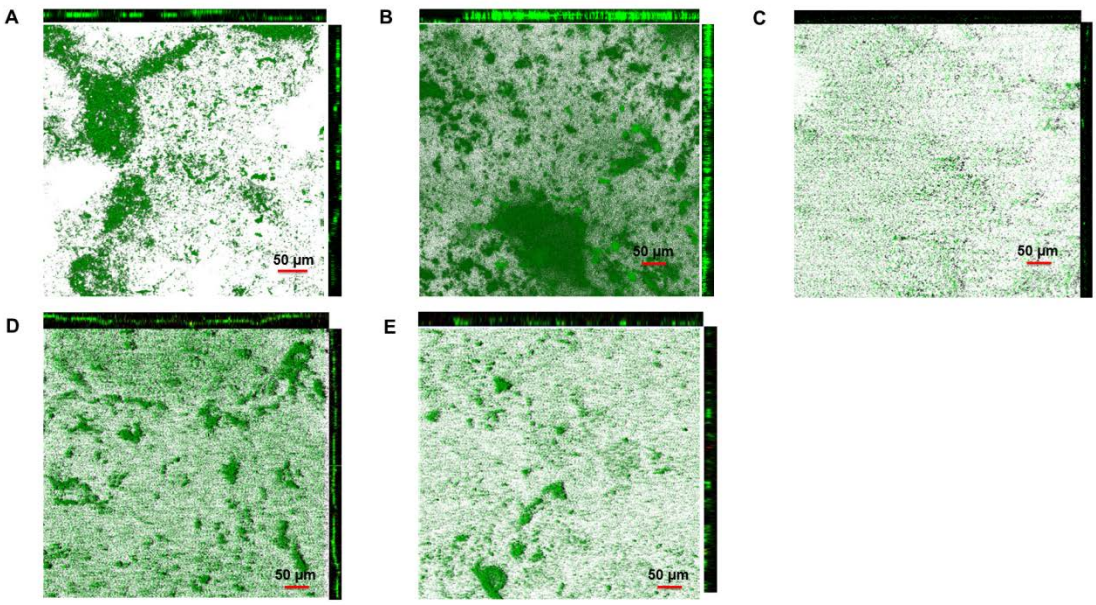

Figure S2. Z-stack CLSM images of graphite stick cathode from MES reactor populated with (A) *S. ovata* DSM-2662, (B) *S. ovata* DSM-2663, (C) *S. ovata* DSM-3300, (D) *S. acidovorans* and (E) *S. malonica*.

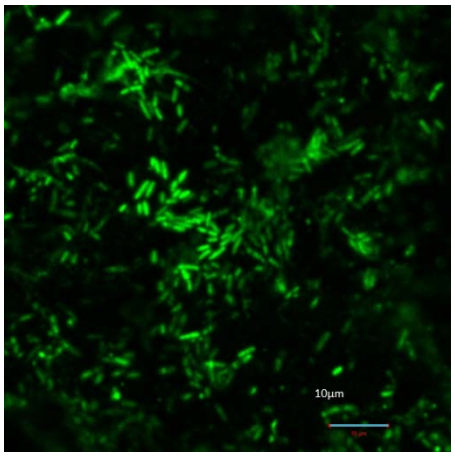

Figure S3. CLSM image of *S. ovata* DSM-2663 at a higher resolution (10 µM) showing individual bacterial cells.

3 Substantial enhancement of MES for acetate production using novel composite cathodes

3.1 Freestanding and flexible graphene papers as bioelectrochemical cathode for selective and efficient CO_2 conversion

Author:

Nabin Aryal[a] Arnab Halder[b], Minwei Zhang[b], Pier-Luc Tremblay[a,c], Qijin Chi[b], Tian Zhang[a,c]*

Affiliation:

[a]The Novo Nordisk Foundation Center for Biosustainability, Technical University of Denmark, DK-2970 Hørsholm, Denmark.

[b]Department of Chemistry, Technical University of Denmark, DK-2800 Kongens Lyngby, Denmark.

[c]School of Chemistry, Chemical Engineering and Life Science, Wuhan University of Technology, Wuhan 430070, PR China

Abstract

During microbial electrosynthesis (MES) driven CO_2 reduction, cathode plays a vital role by donating electrons to microbe. We have exploited the advantage of graphene papers as cathode materials to enhance electron transfer between the cathode and microbe, which in turn facilitates CO2 reduction and acetate production.

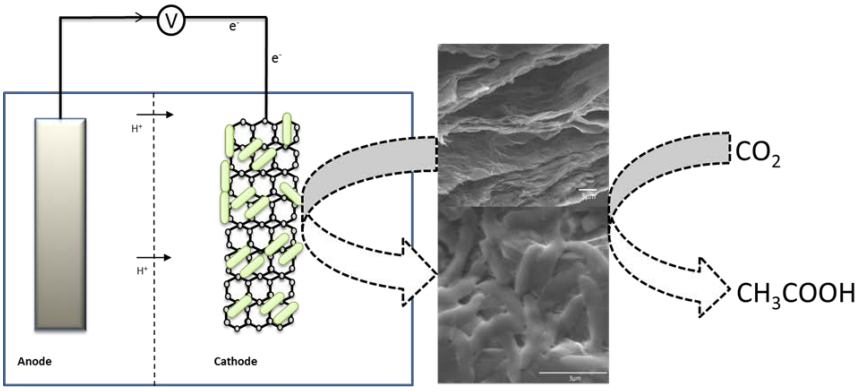

Figure 1. Microbial Electrosynthesis system where Microbes are reducing CO_2 into acetate with electrons from the reduced graphene paper cathode and protons migrating from anode through a proton exchange membrane (PEM).

Manuscript

Thin paper made of reduced graphene oxide (RGO) has a wide range of potential applications in research fields such as materials science, life sciences, environmental engineering, and electrochemical technologies[1–6]. RGO paper attracts interest because of its unique combination of physicochemical properties, which includes large surface area, tough mechanical strength, good biocompatibility, low cost as well as high flexibility, thermal stability, and electrical conductivity[1,7]. In recent years, RGO papers have been explored to fabricate freestanding electrodes for electrochemical sensor applications. For instance, RGO-paper-based electrodes have been used for the detection of H_2O_2, glucose

level in blood, pathogenic bacteria, or to monitor the secretion of nitric oxide by live cells[1,8–10].

Carbon paper is another paper-like material employed in electrochemical devices that share several properties with RGO papers such as high electrical conductivity, large surface area, biocompatibility, and low cost [11]. However, carbon paper has a lower mechanical strength than RGO paper due to its brittleness [7,12]. Carbon paper has been used extensively in the field of bioelectrochemistry to fabricate electrodes for the bioelectrochemical generation of electrical energy via microbial fuel cells[13–16]. Carbon paper electrodes have also been employed in other bioelectrochemical devices such as bioelectric sensors and microbial electrolysis cells[17,18,19].

Microbial electrosynthesis (MES) is a promising bioelectrochemical application in which the greenhouse gas CO_2 is reduced into multicarbon products or methane with electrons derived from the cathode of an electrochemical reactor[20–23]. Until now, multicarbon compounds generated from CO_2 by MES include acetate, butyrate, 2-oxobutyrate, and biofuels[24–26] .MES can be powered by electricity surpluses from the power grid as well as be partially driven by the biological oxidation of wastewater at the

anode[24,27–29,30]. MES reactors can also be integrated into bioinorganic artificial photosynthesis devices aiming at reducing CO_2 with solar energy more efficiently than natural photosynthesis[20,26,31–33].

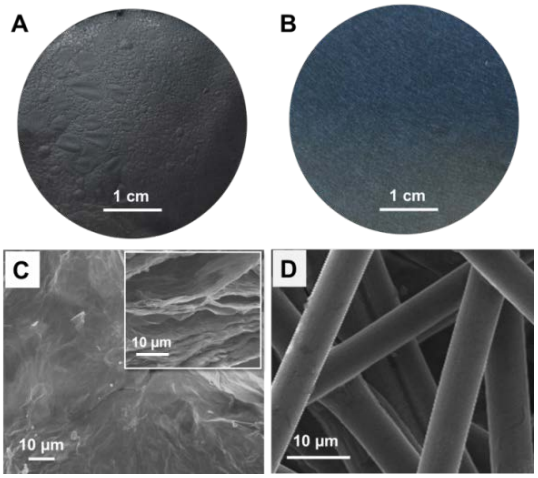

Fig. 2 Digital pictures and SEM images of (A, C) a freestanding RGO paper cathode and (B, D) a freestanding carbon paper cathode. Inset of panel C is a cross-sectional SEM image of RGO paper

To enhance electron transfer rate and productivity of MES reactors, many efforts have focused on the development of high-performance cathode materials, microbial catalysts and growth media [34–41]. To construct an efficient cathode, the ideal material should possess good biocompatibility, high surface area, high durability, low production cost and high electrical conductivity[42].

RGO paper and carbon paper have these favorable characteristics, and thus they are used as cathodes in a MES system with the acetogen *Sporomusa ovata* as the microbial catalyst for the present work. Furthermore, we have investigated the biofilm formation on both RGO and carbon paper electrodes and their electrochemical behavior in detail.

RGO paper tested in MES reactor during this study was fabricated from high-quality graphene oxide (GO) prepared *via* the modified Hummer's method[13] (Experimental details in ESI). UV-vis spectrum of GO showed characteristic peaks at 230 nm due to π-π^* transitions of aromatic C–C bonds and a shoulder peak at ca. 300 nm due to n-π^* transitions of C=O bonds (Fig. S1). Furthermore, the Raman spectrum showed peak shifting around 1400 to 1560 cm^{-1}, which is due to surface defect on the single-layer GO nanosheet (Fig. S1). To synthesize highly-conductive RGO paper, GO paper was first assembled and then reduced with a hydrazine solution and heating process. X-ray photoelectron spectroscopy (XPS) indicated that the reduction of GO paper into RGO paper was successful (Fig.2). The XPS survey spectrum of RGO paper showed a higher C:O ratio than that for GO paper (Fig. S2).

Table 1. Comparison of MES performances with freestanding carbon-based cathodes.[a]

Cathode	Microbial catalyst[b]	Production rate[c] (mmol d^{-1} m^{-2})	Current density[c] (mA m^{-2})	Coulombic efficiency[c] (%)	Reference
RGO paper	*S. ovata*	168.5 ± 22.4	2580 ± 540	90.7 ± 9.3	This work
Carbon paper	*S. ovata*	20.9 ± 5.0	370 ± 100	83.8 ± 4.2	This work
RGO paper	Sterile	N.D.[d]	434± 54	N.A.[e]	This work
Carbon paper	Sterile	N.D.[d]	33 ± 12	N.A.[e]	This work
Carbon cloth	*S. ovata*	22.0 ± 2.0	191 ± 10	82.0 ± 3.0	Chen, 2016
Carbon felt	*S. ovata*	34.1 ± 10.9	400 ± 10	76.6 ± 2.3	Aryal, 2016
Graphite stick	*S. ovata*	33.4 ± 10.8	320 ± 98	85.3 ± 8.3	Tremblay, 2015

[a] MES at a cathode potential of -690 mV vs SHE. [b] *S. ovata* is the wild type strain DSM-2662.
[c] Each value is the mean and standard deviation of three replicates. [d]Not detected. [e]Not applicable.

Furthermore, a supplementary peak corresponding to nitrogen from the hydrazine reduction was observed at ca. 402 eV. The high resolution C1s spectrum from GO paper showed three different peaks centered at 284.2, 286.4, and 288.3 eV, corresponding to C–C in aromatic rings, C–O-C (epoxy and alkoxy), and O-C=O groups, respectively. As expected, the intensity of all peaks corresponding to carbon-oxygen groups, especially the C–O-C peak, decreased significantly for RGO paper, revealing that most oxygen-containing functional groups were removed during the reduction reaction.

During the fabrication process, the thickness of RGO paper was controlled at 0.36 ± 0.02 mm. This is comparable to the 0.37 mm thickness of commercially available carbon paper (AvCarb MGL370). The diameter of 4 cm was also the same for both types of cathode (Fig. 1A-B). Both carbon paper and RGO paper tested here were freestanding and are known to have high electrical conductivity[7,43,44.] Scanning electron microscope (SEM) images of the RGO paper cathode showed a wrinkled and continuous surface structure (Fig. 2C). Cross-sectional SEM image indicated that the RGO paper had a characteristic multilayered arrangement[7] (Fig. 2C inset). In comparison, the carbon paper cathode comprised a network of fibers with relatively smooth surface (Fig 2D). The specific surface area of the RGO paper cathode was 0.29 $m^2 g^{-1}$,

which is 5.4 fold higher than the carbon paper cathode with similar diameter and thickness. Furthermore, contrary to carbon paper, RGO paper can be bent or rolled exhibiting a higher flexibility and durability (Fig. S3). All these characteristics of RGO paper make it a good cathode candidate for MES and could be exploited to increase substantially the electrode surface area available in the MES reactor for electronic interactions with microbes. In recent studies, performance improvement observed for MES reactors equipped with carbon felt or carbon cloth cathodes coated with unfunctionalized or functionalized RGO has been attributed in part to higher specific surface area and electrical conductivity compared to unmodified cathodes[35,36].

With a carbon paper cathode poised at -690 mV versus standard hydrogen electrode (SHE), the acetate production rate from CO_2 of *S. ovata*-driven MES reactors was 20.9 ± 5.0 mmol m^{-2} d^{-1} (Fig. 3A; Table 1). When a RGO paper cathode poised at the same potential was employed, the acetate production rate was increased to 168.5 ± 22.4 mmol m^{-2} d^{-1}, approximately 8-fold enhancement Furthermore, the CO_2 conversion is highly selective, as there were no multicarbon compounds other than acetate produced from CO_2 in noticeable quantity in this study. The current density of 2580 ± 540 mA m^{-2} was 7 fold higher with the RGO paper cathode compared to the

carbon paper cathode (Fig. 3B; Table 1). Coulombic efficiency for the conversion of electrons into acetate was 90.7 ± 9.3% for RGO paper cathode and 83.8 ± 4.2% for carbon paper cathode, respectively (Table 1). The improved MES performance with RGO paper cathode could be attributed to the higher specific surface area and better biocompatibility of RGO papers.

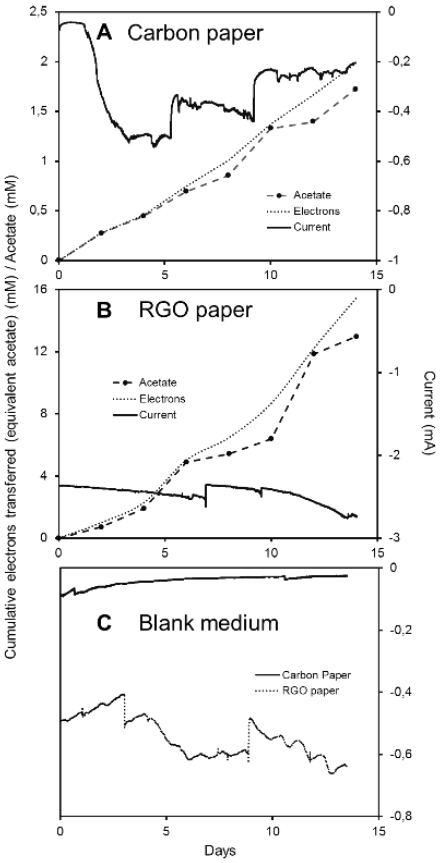

Fig. 3 Acetate concentration, electron transferred and current

consumption during MES with (A) a carbon paper cathode or (B) a RGO paper cathode. (C) Current consumption with carbon paper cathode or RGO paper cathode in sterile medium. The acetate concentration in mM corresponds to the analytical concentration of acetate in the reactor measured from high-pressure liquid chromatography (HPLC). Electron transferred curves measured from potentiostat refer to the acetate concentration in mM if all the electrons transferred were converted to acetate in the system. Results shown are from a representative example of three replicate bioelectrochemical reactors.

In the absence of *S. ovata*, MES reactors with either carbon or RGO paper cathode did not generate any acetate from CO_2 confirming that the MES processes observed in this study were biologically-driven (Fig. 4C). Furthermore, current densities were significantly lower for abiotic MES reactors compared to MES reactors colonized by *S. ovata* for both materials (Table 1). Interestingly, the current density of abiotic MES reactors equipped with RGO paper cathode was 434.4 ± 53.8 mA m^{-2}, which was 13.4-fold higher than abiotic MES reactor equipped with carbon paper cathode (Table 1). This superior current density observed with the abiotic RGO paper-equipped MES reactors is probably related to the higher specific surface area and the outstanding electrical conductivity of this material.

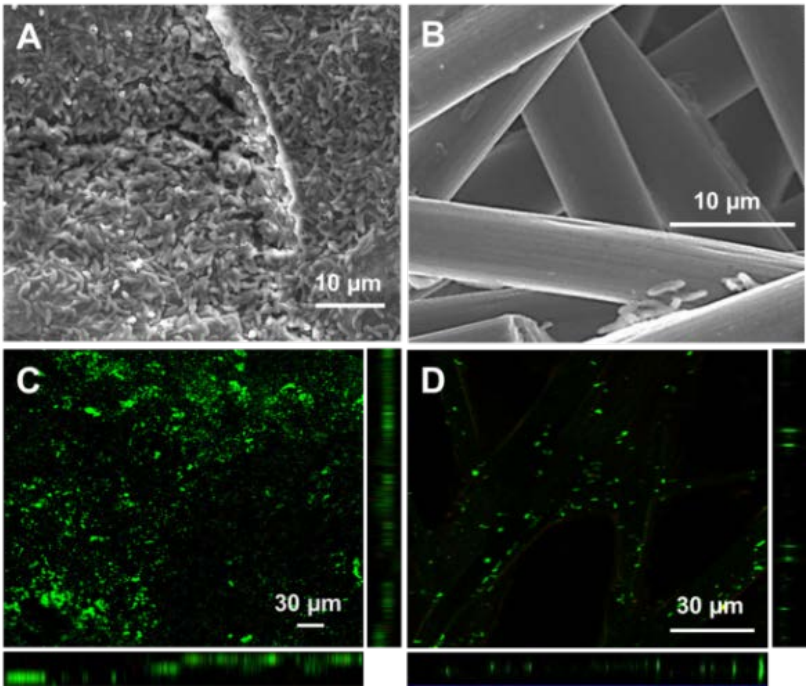

Fig. 4 SEM and CLSM images of (A, C) a freestanding RGO paper cathode and (B, D) a carbon paper cathode in a *S. ovata*-driven MES reactor.

SEM image of RGO paper cathode from a MES system colonized by *S. ovata* and running for 12 days showed a dense biofilm composed of tightly packed bacterial cells (Fig. 4A). In comparison, only scarce and isolated bacterial cells can be observed on the SEM image of the carbon paper cathode coming from a *S. ovata*-driven MES reactor (Fig. 4B). Confocal laser scanning microscopy (CLSM) images confirmed that a more substantial *S. ovata* biofilm

was formed on the RGO paper cathode than on the carbon paper cathode (Fig. 4C-D). The larger number of bacterial cells present at the surface of the RGO paper cathode indicated that this material is more compatible for colonization by *S. ovata* in MES reactors, which led to faster acetate production and higher current density.

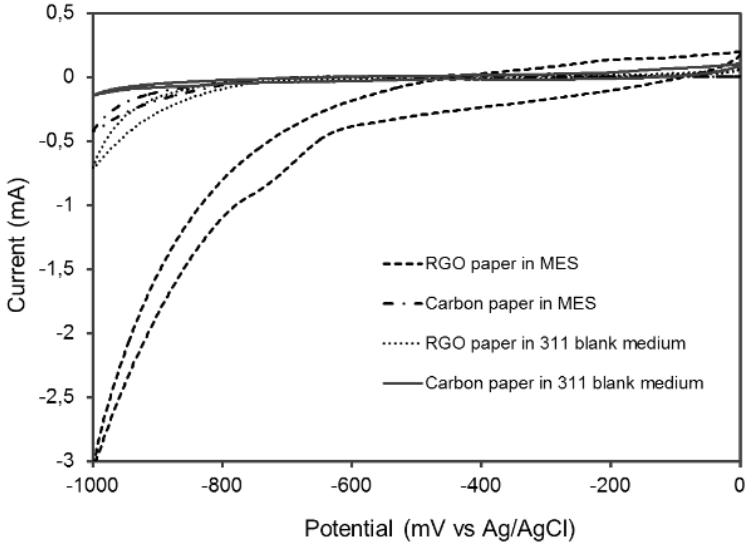

Fig. 5 Cyclic voltammograms obtained at a RGO paper cathode or at a carbon paper cathode in *S. ovata*-driven MES reactor and in sterile blank medium. The potential window was set between -1.0 V to 0 V versus Ag/AgCl at a scan rate of 1 mV s^{-1}.

The electrochemical behavior of RGO and carbon paper cathode before and after colonization by *S. ovata* during MES was investigated with cyclic voltammetry (CV) (Fig. 5). There was no reversible redox peaks detected on the current–potential curves for

all the tested conditions, indicating that no electroactive species were acting as electron shuttles between *S. ovata* and the cathodes. Furthermore, in the presence of a biofilm, the RGO paper cathode exhibited a cathodic current response at -900 mV versus Ag/AgCl ca. 8 fold and 6.7 fold higher than the colonized carbon paper cathode and the sterile control RGO paper cathode, respectively (Fig.4). Additionally, the RGO paper cathode with sterile blank medium also exhibited a higher cathodic current response than either the carbon paper cathode with a biofilm or with sterile blank medium. These results correlated well with what has been observed with the current densities of abiotic or *S. ovata*-driven MES reactors equipped with either a RGO or a carbon paper cathode.

In conclusion, with wild type *S. ovata* as the microbial catalyst and at a cathode potential of -690 mV versus SHE, MES system equipped with RGO paper cathode is more performant than MES systems equipped with other types of freestanding carbonaceous cathode including carbon paper (Table 1). Besides higher acetate production rate and current density (Table 1), RGO paper cathode also has better durability and flexibility that make it possible to be Feld in the MES reactor to increase its surface area and thus improve electron exchange with microbial catalysts. Further experiments are warranted to find novel RGO paper electrode conformation that may

increase the productivity of MES towards practical application.

T.Z. acknowledges financial support by the Novo Nordisk Foundation. Q.C. is grateful to the financial support from DFF-FTP (Project No.12-127447). M.Z. acknowledges the CSC PhD scholarship (No. 201306170047).

Notes and references

1 M. Zhang, A. Halder, C. Hou, J. Ulstrup and Q. Chi, *Bioelectrochemistry*, 2016, **109**, 87–94.

2 H. Gao and H. Duan, *Biosens. Bioelectron.*, 2015, **65**, 404–419.

3 Y. Song, Y. Luo, C. Zhu, H. Li, D. Du and Y. Lin, *Biosens. Bioelectron.*, 2016, **76**, 195–212.

4 M. Carbone, L. Gorton and R. Antiochia, *Electroanalysis*, 2015, **27**, 16–31.

5 A. T. Lawal, *Talanta*, 2015, **131**, 424–443.

6 M. Zhang, C. Hou, A. Halder, H. Wang and Q. Chi, *Mater. Chem. Front.*, 2017, **1**, 37–60.

7 H. Chen, M. B. Müller, K. J. Gilmore, G. G. Wallace and D. Li, *Adv. Mater.*, 2008, **20**, 3557–3561.

8 F. Xiao, Y. Li, H. Gao, S. Ge and H. Duan, *Biosens. Bioelectron.*, 2013, **41**, 417–423.

9 X. Zan, Z. Fang, J. Wu, F. Xiao, F. Huo and H. Duan,

Biosens. Bioelectron., 2013, **49**, 71–78.

10 Y. Wang, J. Ping, Z. Ye, J. Wu and Y. Ying, *Biosens. Bioelectron.*, 2013, **49**, 492–8.

11 M. Zhou, M. Chi, J. Luo, H. He and T. Jin, *J. Power Sources*, 2011, **196**, 4427–4435.

12 J. Wei, P. Liang and X. Huang, *Bioresour. Technol.*, 2011, **102**, 9335–9344.

13 M. Rahimnejad, A. Adhami, S. Darvari, A. Zirepour and S.-E. Oh, *Alexandria Eng. J.*, 2015, **54**, 745–756.

14 S. Jung and J. M. Regan, *Appl. Microbiol. Biotechnol.*, 2007, **77**, 393–402.

15 S. H. A. Hassan, Y. S. Kim and S. E. Oh, *Enzyme Microb. Technol.*, 2012, **51**, 269–273.

16 B. E. Logan and J. M. Regan, *Trends Microbiol.*, 2006, **14**, 512–518.

17 C. J. Yuan, C. L. Wang, T. Y. Wu, K. C. Hwang and W. C. Chao, *Biosens. Bioelectron.*, 2011, **26**, 2858–2863.

18 T. Wang, R. C. Reid and S. D. Minteer, *Electroanalysis*, 2016, **28**, 854–859.

19 H. Liu and S. Grot, 2005, **39**, 4317–4320.

20 D. R. Lovley and K. P. Nevin, *Curr. Opin. Biotechnol.*, 2013, **24**, 385–390.

21 K. P. Nevin, T. L. Woodard and A. E. Franks, *MBio*, 2010,

1, e00103-10.

22 K. Rabaey and R. a Rozendal, *Nat. Rev. Microbiol.*, 2010, **8**, 706–716.

23 P.-L. Tremblay, L. T. Angenent and T. Zhang, *Trends Biotechnol.*, 2016, **xx**, 1–12.

24 P.-L. Tremblay and T. Zhang, *Microb. Physiol. Metab.*, 2015, 201.

25 R. Ganigué, S. Puig, P. Batlle-vilanova and M. D. Balaguer, 2015, 1–4.

26 H. Li, P. H. Opgenorth, D. G. Wernick, S. Rogers, T.-Y. Wu, W. Higashide, P. Malati, Y.-X. Huo, K. M. Cho and J. C. Liao, *Science (80-.).*, 2012, **335**, 1596–1596.

27 Y. Gong, A. Ebrahim, A. M. Feist, M. Embree, T. Zhang, D. Lovley and K. Zengler, 2013.

28 Y. Jiang, M. Su and D. Li, *Appl. Biochem. Biotechnol.*, 2014, **172**, 2720–2731.

29 M. Zeppilli, M. Villano, F. Aulenta, S. Lampis, G. Vallini and M. Majone, *Environ. Sci. Pollut. Res. Int.*, 2015, **22**, 7349–7360.

30 M. Siegert, X. F. Li, M. D. Yates and B. E. Logan, *Front. Microbiol.*, 2015, **6**, 1–12.

31 T. Zhang, *Science (80-.).*, 2015, **350**, 738–739.

32 C. Liu, J. J. Gallagher, K. K. Sakimoto, E. M. Nichols, C. J.

Chang, M. C. Y. Chang and P. Yang, *Nano Lett.*, 2015, **15**, 3634–3639.

33 E. M. Nichols, J. J. Gallagher, C. Liu, Y. Su, J. Resasco, Y. Yu, Y. Sun, P. Yang, M. C. Y. Chang and C. J. Chang, *Proc. Natl. Acad. Sci. U. S. A.*, 2015, **112**, 11461–11466.

34 F. Ammam, P.-L. Tremblay, D. M. Lizak and T. Zhang, *Biotechnol. Biofuels*, 2016, **9**, 163.

35 N. Aryal, A. Halder, P. L. Tremblay, Q. Chi and T. Zhang, *Electrochim. Acta*, 2016, **217**, 117–122.

36 L. Chen, P.-L. Tremblay, S. Mohanty, K. Xu and T. Zhang, *J. Mater. Chem. A*, 2016, **4**, 8395–8401.

37 L. Jourdin, T. Grieger, J. Monetti, V. Flexer, S. Freguia, Y. Lu, J. Chen, M. Romano, G. G. Wallace and J. Keller, *Environ. Sci. Technol.*, 2015, acs.est.5b03821.

38 L. Jourdin, S. Freguia, B. C. Donose, J. Chen, G. G. Wallace, J. Keller and V. Flexer, *J. Mater. Chem. A*, 2014, **2**, 13093.

39 S. Bajracharya, A. ter Heijne, X. Dominguez Benetton, K. Vanbroekhoven, C. J. N. Buisman, D. P. B. T. B. Strik and D. Pant, *Bioresour. Technol.*, 2015.

40 H. Nie, T. Zhang, M. Cui, H. Lu, D. R. Lovley and T. P. Russell, *Phys. Chem. Chem. Phys.*, 2013, **15**, 14290–4.

41 T. Zhang, H. Nie, T. S. Bain, H. Lu, M. Cui, O. L. Snoeyenbos-West, A. E. Franks, K. Nevin, T. P. Russell and

D. Lovley, *Energy Environ. Sci.*, 2013, **6**, 217–224.

42 K. Guo, A. Prévoteau, S. a Patil and K. Rabaey, *Curr. Opin. Biotechnol.*, 2015, **33**, 149–156.

43 S. Zhu, J. H. So, R. Mays, S. Desai, W. R. Barnes, B. Pourdeyhimi and M. D. Dickey, *Adv. Funct. Mater.*, 2013, **23**, 2308–2314.

44 The Fuel cell Store http://www.fuelcellstore.com/ , (accessed January 2017).

Electronic Supplementary Information File

Experimental details

1. The microbial catalyst *Sporomusa ovata*

Sporomusa ovata DSM 2662 wild type strain was acquired from the Deutsche Sammlung Mikroorganismen und Zellkulturen (DSMZ)[1]. *S. ovata* cultures were routinely maintained in the 311 medium with 40 mM betaine as substrate under a N_2-CO_2 (80:20) atmosphere. For growth with H_2 as the electron source and CO_2 as the carbon source, no betaine was added to the 311 medium and the atmosphere was N_2-CO_2-H_2 (83:10:7). For all growth conditions presented in this study, casitone, sodium sulfide, yeast extract, and resazurin were omitted from the 311 medium. For microbial electrosynthesis (MES) experiments, cysteine was also omitted from the 311 medium.

2. Construction of freestanding reduced graphene oxide (RGO) paper cathode

High quality graphene oxide (GO) was synthesized by the modified Hummer's method as previously reported[2,3]. GO solution was then used for the fabrication of RGO paper as described before[4]. Briefly, 50 ml of a 1 mg/ml GO solution was sonicated for 15 minutes before being filtered with a vacuum filtration system. Then, two-

dimensional GO nanosheets were assembled into a flexible layer-by-layer GO paper structure directly on the filter membrane. The thickness and layered structural orientation of the GO paper was tuned by adjusting the volume and the concentration of the GO solution added to the vacuum filtration system. Subsequently, the GO paper was reduced to obtain highly conductive RGO paper. To this end, the GO paper was put in an autoclave container along with a few drops of hydrazine solution and heated at 180 °C overnight. After cooling to room temperature, RGO paper was washed with Milli-Q water several times and annealed further at 200 °C to remove residual hydrazine as well as to enhance its electrical conductivity. After reduction and annealing, the amount of oxygen-containing groups was significantly reduced, as evidenced by the increased C/O ratio measured by X-ray photoelectron spectroscopy (XPS). The resulting RGO paper was cut into discs with a diameter of 4 cm as cathodes.

3. Microbial electrosynthesis of acetate and cyclic voltammetry

RGO paper and AvCarb carbon paper MGL 370 (AvCarb Material Solutions, USA) cathodes were tested at least in triplicate in three-electrode, dual chambered bioelectrochemical reactors. MES experiments were conducted at 25 °C with *S. ovata* DSM-2662

grown in the cathode chamber performing CO_2 reduction to acetate as previously described[5–7]. The RGO paper or carbon paper cathode (4 cm diameter, 0.36-0.37 mm thickness) and graphite stick anode (36 cm^2) were immerged in 250 ml of 311 medium in two chambers separated by a Nafion 115 ion-exchange membrane (Ion Power, Inc., New Castle, DE, USA). The reference electrode was a sealed miniature Ag/AgCl electrode model ET072 (eDAQ, Denmark) and the cathode potential was set at –690 mV versus SHE during MES. H_2-grown *S. ovata* cultures were established in the cathode chamber with a hydrogen-containing gas mix N_2-CO_2-H_2 (83:10:7). The gas mix was switched to N_2-CO_2 (80:20) after several fresh medium swaps at which point data start being collected. During the whole MES experiment, the anode chamber was bubbled with N_2-CO_2. A CH Instrument potentiostat (CH Instruments, Inc, USA) was used to perform both MES as well as cyclic voltammetry (CV) experiments. During the CV experiments, the tested electrodes were scanned at a rate of 1 mV s^{-1} in a potential window of 0 to -1000 mV vs Ag/AgCl. Data generated during MES and CV experiments were analyzed with EC-Lab® software v.10.40 as described previously[8–10].

4. High-pressure liquid chromatography

Acetate concentration were measured by high-performance liquid chromatography (HPLC) with an apparatus equipped with a HPX-87H anion exchange column (Bio-Rad Laboratories Inc., California, USA) at a temperature of 30 °C. The mobile phase was 5 mM H_2SO_4 at a flow rate of 0.6 ml/min. Refractive index detector was used for the detection and data were analyzed with the Chromeleon software (Thermo Fisher Scientific, Denmark). Where indicated, acetate production rate was normalized with respect to the projected area of RGO paper or carbon paper cathodes.

5. Microscopy

For Scanning Electron Microscopy (SEM) images, cathode samples were collected and fixed during 5 hours at room temperature with a 0.1M phosphate buffer at pH 7.0 containing 2.5% glutaraldehyde. Samples were then washed with the buffer solution without glutaraldehyde before being immerged successively in different concentration of ethanol and acetonitrile as described previously[6]. Nitrogen-dried samples were observed with a Quanta 200 FEG scanning electron microscope (FEI) at an accelerating voltage of 10 V under high vacuum condition. For Confocal Laser Scanning Microscopy (CLSM) images, RGO paper and carbon paper biocathodes were removed from the MES reactor and were stained

with the LIVE/DEAD® BacLight™ Bacterial Viability Kit (ThermoFisher Scientific) as described previously[6]. CLSM image were taken with a Zeiss LSM 5 Pascal microscope and analyzed with the ZEN imaging software (Zeiss, Germany).

6. Analytical methods

Specific surface area of RGO paper or carbon paper cathodes was determined with the Brunauer–Emmett–Teller (BET) method as previously described[8]. The Agilent 8453 G1103A spectrophotometer (Agilent, Denmark) was used to measure the UV-vis spectrum of the GO solution. X-ray photoelectron spectroscopy (XPS) was performed with a Thermo Scientific™ K-Alpha™⁺ X-ray Photoelectron Spectrometer System with an aluminum K-Alpha (1486 eV) as x-ray source. All the samples were deposited on polished Si-wafer by drop casting for XPS measurements. X-ray spot area for measurement was set at 400 μm and flood gun was used for charge compensation.

7. Supporting data

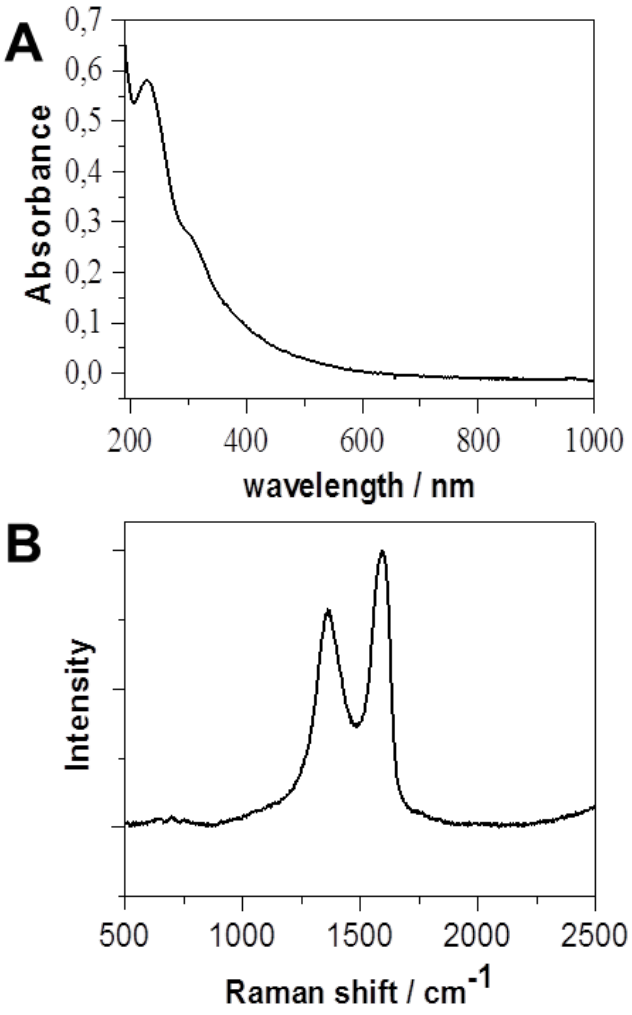

Figure S1. (A) UV-vis and (B) Raman spectra of GO.

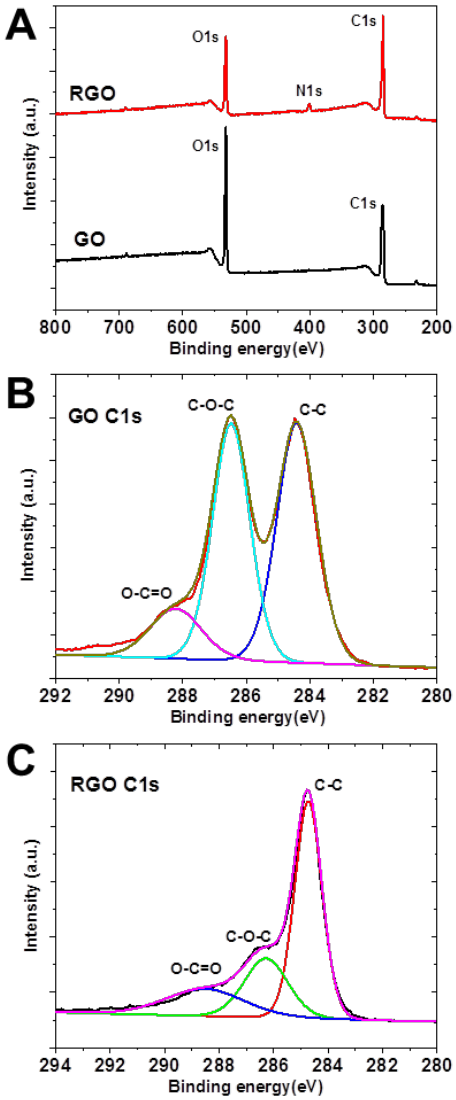

Figure S2. (A) The XPS survey spectra for GO and RGO. The high resolution C 1s spectra for (B) GO and (C) RGO.

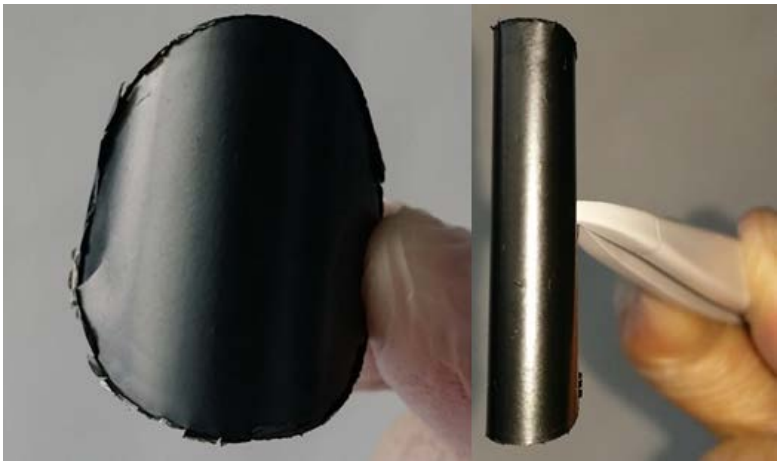

Figure S3. Bent RGO papers for demonstrating their mechanical flexibility.

8. References

1 E. Smith and A. Badawy, *Water Sci. Technol.*, 2010, **61**, 2251–8.

2 N. Aryal, A. Halder, P. L. Tremblay, Q. Chi and T. Zhang, *Electrochim. Acta*, 2016, **217**, 117–122.

3 N. Zhu, S. Han, S. Gan, J. Ulstrup and Q. Chi, *Adv. Funct. Mater.*, 2013, **23**, 5297–5306.

4 M. Zhang, A. Halder, C. Hou, J. Ulstrup and Q. Chi, *Bioelectrochemistry*, 2016, **109**, 87–94.

5 P.-L. Tremblay, D. Höglund, A. Koza, I. Bonde and T. Zhang, *Sci. Rep.*, 2015, **5**, 16168.

6 T. Zhang, H. Nie, T. S. Bain, H. Lu, M. Cui, O. L. Snoeyenbos-

West, A. E. Franks, K. Nevin, T. P. Russell and D. Lovley, *Energy Environ. Sci.*, 2013, **6**, 217–224.

7 K. P. Nevin, T. L. Woodard and A. E. Franks, *MBio*, 2010, **1**, e00103-10.

8 R. Poreddy, C. Engelbrekt and A. Riisager, *Catal. Sci. Technol.*, 2015, **5**, 2467–2477.

9 M. Sharma, N. Aryal, P. M. Sarma, K. Vanbroekhoven, B. Lal, X. D. Benetton and D. Pant, *Chem. Commun.*, 2013, **49**, 6495–6497.

10 G. Lepage, G. Perrier, G. Merlin, N. Aryal and X. Dominguez-Benetton, *RSC Adv.*, 2014, **4**, 23815.

Chapter 3.2

3.2 Enhanced microbial electrosynthesis with 3D-graphene functionalized cathodes through solvothermal grapheme synthesis.

Authors:
Nabin Aryal,[1] Arnab Halder,[2] Pier-Luc Tremblay,[1,3] Qijin Chi,[2] Tian Zhang[*,1,3]

Affiliation:
[1]The Novo Nordisk Foundation Center for Biosustainability, Technical University of Denmark, DK-2970 Hørsholm, Denmark.

[2]Department of Chemistry, Technical University of Denmark, DK-2800 Kongens Lyngby, Denmark.

[3]School of Chemistry, Chemical Engineering and Life Science, Wuhan University of Technology, Wuhan 430070, PR China

Keywords: Biolectrochemical system, Carbon dioxide fixation, Cathode electrode, Graphene, Microbial electrosynthesis

Electrochimica Acta 217 (2016) 117–122

Contents lists available at ScienceDirect

Electrochimica Acta

journal homepage: www.elsevier.com/locate/electacta

Enhanced microbial electrosynthesis with three-dimensional graphene functionalized cathodes fabricated *via* solvothermal synthesis

Nabin Aryal[a], Arnab Halder[b], Pier-Luc Tremblay[a,c], Qijin Chi[b], Tian Zhang[a,c,*]

[a] The Novo Nordisk Foundation Center for Biosustainability, Technical University of Denmark, DK-2970 Hørsholm, Denmark
[b] Department of Chemistry, Technical University of Denmark, DK-2800 Kongens Lyngby, Denmark
[c] School of Chemistry, Chemical Engineering and Life Science, Wuhan University of Technology, Wuhan 430070, PR China

ARTICLE INFO

Article history:
Received 30 July 2016
Received in revised form 11 September 2016
Accepted 12 September 2016
Available online 15 September 2016

Keywords:
Biolectrochemical system
Carbon dioxide fixation
Cathode electrode
Graphene
Microbial electrosynthesis

ABSTRACT

The biological reduction of CO_2 into multicarbon chemicals can be driven by electrons derived from the cathode of a bioelectrochemical reactor via microbial electrosynthesis (MES). To increase MES productivity, conditions for optimal electron transfer between the cathode and the microbial catalyst must be implemented. Here, we report the development of a 3D-graphene functionalized carbon felt composite cathode enabling faster electron transfer to the microbial catalyst *Sporomusa ovata* in a MES reactor. Modification with 3D-graphene network increased the electrosynthesis rate of acetate from CO_2 by 6.8 fold. It also significantly improved biofilm density and current consumption. A 2-fold increase in specific surface area of the 3D-graphene/carbon felt composite cathode explained in part the formation of more substantial biofilms compared to untreated control. Furthermore, in cyclic voltammetry analysis, 3D-graphene/carbon felt composite cathode exhibited higher current response. The results indicate that the development of a 3D-network cathode is an effective approach to improve microbe-electrode interactions leading to productive MES systems.

1. Introduction

Microbial electrosynthesis (MES) is an attractive strategy for the conversion of the greenhouse gas CO_2 into multicarbon products or methane with electrons derived from the cathode of a bioelectrochemical system (BES) [1–3]. MES reactors can be powered by an external source of electricity generated from renewable energy. Under these circumstances, one of the purposes of MES is to store electricity surpluses associated with intermittent energy sources such as wind and solar into useful products [4,5]. Interestingly, when a MES reactor is powered by solar cells or when the MES electrodes are modified to enable the direct capture of light energy, it effectively becomes an artificial photosynthesis apparatus with potentially higher solar-to-product efficiency than natural photosynthesis [1,6–9]. MES can also be driven by the biological oxidation of pollutants at the anode effectively coupling the production of useful chemicals at the cathode with environment cleaning processes. Experimental demonstrations include sulfide removal and wastewater polishing in a bioanodic chamber generating electrons used by a microbial catalyst at the cathode to reduce CO_2 to methane or acetate [10–12].

One of the key steps of the MES process is the transfer of electrons from cathode to microbe. Successful strategies focusing on the cathode have been developed to improve electron transfer rates and production rates [4]. These include modifications of the spatial arrangement as well as of the surface of carbonaceous cathodes [13–17]. For instance, carbon cloth cathode coated with chitosan became positively charged and thus more suitable for interactions with negatively-charged microbes as demonstrated by higher cell density, electron transfer rates and acetate production rates [16]. Other cathode modifications including treatments with metallic nanoparticles, nickel nanowires or carbon nanotubes resulted in better MES performance because of better catalytic properties, enhanced surface-area-to-volume ratio and increased porosity [14–17].

* Corresponding author at: Technical University of Denmark, Novo Nordisk Foundation Center for Biosustainability, Kogle Alle 6, DK - 2970 Hørsholm, Denmark.
E-mail addresses: zhang@biosustain.dtu.dk, zhangdtu@gmail.com (T. Zhang).

http://dx.doi.org/10.1016/j.electacta.2016.09.063
0013-4686/

Graphene is a two-dimensional and one-atom-thick carbon material. This material has many extraordinary properties, including high electronic conductivity, low charge-transfer resistance, large specific surface area, exceptional mechanical strength and biocompatibility [18–20], which could be used to augment electron transfer rate in MES system. This has been demonstrated recently with improved MES performance observed with a carbon cloth-based biocathode modified by the injection of graphene functionalized with positively-charged tetraethylenepentamine (TEPA) [21].

Three-dimensional graphene (3D-G) formed by the coating of graphene nanosheets on a scaffold has even higher specific surface and catalytic activity [22–27]. To investigate the impact of 3D-G on MES, carbon felt (CF) cathode coated with 3D-G was fabricated *via* a solvothermal synthesis process and used to transfer electrons to a pure culture of the highly-efficient MES microbial catalyst *Sporomusa ovata* [28] for the reduction of CO_2 into acetate.

2. Experimental

2.1. Organism source and growth conditions

Sporomusa ovata DSM 2662 [29] was acquired from the Deutsche Sammlung Mikroorganismen und Zellkulturen (DSMZ). *S. ovata* strains were routinely maintained in 311 medium with 40 mM betaine as substrate under a N_2-CO_2 (80:20) atmosphere. For growth with H_2 as the electron source and CO_2 as the carbon source, no betaine was added to the 311 medium and the atmosphere was N_2-CO_2-H_2 (83:10:7). For all growth conditions presented in this study, casitone, sodium sulfide, yeast extract, and resazurin were omitted from the 311 medium. For bioelectrochemical experiments, cysteine was also omitted from the 311 medium.

2.2. Synthesis of graphene oxide (GO)

GO was prepared by a two-step synthetic procedure as reported previously [30,31]. Pre-oxidized graphite was prepared in the first step and in the next step GO was obtained through exfoliation and strong oxidation. In the first step, graphite powder (10 g) was added to a concentrated H_2SO_4 solution (7.5 ml) containing $K_2S_2O_8$ (2.5 g) and P_2O_5 (2.5 g) and kept in a hot water bath (80 °C) under strong stirring for 3 hours. After being cooled down to room temperature, the dark green mixture was diluted with Milli-Q water. The mixture was then filtered before being washed several times with Milli-Q water until the washed out solution had a neutral pH. The pre-oxidized graphite powder was then collected and air-dried overnight at room temperature.

In the second step, pre-oxidized graphite powder (1.0 g) was added to H_2SO_4 solution (25 ml) and maintained at 0 °C. $KMnO_4$ (3.0 g) was added to the mixture under slow stirring while the temperature was below 20 °C. The mixture was then heated at 35 °C under continuous stirring for 2 hours before the addition of Milli-Q water (46 ml). After two minutes, a 0.5% H_2O_2 (140 ml) solution was added to the mixture and the solution color changed immediately to bright yellow. The mixture was filtered and then the retained material was washed thoroughly with 10% HCl solution (250 ml) to remove residual metal ions. The filtered-out material was resuspended into Milli-Q water before being centrifuged at 12000 rpm in a benchtop centrifuge. The supernatant containing highly dispersed and stable GO nanosheets was collected. To remove residual salts and acids, the sample was dialyzed using a dialysis tube (cut-off molecular weight of 12-14 KDa) for one week by regularly replacing the water in a water bath with fresh Milli-Q water 4 times per day.

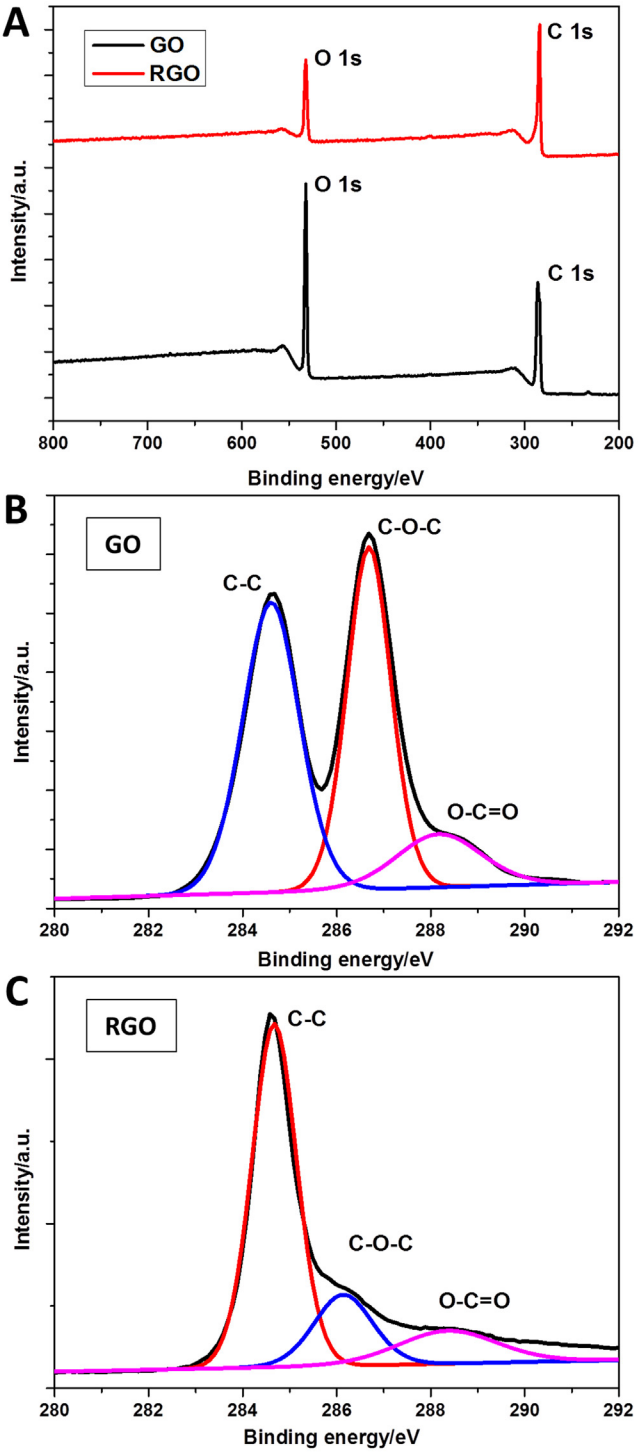

Fig. 1. Comparison of XPS spectra of GO and RGO with the survey spectra (A) and the C 1 s XPS spectra (B-C).

2.3. Reduction of GO and fabrication of 3D-graphene (3D-G) cathode electrodes

CF electrodes (Jiangsu Tongkang Special Activated Carbon Fiber & Fabric Co., Ltd, China) were pretreated with 3 M HNO_3 for 12 hours and then extensively washed with Milli-Q water [16]. The acid treated electrodes were dried by nitrogen gas flow, prior to modification with 3D-G.

The biocompatible reduction of GO and the fabrication of 3D-G coated CF cathode was done in a single step *via* a solvothermal

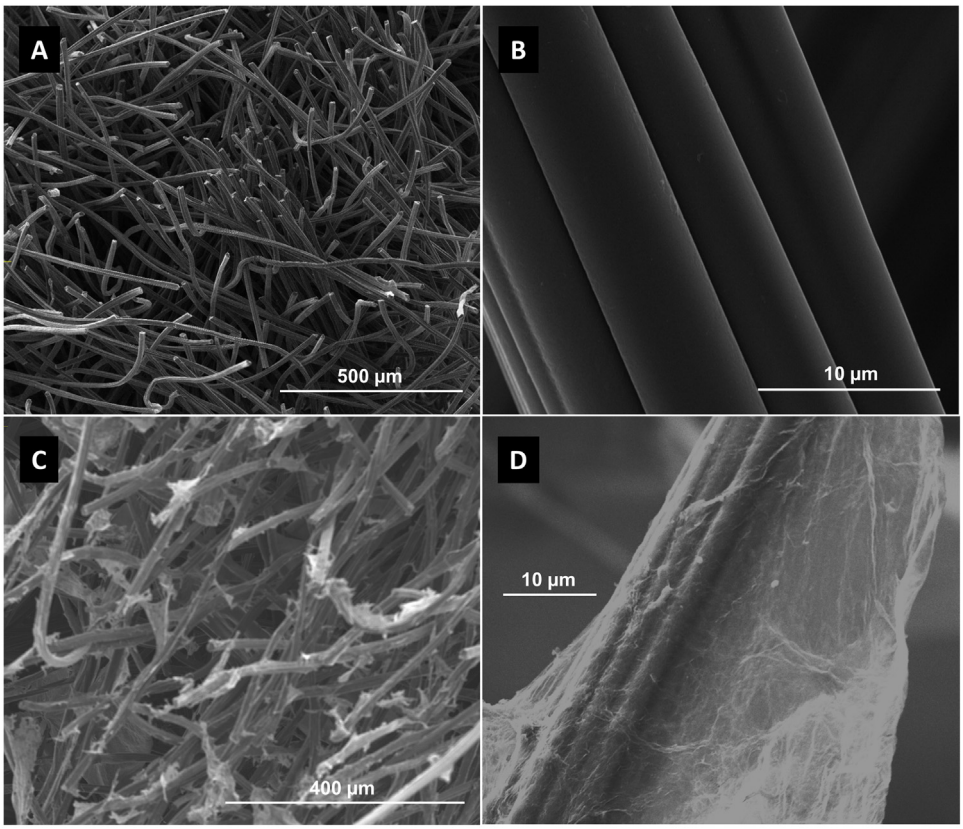

Fig. 2. SEM images (A and B) low- and high-magnification of unmodified CF cathode, and (C and D) low- and high-magnification of 3D-G-CF cathode.

synthesis process. Briefly, a pre-synthesized 60 ml (0.5 mg/ml) GO solution was mixed with 30 mg of ascorbic acid, and the mixture was then sonicated for 10 minutes. The pre-treated CF was then soaked in the GO solution and incubated at 160 °C in an oven for 12 h. During this incubation, GO was reduced and assembled into the pores of the CF to create a 3D-G network. The 3D-G coated CF was washed with Milli-Q water several times to remove loosely-bound RGO sheets and excess ascorbic acid. The 3D-G coated CF materials were dried in vacuum for 4 days before use for MES and electrochemical experiments.

2.4. Microbial electrosynthesis (MES) of acetate from CO_2 and cyclic voltammetry (CV)

The cathode materials were tested at least in triplicate in three-electrode, dual chambered reactors that were operated at room temperature with *S. ovata* grown in the cathode chamber performing CO_2 reduction to acetate by MES as previously described [2,16]. The CF-based cathodes (22.5 cm^2) and graphite stick anode (36 cm^2) were immerged in 250 ml of 311 media in two chambers separated by a Nafion 115 ion-exchange membrane (Ion Power, Inc., New Castle, DE, USA). The experiments were performed with a CH Instrument potentiostat (CH Instruments, Inc, USA) and the cathode potential was set at −690 mV versus SHE. H_2-grown *S. ovata* cultures were established in the cathode chamber with a hydrogen-containing gas mix N_2-CO_2-H_2 (83:10:7). The gas mix was switched to N_2-CO_2 (80:20) after several fresh medium swaps at which point data start being collected. During the whole experiment, the anode chamber was bubbled with N_2-CO_2.

The cyclic voltammetry experiments were performed at the end of the MES experiments with applied potentials from −0.8 to 0.2 V vs Ag/AgCl reference electrode with a scan rate of 1 mV s^{-1}. The solution was purged with N_2 for at least 30 min before

Table 1
Average rate of acetate production from CO_2 and current consumption density of MES.

Cathode	Acetate production[a] g L^{-1} h^{-1} m^{-2}	mM m^{-2} day^{-1}[b]	mM day^{-1}	Current density[a] (mA m^{-2})	Coulombic efficiency (%)
Sterile CF	n.d.[c]	n.d.[c]	n.d.[c]	80 ± 40	NA[d]
Sterile 3D-G-CF	n.d.[c]	n.d.[c]	n.d.[c]	140 ± 40	NA[d]
CF with *S. ovata*	0.34 ± 0.11	136.5 ± 43.5	0.31 ± 0.10	400 ± 100	76.6 ± 2.3
3D-G-CF with *S. ovata*	2.28 ± 0.07	925.5 ± 29.4	2.08 ± 0.07	2450 ± 160	86.5 ± 3.2

[a] Each value is the mean and standard deviation of three replicates.
[b] Values normalized with respect to the CF-based cathodes projected surface area.
[c] Not detected.
[d] Not applicable.

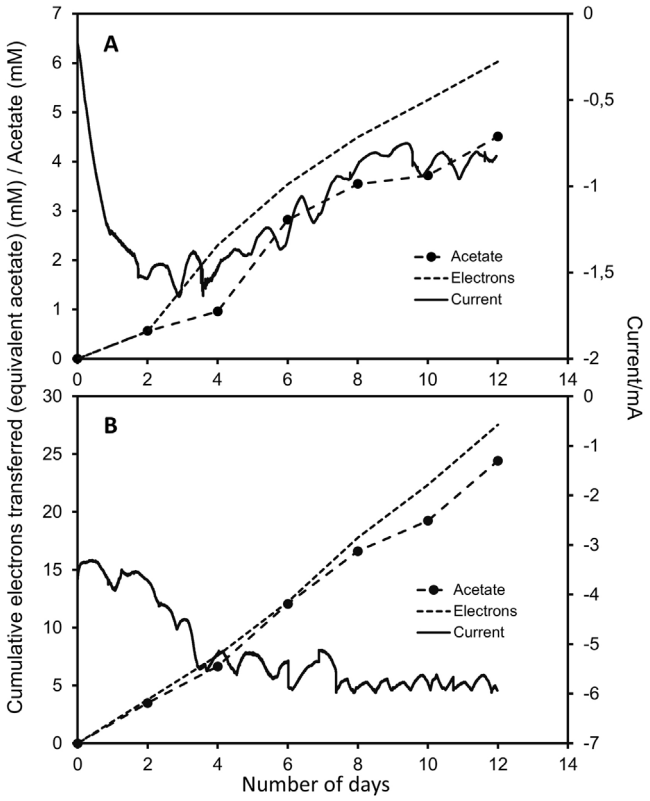

Fig. 3. Electron transferred, acetate and current consumption with (A) the unmodified CF cathode and (B) the 3D-G-CF cathode. Electron transferred curves correspond to the acetate concentration in mM if all the electrons transferred were converted to acetate. Acetate production curves in mM correspond to the real progression of acetate concentration in the MES reactor detected by high-pressure liquid chromatography. Results shown are from a representative example of three replicate MES reactors.

electrochemical measurements. CO_2 was omitted from the gas mix to avoid its electrochemical reduction.

2.5. Analytical methods

Acetate was measured with High Performance Liquid Chromatography (HPLC) as previously described [28]. Where indicated, acetate production rate was normalized with respect to the projected area of CF-based cathodes. The electrochemical data were processed with the EC-Lab® software v.10.40, with data imported as text files from a CH Instrument potentiostat. The LIVE/DEAD® BacLight™ Bacterial Viability Kit (ThermoFisher Scientific) was used to stain *S. ovata* cells at the surface of cathodes and Confocal Laser Scanning Microscopy (CLSM) images were taken with a LSM5 Pascal laser scanning microscope (Zeiss). For Scanning Electron Microscopy (SEM) image, cathode samples were collected and fixed overnight with a buffered solution (0.1 M phosphate buffer, pH 7.0) containing 2.5% glutaraldehyde at room temperature. Samples were washed with the buffer solution without glutaraldehyde before being immerged successively in different concentration of ethanol and acetonitrile as described previously [16]. Air-dried samples were observed with a Quanta 200 FEG scanning electron microscope (FEI) at an accelerating voltage of 15 V under high vacuum condition. CLSM and SEM images presented in this study at Figs. 2 and 4 are representative of at least 3 samples. Specific surface area of cathode samples was determined by the Brunauer–Emmett–Teller (BET) method as previously described [32]. X-ray photoelectron spectroscopy (XPS) was performed with a Thermo Scientific™ K-Alpha™+ X-ray Photoelectron Spectrometer System with an aluminum K-Alpha (1486 eV) as x-ray source. All the samples were deposited on polished Si-wafer by drop casting for XPS measurements. X-ray spot area for measurement was set at 400 μm and flood gun was used for charge compensation.

3. Results and discussion

3.1. Fabrication and characterization of the 3D-graphene carbon felt cathode (3D-G-CF)

Graphene oxide (GO) was reduced (RGO) via a biocompatible method with ascorbic acid as reducing agent [33] to provide an optimal microenvironment for *S. ovata*. Reduction of GO was successful as indicated by the lower C/O ratio detected by X-ray photoelectron spectroscopy (XPS) as well as by the weakened intensities of all the C1 s peaks corresponding to carbon molecules binding to oxygen (Fig. 1). SEM indicates that after the solvothermal synthesis process a 3D-G network was formed with RGO nanosheets on the carbon felt substrate (Fig. 2). The unmodified CF consists of large quantities of carbon fibers with smooth surface area (Fig. 2A and B), while 3D-G modified CF is formed of carbon fibers coated with crumpled paper-like RGO sheets (Fig. 2C and D). The specific surface area measured with the BET method was increased by 2.2-fold with 3D-G-CF composite (surface area of 2.99 $m^2 g^{-1}$) compared to untreated CF (surface area of 1.36 $m^2 g^{-1}$).

3.2. Microbial electrosynthesis of acetate from CO_2 with the 3D-G-CF cathode

Production of acetate from CO_2 by *S. ovata*-driven MES reactors equipped with the newly-developed 3D-G-CF composite cathode was increased by 6.8 fold compared to MES reactors equipped with unmodified CF (Table 1; Fig. 3). The acetate production rate of 3D-G-CF MES reactors per m^{-2} of electrode surface was 925.5 ± 29.4 mM day^{-1} (n = 3). Average current consumption density was also improved accordingly by 6.1 fold to 2450 ± 160 mA m^{-2} (n = 3) with a better coulombic efficiency of 86.5% ± 3.2% (n = 3) than that of the unmodified CF cathode of 76.6% ± 2.3% (n = 3). No acetate production was detected in abiotic MES systems equipped with an unmodified CF cathode or a 3D-G-CF cathode and their abiotic current density was only 80 ± 40 mA m^{-2} (n = 3) and 140 ± 30 mA m^{-2} (n = 3), respectively (Table 1).

3.3. Biofilm formation on the 3D-G-F cathode

SEM image of the 3D-G-CF composite cathode from a MES reactor running for 12 days shows significantly higher density of bacterial cells compared to the unmodified CF cathode (Fig. 4A, C). CLSM with live bacteria stained in green also confirmed that a more considerable *S. ovata* biofilm was present at the surface of the 3D-G-CF cathode (Fig. 4B, D). These observations combined with the increased BET surface area of 3D-G-CF cathode clearly indicate that a greater number of bacterial cells are attached to 3D-G-CF electrodes increasing the quantity of electronic interactions and leading to significantly enhanced current consumption and acetate production rates.

3.4. Cyclic voltammetry analysis

Cyclic voltammetry (CV) was performed in MES reactor to investigate the electrochemical behavior of 3D-G-CF cathode during acetate electrosynthesis. As shown by cyclic voltammograms in Fig. 5, a similar pair of redox peaks featured with weak

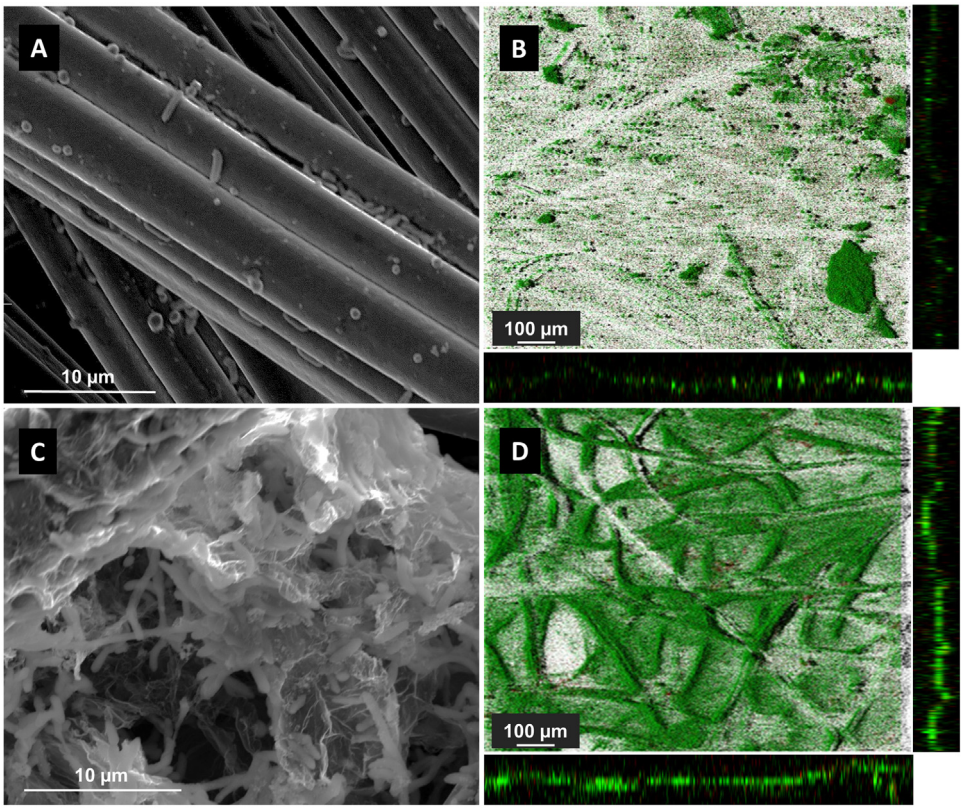

Fig. 4. SEM and CLSM images of (A, B) a CF cathode and (C, D) a 3D-G-CF cathode in a *S. ovata*-driven MES reactor.

current signals and broaden shape is observed for all the tested conditions. Although the redox potentials vary slightly with the experimental conditions, all the oxidation peaks follow in the range of −0.35 V to −0.1 V and all the reduction peaks appear around −0.3 V. These observations strongly suggest that there were no electroactive species involved in electron transport processes of *S. ovata*-driven MES, although the mechanistic detail of electron transfer is not fully understood. More importantly, 3D-G-CF composite cathode exhibited a higher cathodic current response than the CF cathode in the potential scan range of −0.8 V to 0.2 V (Fig. 5). This observation in combination with the higher specific surface area and higher current draw during MES with the 3D-G-CF cathode indicates that the 3D-G network formed on the CF substrate created more electroactive sites for microbially-catalyzed reaction in MES, resulting in an increased electron-exchange capacity.

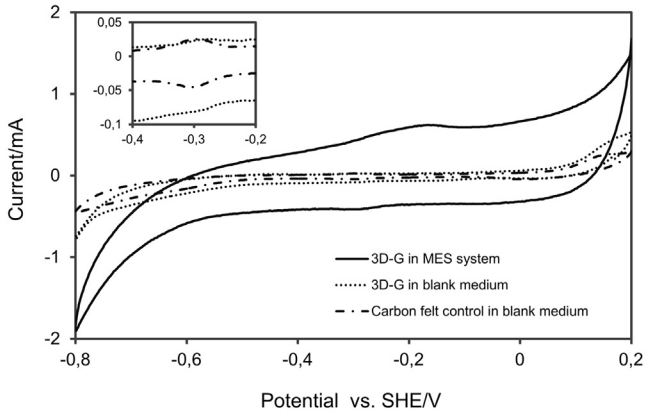

Fig. 5. Cyclic voltammograms obtained at a 3D-G-CF electrode in S. ovata-driven MES reactor and in sterile blank medium, and at the untreated carbon felt electrode in sterile blank medium. The inset is the cyclic voltammograms of both electrodes in sterile blank medium in the potential window of −0.4 V to −0.2 V. Scan rate: 1 mV s^{-1}.

4. Conclusions

The study presented here demonstrated that functionalizing the cathode of a *S. ovata*-driven MES system with 3D-G enhances significantly current consumption density and chemicals production rates. CV analysis, SEM and CLSM images show that the improved performance of MES systems equipped with 3D-G-CF composite cathodes is due to an augmentation of the electrode surface area available for electron exchange with microbes, a higher electronic conductivity and the formation of a more substantial biofilm. These results are in accordance with other bioelectrochemical studies where bioelectrodes modified with 3D-G are more performant for power generation *via* microbial fuel cells (MFCs). In those MFC reactors, 3D-G is thought to improve specific surface area and conductivity of the electrode as well as the strength of electrostatic interactions between the electrode and the microbes resulting in stronger bacterial adhesion [19,26,34,35].

Besides productivity, the integration of 3D-G composite cathode in MES reactor would be particularly attractive in terms of cost-effectiveness, since graphene production cost by wet-chemical methods is much lower than other carbon nanomaterials such as carbon nanotubes used to improve the performance of MES cathodes [15,36,37]. This is one of the key reasons why graphene is an attractive material for various applications such as solar cells, batteries and biosensors [37]. Unfunctionalized 3D-G would also

be a more cost-effective material than TEPA-modified graphene for the fabrication of cathode for high-performance MES [21]. Hence, the production rates observed with the 3D-G-CF cathode as well as the associated reduced cost are promising for the potential industrial development of MES technology.

Acknowledgements

T.Z. acknowledges financial support by the Novo Nordisk Foundation. Q.C. is grateful to the financial support from DFF-FTP (Project No. 12-127447).

References

[1] D.R. Lovley, K.P. Nevin, Electrobiocommodities: powering microbial production of fuels and commodity chemicals from carbon dioxide with electricity, Curr. Opin. Biotechnol. 24 (2013) 385–390, doi:http://dx.doi.org/10.1016/j.copbio.2013.02.012.
[2] K.P. Nevin, T.L. Woodard, A.E. Franks, Z.M. Summers, D.R. Lovley, Microbial electrosynthesis: feeding microbes electricity to convert carbon dioxide and water to multicarbon extracellular organic compounds, mBio 1 (2010), doi:http://dx.doi.org/10.1128/mBio. 00103-10.
[3] K. Rabaey, R.A. Rozendal, Microbial electrosynthesis — revisiting the electrical route for microbial production, Nat. Rev. Microbiol. 8 (2010) 706–716, doi:http://dx.doi.org/10.1038/nrmicro2422.
[4] P.-L. Tremblay, T. Zhang, Electrifying microbes for the production of chemicals, Front. Microbiol. 6 (2015) 201, doi:http://dx.doi.org/10.3389/fmicb.2015.00201.
[5] L. Jürgensen, E.A. Ehimen, J. Born, J.B. Holm-Nielsen, Utilization of surplus electricity from wind power for dynamic biogas upgrading: Northern Germany case study, Biomass Bioenergy 66 (2014) 126–132, doi:http://dx.doi.org/10.1016/j.biombioe.2014.02.032.
[6] E.M. Nichols, J.J. Gallagher, C. Liu, Y. Su, J. Resasco, Y. Yu, Y. Sun, P. Yang, M.C.Y. Chang, C.J. Chang, Hybrid bioinorganic approach to solar-to-chemical conversion, Proc. Natl. Acad. Sci. U. S. A. 112 (2015) 11461–11466, doi:http://dx.doi.org/10.1073/pnas.1508075112.
[7] C. Liu, B.C. Colón, M. Ziesack, P.A. Silver, D.G. Nocera, Water splitting–biosynthetic system with CO_2 reduction efficiencies exceeding photosynthesis, Science 352 (2016) 1210–1213, doi:http://dx.doi.org/10.1126/science.aaf5039.
[8] C. Liu, J.J. Gallagher, K.K. Sakimoto, E.M. Nichols, C.J. Chang, M.C.Y. Chang, P. Yang, Nanowire-bacteria hybrids for unassisted solar carbon dioxide fixation to value-added chemicals, Nano Lett. 15 (2015) 3634–3639, doi:http://dx.doi.org/10.1021/acs.nanolett.5b01254.
[9] T. Zhang, More efficient together, Science 350 (2015) 738–739, doi:http://dx.doi.org/10.1126/science.aad6452.
[10] S. Cheng, D. Xing, D.F. Call, B.E. Logan, Direct Biological Conversion of Electrical Current into Methane by Electromethanogenesis, Environ. Sci. Technol. 43 (2009) 3953–3958, doi:http://dx.doi.org/10.1021/es803531g.
[11] Y. Gong, A. Ebrahim, A.M. Feist, M. Embree, T. Zhang, D. Lovley, K. Zengler, Sulfide-driven microbial electrosynthesis, Environ. Sci. Technol. 47 (2013) 568–573, doi:http://dx.doi.org/10.1021/es303837j.
[12] M. Villano, F. Aulenta, C. Ciucci, T. Ferri, A. Giuliano, M. Majone, Bioelectrochemical reduction of CO(2) to CH(4) via direct and indirect extracellular electron transfer by a hydrogenophilic methanogenic culture, Bioresour. Technol. 101 (2010) 3085–3090, doi:http://dx.doi.org/10.1016/j.biortech.2009.12.077.
[13] E.V. LaBelle, C.W. Marshall, J.A. Gilbert, H.D. May, Influence of Acidic pH on Hydrogen and Acetate Production by an Electrosynthetic Microbiome, PLoS ONE 9 (2014) e109935, doi:http://dx.doi.org/10.1371/journal.pone.0109935.
[14] L. Jourdin, S. Freguia, B.C. Donose, J. Chen, G.G. Wallace, J. Keller, V. Flexer, A novel carbon nanotube modified scaffold as an efficient biocathode material for improved microbial electrosynthesis, J. Mater. Chem. A 2 (2014) 13093–13102, doi:http://dx.doi.org/10.1039/C4TA03101F.
[15] L. Jourdin, T. Grieger, J. Monetti, V. Flexer, S. Freguia, Y. Lu, J. Chen, M. Romano, G.G. Wallace, J. Keller, High Acetic Acid Production Rate Obtained by Microbial Electrosynthesis from Carbon Dioxide, Environ. Sci. Technol. 49 (2015) 13566–13574, doi:http://dx.doi.org/10.1021/acs.est.5b03821.
[16] T. Zhang, H. Nie, T.S. Bain, H. Lu, M. Cui, O.L. Snoeyenbos-West, A.E. Franks, K.P. Nevin, T.P. Russell, D.R. Lovley, Improved cathode materials for microbial electrosynthesis, Energy Environ. Sci. 6 (2013) 217–224, doi:http://dx.doi.org/10.1039/C2EE23350A.
[17] H. Nie, T. Zhang, M. Cui, H. Lu, D.R. Lovley, T.P. Russell, Improved cathode for high efficient microbial-catalyzed reduction in microbial electrosynthesis cells, Phys. Chem. Chem. Phys. 15 (2013) 14290–14294, doi:http://dx.doi.org/10.1039/c3cp52697f.
[18] S. Ci, P. Cai, Z. Wen, J. Li, Graphene-based electrode materials for microbial fuel cells, Sci. China Mater. 58 (2015) 496–509, doi:http://dx.doi.org/10.1007/s40843-015-0061-2.
[19] J. Hou, Z. Liu, P. Zhang, A new method for fabrication of graphene/polyaniline nanocomplex modified microbial fuel cell anodes, J. Power Sources 224 (2013) 139–144, doi:http://dx.doi.org/10.1016/j.jpowsour.2012.09.091.
[20] H. Yuan, Z. He, Graphene-modified electrodes for enhancing the performance of microbial fuel cells, Nanoscale 7 (2015) 7022–7029, doi:http://dx.doi.org/10.1039/C4NR05637J.
[21] L. Chen, P.-L. Tremblay, S. Mohanty, K. Xu, T. Zhang, Electrosynthesis of acetate from CO_2 by a highly structured biofilm assembled with reduced graphene oxide?tetraethylene pentamine, J. Mater. Chem. A 4 (2016) 8395–8401, doi:http://dx.doi.org/10.1039/C6TA02036D.
[22] B.G. Choi, M. Yang, W.H. Hong, J.W. Choi, Y.S. Huh, 3D Macroporous Graphene Frameworks for Supercapacitors with High Energy and Power Densities, ACS Nano 6 (2012) 4020–4028, doi:http://dx.doi.org/10.1021/nn3003345.
[23] X. Dong, X. Wang, L. Wang, H. Song, H. Zhang, W. Huang, P. Chen, 3D Graphene Foam as a Monolithic and Macroporous Carbon Electrode for Electrochemical Sensing, ACS Appl. Mater. Interfaces 4 (2012) 3129–3133, doi:http://dx.doi.org/10.1021/am300459m.
[24] X. Ji, X. Zhang, X. Zhang, X. Ji, X. Zhang, X. Zhang, Three-Dimensional Graphene-Based Nanomaterials as Electrocatalysts for Oxygen Reduction Reaction, Three-Dimensional Graphene-Based Nanomaterials as Electrocatalysts for Oxygen Reduction Reaction, J. Nanomater. 2015 (2015) e357196, doi:http://dx.doi.org/10.1155/2015/357196.
[25] H. Wang, G. Wang, Y. Ling, F. Qian, Y. Song, X. Lu, S. Chen, Y. Tong, Y. Li, High power density microbial fuel cell with flexible 3D graphene-nickel foam as anode, Nanoscale 5 (2013) 10283–10290, doi:http://dx.doi.org/10.1039/c3nr03487a.
[26] Y.-C. Yong, X.-C. Dong, M.B. Chan-Park, H. Song, P. Chen, Macroporous and Monolithic Anode Based on Polyaniline Hybridized Three-Dimensional Graphene for High-Performance Microbial Fuel Cells, ACS Nano 6 (2012) 2394–2400, doi:http://dx.doi.org/10.1021/nn204656d.
[27] H. Gao, H. Duan, 2D and 3D graphene materials: Preparation and bioelectrochemical applications, Biosens. Bioelectron. 65 (2015) 404–419, doi:http://dx.doi.org/10.1016/j.bios.2014.10.067.
[28] P.-L. Tremblay, D. Höglund, A. Koza, I. Bonde, T. Zhang, Adaptation of the autotrophic acetogen *Sporomusa ovata* to methanol accelerates the conversion of CO_2 to organic products, Sci. Rep. 5 (2015) 16168, doi:http://dx.doi.org/10.1038/srep16168.
[29] B. Möller, R. Oßmer, B.H. Howard, G. Gottschalk, H. Hippe, Sporomusa, a new genus of gram-negative anaerobic bacteria including Sporomusa sphaeroides spec nov. and Sporomusa ovata spec. nov, Arch. Microbiol. 139 (1984) 388–396, doi:http://dx.doi.org/10.1007/BF00408385.
[30] N. Zhu, S. Han, S. Gan, J. Ulstrup, Q. Chi, Graphene Paper Doped with Chemically Compatible Prussian Blue Nanoparticles as Nanohybrid Electrocatalyst, Adv. Funct. Mater. 23 (2013) 5297–5306, doi:http://dx.doi.org/10.1002/adfm.201300605.
[31] R.S. Dey, H.A. Hjuler, Q. Chi, Approaching the theoretical capacitance of graphene through copper foam integrated three-dimensional graphene networks, J. Mater. Chem. A 3 (2015) 6324–6329, doi:http://dx.doi.org/10.1039/C5TA01112D.
[32] R. Poreddy, C. Engelbrekt, A. Riisager, Copper oxide as efficient catalyst for oxidative dehydrogenation of alcohols with air, Catal. Sci. Technol. 5 (2015) 2467–2477, doi:http://dx.doi.org/10.1039/C4CY01622J.
[33] J. Zhang, H. Yang, G. Shen, P. Cheng, J. Zhang, S. Guo, Reduction of graphene oxide viaL-ascorbic acid, Chem. Commun. 46 (2010) 1112–1114, doi:http://dx.doi.org/10.1039/B917705A.
[34] Y. Zhang, G. Mo, X. Li, W. Zhang, J. Zhang, J. Ye, X. Huang, C. Yu, A graphene modified anode to improve the performance of microbial fuel cells, J. Power Sources 196 (2011) 5402–5407, doi:http://dx.doi.org/10.1016/j.jpowsour.2011.02.067.
[35] L. Xiao, J. Damien, J. Luo, H.D. Jang, J. Huang, Z. He, Crumpled graphene particles for microbial fuel cell electrodes, J. Power Sources 208 (2012) 187–192, doi:http://dx.doi.org/10.1016/j.jpowsour.2012.02.036.
[36] X.-M. Liu, Z. dong Huang, S. woon Oh, B. Zhang, P.-C. Ma, M.M.F. Yuen, J.-K. Kim, Carbon nanotube (CNT)-based composites as electrode material for rechargeable Li-ion batteries: A review, Compos. Sci. Technol. 72 (2012) 121–144, doi:http://dx.doi.org/10.1016/j.compscitech.2011.11.019.
[37] M. Segal, Selling graphene by the ton, Nat. Nanotechnol. 4 (2009) 612–614, doi:http://dx.doi.org/10.1038/nnano.2009.279.

4 Reduced graphene oxide-copper foam composite cathode for the microbial electrosynthesis of acetate from carbon dioxide

Authors:

Nabin Aryal[1], Pier-Luc Tremblay[1, 4] Marc Hvid Overgaard[2], Adam C. Stoot[3],Tian Zhang[1,4]

Affiliation:

[1] Novo Nordisk Foundation Center for Biosustainability, Technical University of Denmark, Kemitorvet-220, 2800 Lyngby, Denmark

[2]Department of Chemistry, University of Copenhagen Universitetsparken 5, 2100 København, Denmark

[3]DTU Nanotech, Technical University of Denmark, 2800 Kgs. Lyngby

[4] School of Chemistry, Chemical Engineering and Life Science, Wuhan University of Technology, Wuhan 430070, PR China

Abstract

Copper and reduced graphene oxide (rGO) are two highly conductive and inexpensive cathode materials that have been employed for the development of high-performance electrochemical applications. In this study, the performance of a

cathode fabricated with copper foam coated with rGO was tested for the microbial electrosynthesis (MES) of acetate from CO_2. The composite cathode combined the outstanding physicochemical and electrical properties of copper and rGO to enable the fast MES of acetate at a rate of 1708. 3 mmol m^{-2} d^{-1}. A substantial current density of -20.4 A m^{-2} and a coulombic efficiency of 74.5 % were also observed. With this MES system, electrons were transferred from the cathode to the microbial catalyst *via* H_2. Electron transfer was not limiting for the bioproduction of acetate since H_2 surplus accumulated at a rate of 4184.0 mmol m^{-2} d^{-1} in the gas phase of the MES reactor. Comparing the rGO-copper foam cathode with an uncoated copper foam cathode elucidated in part the superior MES performance associated with the composite material. The rGO-copper foam cathode evolved the electron shuttle H_2 3.1 times faster probably due to a specific surface area 161-fold larger than the uncoated copper foam cathode. Furthermore, a healthier and more substantial biofilm comprised of *Sporomusa ovata* cells was attached on the biocompatible rGO surface of the composite cathode while the copper foam cathode was covered mainly by broken bacteria. This study concluded that rGO-copper foam composite is a promising cathode material for high-performance MES or for other bioelectrochemical application

1. Introduction

Microbial electrosynthesis (MES) is an emerging biotechnology where electrons coming from the cathode of a bioelectrochemical reactor are used by a microbial catalyst for the reduction of CO_2 into multicarbon compounds or methane.[1-3] In MES, electrons and protons driving biological reduction reactions at the cathode are coming from chemical or biological oxidation reactions occurring at the anode.[4-6] The electricity required to drive MES processes can be generated from multiple renewable energy sources including wind turbine and sunlight.[7,8] Under these circumstances MES is a technology developed for the storage of electricity from intermittent energy sources into the chemical bonds of easy-to-store molecules.[9]

Copper, which has high electrical conductivity and a relatively low price, could be an interesting alternative for the fabrication of high-performance MES cathodes. In bioelectrochemical systems aiming at the generation of an electrical current from the microbial oxidation of organic carbon molecules, copper anode have been shown to have a comparable performance to benchmark graphite anode.[20] For this application, fabrication of copper anode should reduce cost because the higher conductivity of copper allows the utilization of thinner electrode for the same productivity. In many MES systems, electrons are shuttled from the cathode to the

microbes *via* H_2.[3,21] Cathodes made of metallic copper, copper alloys or comprising copper oxides have been used for the electrochemical or photoelectrochemical evolution of H_2.[22-24] However, copper surfaces are known to inhibit microbial cell growth, which could be incompatible with MES applications.[25,26]

Reduced graphene oxide (rGO) is a honeycombed one-atom-thick carbon material with many of the qualities required for the development of high-performance electrodes for bioelectrochemical applications such as biocompatibility, high electrical conductivity and low production cost.[27-30] In the case of MES, composite carbonaceous cathodes comprising rGO or its derivative have been shown to increase significantly acetate production rates and current density.[15,16] Because of its large specific surface area and superior electron mobility, graphene-based materials have also been used in the fabrication of cathode for the photoelectrochemical or electrochemical H_2 evolution.[31-35] Furthermore, when graphene-based materials were combined with copper-based materials for the fabrication of inexpensive electrodes, a synergistic effect improving H_2 evolution further was observed.[36,37]

During MES, electron transfer rate from the cathode to the microbe can be an important bottleneck restraining productivity. The purpose of this study was to develop a MES system where the flux

of reducing equivalents under the form of H_2 would be sufficient to drive the biological reduction of CO_2 without being a limitation. To achieve this goal, we investigate the performance and bioelectrochemical behavior of *S. ovata*-driven MES reactors equipped with copper foam cathode or copper-foam-rGO composite cathode poised at low potential. Biofilm formation at the surface of the different cathodes was also studied via confocal lase microscopy (CLSM) and scanning electron microscopy (SEM).

2. Materials and methods

2.1 The microbial catalyst *Sporomusa ovata* DSM 2662

Wild-type *Sporomusa ovata* DSM-2662 was acquired from the Deutsche Sammlung Mikroorganismen und Zellkulturen (DSMZ).[38] Bacterial cultures were routinely maintained anaerobically in 311 medium with 40 mM betaine as carbon source and electron donor under N_2:CO_2 (80:20). For autotrophic cultivation with H_2 as the electron source, no betaine was added to 311 medium and the atmosphere was N_2:CO_2:H_2 (83:10:7). Casitone, sodium sulfide, yeast extract, and resazurin were omitted from 311 medium under all growth conditions. Cysteine was also omitted from 311 medium for MES experiments.

2.2 Synthesis of graphene oxide

Graphene oxide (GO) was prepared *via* a modified version of the Hummers' method.[39] 0.5 g of graphite (325 mesh, Alfa Aesar) was loaded into a round bottom flask. 24 ml concentrated H_2SO_4 (95-98%, Sigma-Aldrich) was added, and the reaction mixture was cooled on ice with stirring. After 10 minutes 3 g of $KMnO_4$ (Sigma-Aldrich) was added in small portions over 30 minutes and the reaction was maintained on ice for an additional 1.5 hour. The mixture was then transferred to an oil bath heated to 35 °C and incubated for 16 hours. 80 ml Milli-Q water was added slowly into the reaction mixture and the temperature was subsequently raised to 90 ˚C for 15 minutes. The reaction mixture was allowed to cool down to room temperature and 100 ml Milli-Q water was added followed by 8 ml H_2O_2 (33%, Sigma-Aldrich). The obtained GO was then washed five times with Milli-Q water by centrifugation.[40] GO flake exfoliation was done subsequently using bath sonication for 30 minutes. Large aggregates were removed and further refining to mono- and few-layer GO was achieved by centrifuging 5 times at 2000 rpm. Finally, the GO solution was centrifuged two times at 8000 rpm for 20 minutes to remove oxidative debris.

2.3 Coating of copper foam with reduced graphene oxide

Handling of the copper foam (Goodfellow, UK) was done under a nitrogen atmosphere to avoid extensive copper oxidation. Initially, the copper foam scaffold was washed in isopropanol, ethanol and Milli-Q water for 15 minutes each prior to GO coating. Coating of the copper foam was carried out at 120 ˚C in a round bottom flask under a continuous flow of nitrogen. A 0.5 mg/ml GO solution was dropped on both sides of the copper foam, and the GO solution was allowed to dry. This step was repeated 3 times until full coverage of the copper foam was achieved. GO was subsequently reduced to rGO with 60 ml ascorbic acid solution (0.5 mg/ml) for 2 hours. Finally, the rGO-copper foam electrode was washed extensively with Milli-Q water to remove residual ascorbic acid and loosely-bound rGO flakes.

2.4 Microbial electrosynthesis and cyclic voltammetry

The copper foam and rGO-copper foam cathodes were tested in triplicate MES experiments in dual chambered, three-electrode bioelectrochemical reactors. The MES experiments were conducted at 25 °C with *S. ovata* DSM-2662 for the reduction of CO_2 into acetate as previously described.[2,10] Copper foam or rGO-copper foam cathodes (5.2 cm^2) and graphite stick anode (36 cm^2) were immersed in 250 ml 311 medium in two chambers separated by a

Nafion 115 ion-exchange membrane (Ion Power, Inc., New Castle, DE, USA). An Ag/AgCl electrode model ET072 (eDAQ, Denmark) was used as a reference electrode and the cathode was poised at a potential of –990 mV versus standard hydrogen electrode (SHE) with a CH Instrument potentiostat (CH Instruments, Inc, USA). *S. ovata* cultures were pre-grown under a N_2:CO_2:H_2 atmosphere in the cathode chamber of the MES reactor. After two fresh 311 medium swaps, the gas mix was switched to N_2:CO_2 at which point data start being collected. The anode compartment was also bubbled with N_2:CO_2 during the MES experiment. During the cyclic voltammetry (CV) experiments, the tested electrodes were scanned at a rate of 1 mV s^{-1} in a potential window of 0 to -1300 mV versus Ag/AgCl. Data generated during MES and CV experiments were analyzed with EC-Lab® software v.10.40.

2.5 Gas chromatography and High-pressure liquid chromatography

For H_2 detection, gas samples from the headspace of MES reactors were collected in N_2-flushed serum tubes and concentration was measured by gas chromatography with a Trace 1300 gas chromatograph (ThermoFisher Scientific, Denmark). Argon was used as a carrier gas with a HP-PLOT Molesieve column (Agilent) and H_2 was detected with a thermal conductivity detector (TCD).

The oven temperature of the gas chromatograph was maintained at 130 °C. High-pressure liquid chromatography (HPLC) was used for the quantification of acetate. The HPLC apparatus was equipped with an HPX-87H anion exchange column (Bio-Rad Laboratories Inc., California, USA) set at a temperature of 30 °C. 5 mM H_2SO_4 was the mobile phase at a flow rate of 0.6 ml/min. Acetate was detected with a refractive index (RI) detector and data were analyzed with the Chromeleon software (ThermoFisher Scientific). As described previously[2,10,17], acetate production rate and current density were normalized to the whole geometric surface area of copper foam or rGO-copper foam cathodes, which were rectangular prisms, according to equation 1:

$$A = 2(wl + hl + hw) \quad \text{(Eq. 1)}$$

The whole geometic surface area (A) was 5.2 cm^2 with a width (w) of 0.2 cm, a length (l) of 2 cm and a height (h) of 1 cm.

2.6 Scanning electron microscopy and confocal laser scanning microscopy

For Scanning Electron Microscopy (SEM) images, abiotic cathode and biocathode samples from electrochemical reactors were collected at the end of MES experiments after ten days of operation and fixed with 0.1M buffer solution at pH 7.0 containing 2.5%

glutaraldehyde for 5 hours at room temperature. Cathode samples were then washed with the buffer solution without glutaraldehyde before being immersed successively in acetonitrile and ethanol as described previously.[17] Cathodes were dried under nitrogen and images were taken with a Quanta 200 FEG scanning electron microscope (FEI) at an accelerating voltage of 10 V under high vacuum condition. For Confocal Laser Scanning Microscopy (CLSM) images, copper foam and rGO-copper foam biocathodes were taken from the MES reactor after ten days and stained with the LIVE/DEAD® BacLight™ Bacterial Viability Kit (ThermoFisher Scientific) as described previously.[17] CLSM images were taken with a Zeiss LSM 5 Pascal microscope, and the images were analyzed with the ZEN imaging software (Zeiss, Germany).

2.7 Analytical methods

Raman spectra of copper foam and rGO-copper foam cathodes were obtained with a DXR confocal Raman microscope (ThermoFisher Scientific) at an excitation wavelength of 455 nm with 5 mW of laser power. The Brunauer–Emmett–Teller (BET) method was used as previously described to determine the specific surface area of cathodes.[41]

3. Results and discussion

3.1 The copper foam cathode and the rGO-copper foam composite cathode

Two cathode materials were investigated in this study: commercially-available copper foam and copper-foam-rGO composite. The latter was fabricated by coating copper foam with GO before proceeding to its reduction with ascorbic acid (Fig 1A-B). SEM images of the copper foam cathode show a three dimensional globular structure (Fig. 1C-D). After the coating process, a crumpled paper-like film made of rGO was covering the copper foam surface (Fig. 1E-F). Raman spectroscopy was employed to confirm the successful modification of the copper foam substrate with rGO (Fig. S1). Before modification, the copper foam material exhibited two Raman peaks between 500 and 700 cm^{-1}, which are characteristic of copper oxides found at the surface of metallic copper.[42] After modification, only a single weaker peak at ca. 620 cm^{-1} remained in this region of the Raman spectrum. More importantly, Raman peaks D (1360 cm^{-1}), G (1570 cm^{-1}) and 2D (2700 cm^{-1}) which are characteristic of rGO were present on the Raman spectrum confirming the successful coating of the copper foam. [43] Besides changing the cathode surface structure, coating

rGO on the copper foam substrate resulted in a 161-fold increase of the specific surface area to 1.13 m^2 g^{-1}.

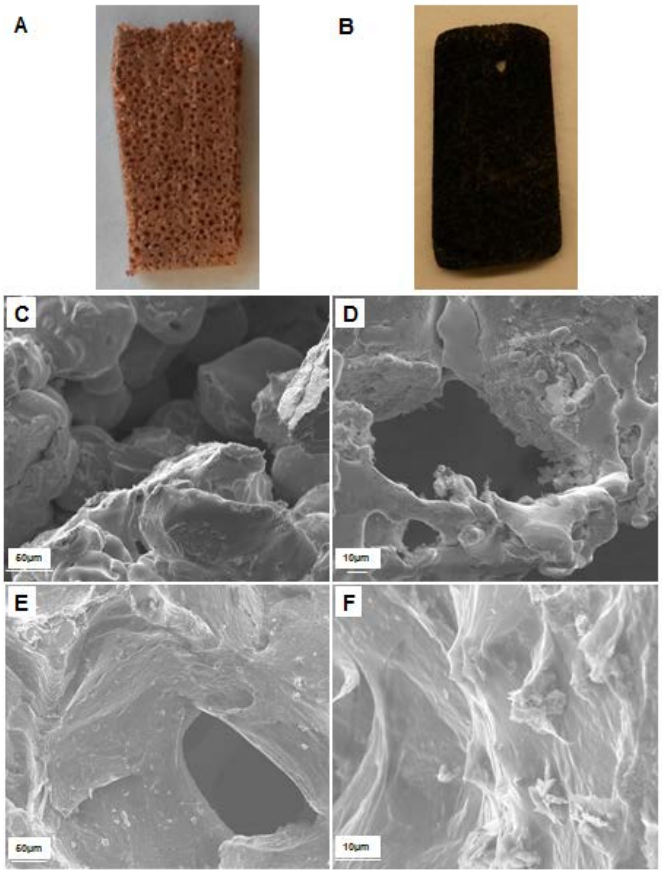

Figure 1. (A) Copper foam and (B) rGO-copper foam cathode. SEM images (C and D) at low- and high-magnification of copper foam cathode, and (E and F) low- and high-magnification of rGO-copper foam cathode.

3.2 Microbial electrosynthesis with the copper foam cathode

A MES system equipped with a copper foam cathode poised at -990 mV vs. SHE and *S. ovata* DSM-2662 as the microbial catalyst had an acetate production rate of 79.6 ± 24.4 mmol m^{-2} d^{-1} and a current density of -7.1 ± 2.5 A m^{-2} (Fig. 2, Table 1). As expected, the abiotic MES system equipped with a copper foam cathode did not generate any acetate while H_2 accumulated in the reactor gas at a rate of 2500.9 ± 461.4 mmol m^{-2} d^{-1}. In the copper foam-MES reactor populated wih *S. ovata*, H_2 also accumulated in the gas phase but at a lower rate of 995.0 ± 63.4 mmol m^{-2} d^{-1}. Assuming that in the MES system described here all the electrons used for the biological reduction of CO_2 into acetate are transferred to the microbe from the cathode under the form of H_2, the electrosynthesis of 1mole of acetate requires 4 moles of H_2 according to equation 2.

$4H_2 + 2CO_2 \rightarrow CH_3COOH + 2H_2O$ (Eq. 2)

This means that to maintain the acetate production rate observed with the copper foam-MES system, bioelectrochemically-evolved H_2 must be oxidized at a rate of 318.4 mmol m^{-2} d^{-1}. Accumulation of large quantity of H_2 in the gas phase at a rate 3.1 fold faster than the predicted H_2 oxidation rate is the main reason why coulombic efficiency is low in this system with only 18.5 ± 12 % of the electrons from the cathode used for the biological synthesis of

acetate from CO_2. Furthermore, results presented here suggest that biomass inhibits H_2 evolution reaction (HER). When the predicted H_2 oxidation rate is added to H_2 accumulation rate in the gas phase, the total H_2 evolution rate of the *S. ovata*-driven MES reactor equipped with a copper foam cathode is still 1.9 fold lower than the H_2 evolution rate of the abiotic reactor.

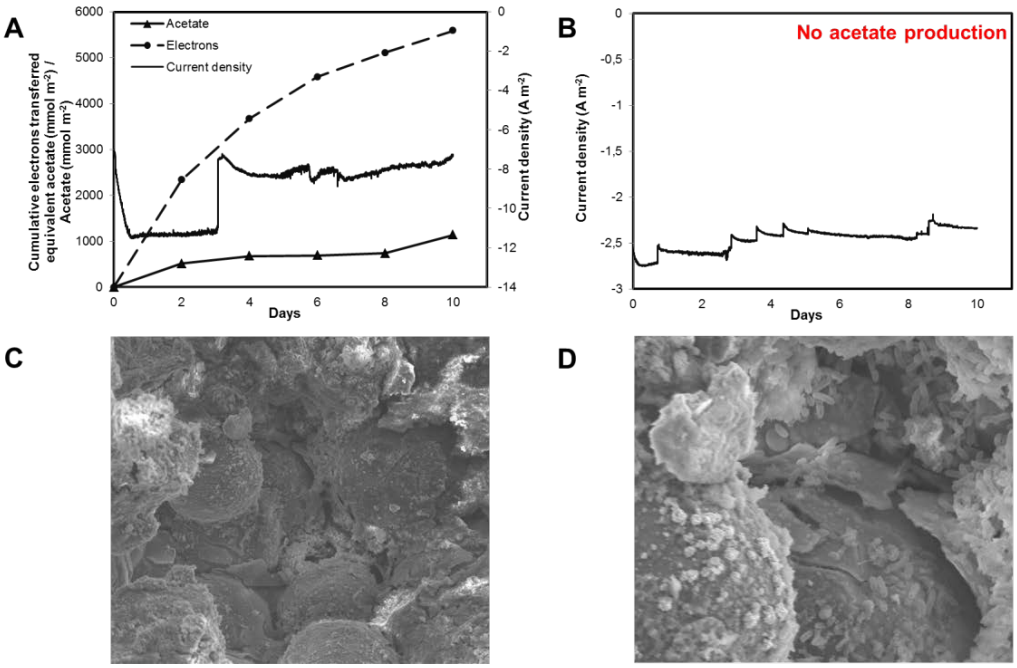

Figure 2. MES with copper foam cathode. (A)Acetate production, current density and electron transferred during *S. ovata*-driven MES. Electron transferred curves correspond to the acetate production in mmol m^{-2} if all the electrons transferred were converted to acetate. Acetate production curves in mmol m^{-2} correspond to the real progression of acetate concentration in the MES reactor detected by HPLC. (B) Current density with an abiotic copper foam cathode. SEM

images (C and D) at low- and high-magnification of a copper foam cathode after 10 days of *S. ovata*-driven MES. Results shown are from a representative example of three replicate MES reactors.

3.3 Cell attachment at the surface of copper foam cathode

SEM images taken after 10 days of operation in the MES reactor shows the presence of *S. ovata* cells attached at the surface of the copper foam cathode (Fig. 2C-D). CLSM images of the same biocathode reveals that a large fraction of *S. ovata* cells stained in red, which indicates that they had a compromised membrane and were either dead or dying (Fig. 3). Presence of multiple dead cells which probably blocked effective reaction sites at the cathode-electrolyte junction where HER happens, possibly explained why copper foam cathode evolved H_2 slower in the *S. ovata*-driven MES system compared to the abiotic reactor. Although copper has many outstanding properties that could be beneficial for MES applications, this material is widely considered as antimicrobial with an oligodynamic effects.[20,26] In this study, the inhibiting impact of copper on *S. ovata* was evident under the MES operational conditions tested here.

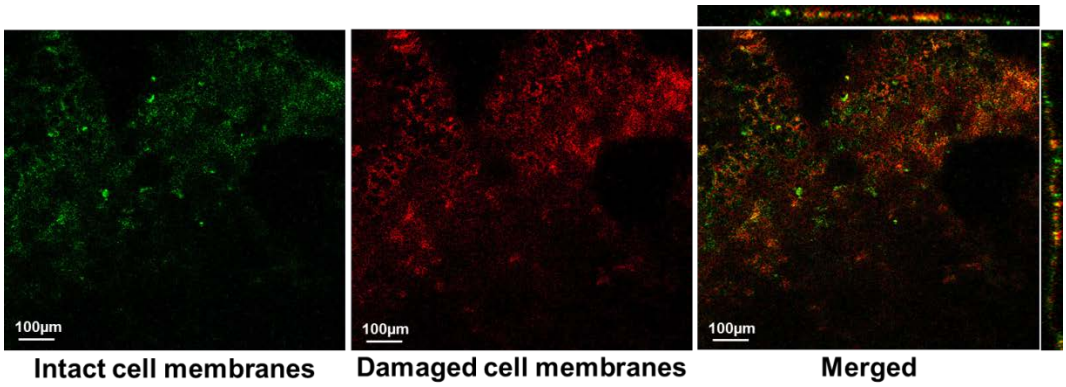

Figure 3. CLSM images of a copper foam cathode from a *S. ovata*-driven MES reactor. Results shown are from a representative example of three replicate.

3.4 Microbial electrosynthesis with the rGO-copper foam cathode

When copper foam was coated with rGO and used as the cathode for *S. ovata*-driven MES, acetate production rates as well as current density were significantly increased to 1708.3 ± 333.3 mmol m^{-2} d^{-1} and -20.4 ± 1.0 A m^{-2}, respectively (Fig 4, Table 1). The acetate production rate observed with this composite cathode is one of the highest reported until now for MES technology. Jourdin et al. reported an acetate production rate of 11407 mmol m^{-2} d^{-1} with a MES system populated with a mixed community and equipped with a reticulated vitreous carbon (RVC) cathode coated with multiwalled carbon nanotubes (MWCN).[19] However, this

outstanding result was normalized to the projected area or footprint of the base of the electrode which was 1.36 cm^2.[12,19,44] If the whole geometric surface area of the RVC-MWCN cathode of ca. 7.82 cm^2 is considered instead, the acetate production rate of 1983.8 mmol m^{-2} d^{-1} becomes comparable to our result.[19] Projected surface area calculated only from one side or the base of the electrode[12,44,45] was not used for normalization in this study because it represents only a minority fraction of the faces of a three-dimensional electrode with which bacteria can interact in a bioelectrochemical reactor. Furthermore, total surface area calculated from the specific surface area was not used for normalization because bacterial cells are too large to interact everywhere on the cathode.

Coulombic efficiency in the MES system with the rGO-copper foam cathode was 74.5 ± 10.9 % (Table 1). Similarly to the copper foam cathode, a large quantity of H_2 was not oxidized by the microbial catalyst and accumulated in the gas phase of the MES reactor. This was the main reason why a fraction of the electrons from the cathode has not been used for the biological reduction of CO_2 into acetate. Still, coulombic efficiency with the rGO-copper foam cathode was significantly better than the one observed with the copper foam cathode.

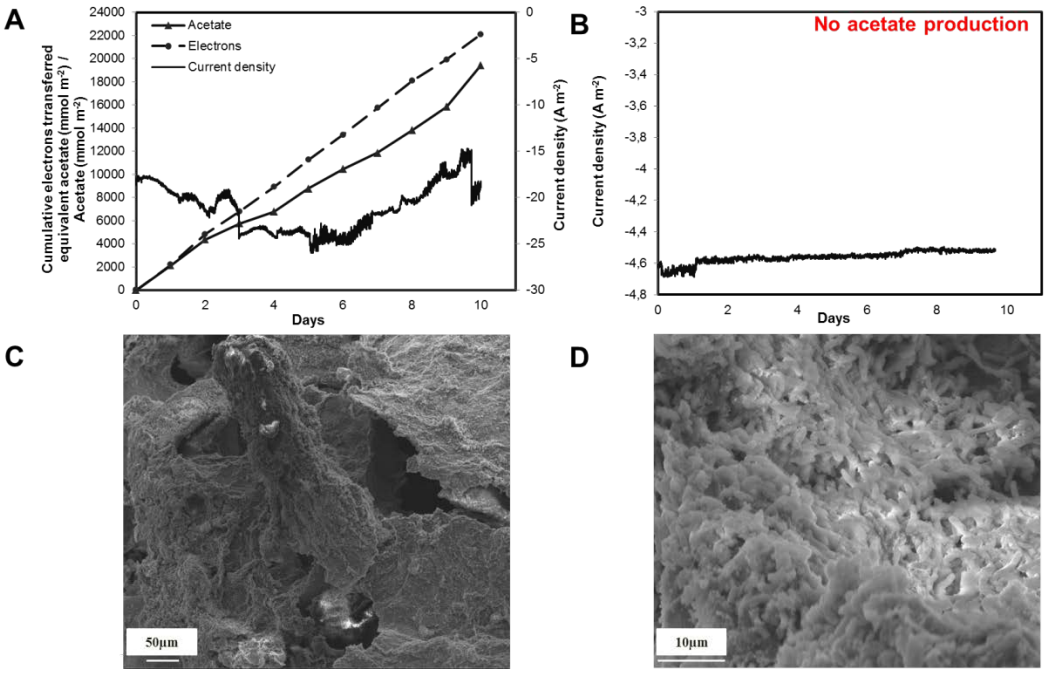

Figure 4. MES with rGO-copper foam cathode. (A)Acetate production, current density and electron transferred during *S. ovata*-driven MES. Electron transferred curves correspond to the acetate production in mmol m^{-2} if all the electrons transferred were converted to acetate. Acetate production curves in mmol m^{-2} correspond to the real progression of acetate concentration in the MES reactor detected by HPLC. (B) Current density with an abiotic rGO-copper foam cathode. SEM images (C and D) at low- and high-magnification of a rGO-copper foam cathode after 10 days of *S. ovata*-driven MES. Results shown are from a representative example of three replicate MES reactor

Table 1. MES performance with copper foam and rGO-copper foam cathodes.[a]

Cathode	Microbial catalyst[b]	Acetate production rate (mmol m^{-2} d^{-1})[c]	Current density (A m^{-2})[c]	Couloumbic efficiency for acetate (%)[c]	Hydrogen accumulation rate (mmol m^{-2} d^{-1})[c,d]
Copper foam	Sterile	N.D.[e]	-2.3 ± 1.1	N.A.[f]	995.0 ± 63.4
Copper foam	*S. ovata*	79.6 ± 24.4	-7.1 ± 2.5	18.5 ± 12.0	2500.9 ± 461.4
rGO-copper foam	Sterile	N.D.	-4.6 ± 0.0	N.A.	7835.3 ± 2177.3
rGO-copper foam	*S. ovata*	1708.3 ± 333.3	-20.4 ± 1.0	74.5 ± 10.9	4184.0 ± 1049.4

[a] Cathode potential set at -990 mV vs SHE., [b] *S. ovata* is the wild type strain DSM-2662, [c] Each value is the mean and standard deviation of three replicates., [d] H_2 accumulation rate in the gas phase of the MES reactor., [e] Not detected., [f] Not applicable.

H_2 accumulation rate in the gas phase of the abiotic rGO-copper foam MES reactor was 7835.3 ± 2177.3 mmol m^{-2} d^{-1}, which is 3.1 fold higher than with the abiotic copper foam MES reactor. Besides the intrinsic properties of rGO, the larger specific area of the rGO-copper foam cathode compared to uncoated copper foam cathode, which increases the quantity of cathode-electrolyte junctions, explains the faster HER observed.

In the *S. ovata*-driven rGO-copper foam MES system, H_2 must be oxidized at a rate of 6833.2 mmol m^{-2} d^{-1} to sustain the observed acetate production rate. Adding the projected H_2 oxidation rate to the H_2 accumulation rate in the gas phase results in an overall H_2 evolution rate of 11017.2 mmol m^{-2} d^{-1}, which is 1.4 fold higher than what was observed in the abiotic rGO-copper foam MES system. This result strongly suggests that, contrary to the copper foam MES system, the presence of biomass accelerate HER. This phenomenon has been observed before with other types of cathode material and it has been proposed that it is caused by the microbial deposition on the MES cathode of redox enzymes or biometals accelerating HER.[3,46,47]

Investigating the bioelectrochemical behavior of the *S. ovata*-driven rGO-copper foam MES system with cyclic voltammetry showed a higher cathodic current response than the abiotic controls as well as

the *S. ovata* copper foam MES system (Fig. S2). This result is consistent with the higher current density and the faster HER observed with the MES reactor equipped with the composite cathode. Furthermore, the abiotic rGO-copper foam MES system exhibited a higher cathodic current response than the abiotic copper foam MES system, a result again consistent with the reported current densities, HER rates as well as with the increase in specific surface area.

3.5 Biofilm formation on the rGO-copper foam cathode

SEM images of the biocathode from the *S. ovata*-driven rGO-copper foam MES system reveal a very dense bacterial population covering the totality of the rGO surface (Fig. 4C-D). CLSM images also show more substantial biomass when compared to the copper foam cathode (Fig. 5). The biocompatibility of rGO was noticeable since almost all the *S. ovata* cells stained in green, which means that they had an intact membrane and were most probably alive. This was expected since Aryal et al. have shown previously that the acetogen *S. ovata* remains viable on rGO.[16] Besides microbial deposition of enzymes or biometals, another possible explanation for the microbial acceleration of HER is that living cells quickly oxidize H_2 present at the cathode-microbe interface, creating conditions in term of H_2 partial pressure that are more favorable for H_2 evolution.[48]

This hypothesis would be in accordance with the observations made in this study which is that HER slowed down when dead *S. ovata* cells are covering a copper foam cathode and accelerated when intact *S. ovata* cells are covering a rGO-copper foam cathode.

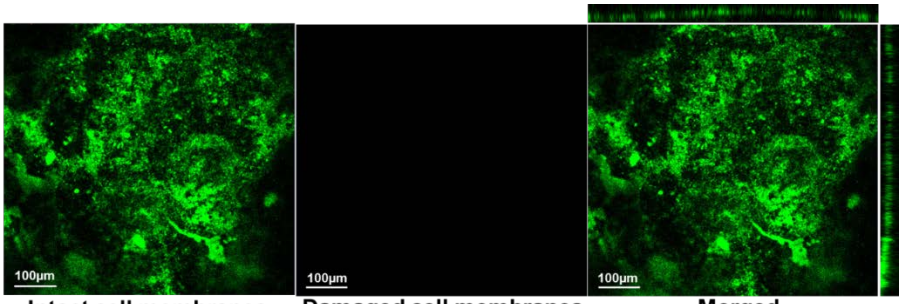

Figure 5. CLSM images of a rGO-copper foam cathode from a *S. ovata*-driven MES reactor. Results shown are from a representative example of three replicate.

4. Conclusion

In this study, a novel MES reactor equipped with a rGO-copper foam cathode evolving large quantity of H_2 to shuttle a non-limiting flux of reducing equivalents to the microbial catalyst *S. ovata* was developed. Copper is a highly conductive and relatively inexpensive material that if used to fabricate electrodes could reduce the cost associated with bioelectrochemical applications.[20] However, the results presented here indicated that a copper foam cathode is unsuitable for the MES of acetate from CO_2 because of its

antimicrobial properties reducing productivity and efficiency. When rGO, which is compatible with *S. ovate*, was coated on the surface of the copper foam cathode, acetate production rate and current density were increased significantly to a level comparable to the most performant MES reactor developed until now.[19] Besides its outstanding physicochemical and electrical properties, rGO is cheaper to produce than other carbon nanomaterials such as MWCN used before in the fabrication of high-performance cathode for MES.[19,30,49] Thus, rGO-copper foam cathodes have multiple features that would be beneficial for the development of productive and cost-effective MES reactors or of other bioelectrochemical applications.

Electronic Supplementary Information

Reduced graphene oxide-copper foam composite cathode for the microbial electrosynthesis of acetate from carbon dioxide

Nabin Aryal[1], Pier-Luc Tremblay[1, 4]Marc Hvid Overgaard[2], Adam C. Stoot[3], Tian Zhang[1,4]

[1] Novo Nordisk Foundation Center for Biosustainability, Technical University of Denmark, Kemitorvet-220, 2800 Lyngby, Denmark

[2]Department of Chemistry, University of Copenhagen Universitetsparken 5, 2100 København, Denmark

[3]DTU Nanotech, Technical University of Denmark, 2800 Kgs. Lyngby

[4] School of Chemistry, Chemical Engineering and Life Science, Wuhan University of Technology, Wuhan 430070, PR China

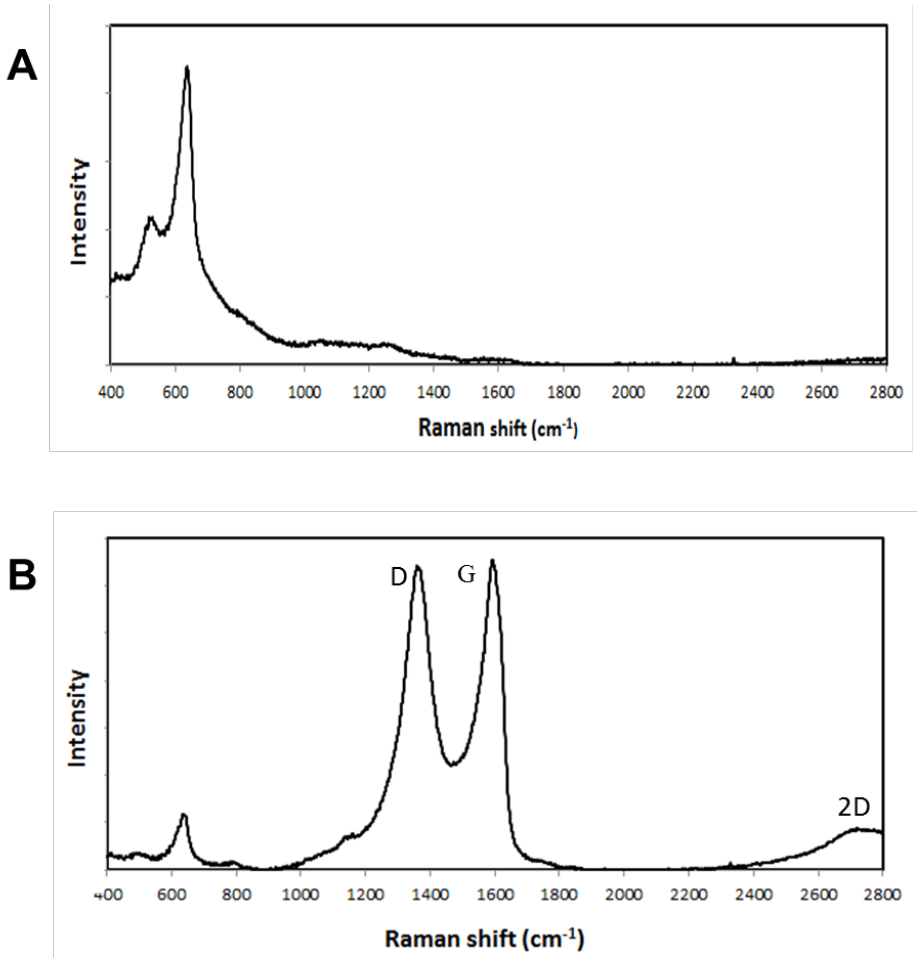

Figure S1. Raman spectra of (A) copper foam and of (B) rGO-copper foam.

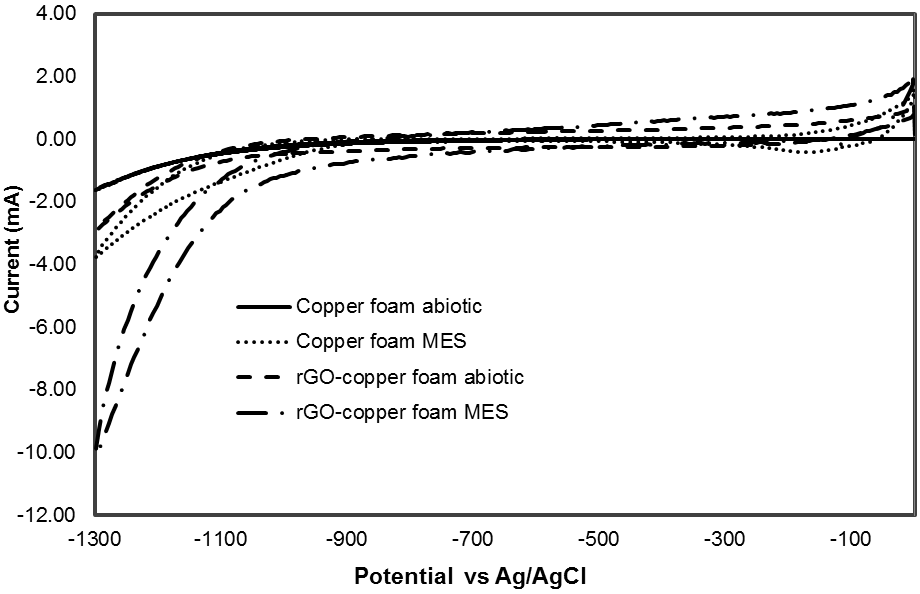

Figure S2. Cyclic voltammograms in a potential window of 0 to -1300 mV versus Ag/AgCl at a rate of 1 mV s^{-1}.

References

1 D. R. Lovley and K. P. Nevin, *Curr. Opin. Biotechnol.*, 2013, **24**, 385–390.

2 K. P. Nevin, T. L. Woodard, A. E. Franks, Z. M. Summers and D. R. Lovley, *mBio*, 2010, **1**, pii: e00103-10.

3 P.-L. Tremblay, L. T. Angenent and T. Zhang, *Trends Biotechnol.*, 2016. doi: 10.1016/j.tibtech.2016.10.004.

4 K. Rabaey and R. A. Rozendal, *Nat. Rev. Microbiol.*, 2010, **8**, 706–716.

5 M. Zeppilli, M. Villano, F. Aulenta, S. Lampis, G. Vallini and M. Majone, *Environ. Sci. Pollut. Res. Int.*, 2015, **22**, 7349–7360.

6 Y. Gong, A. Ebrahim, A. M. Feist, M. Embree, T. Zhang, D. Lovley and K. Zengler, *Environ. Sci. Technol.*, 2013, **47**, 568–573.

7 P.-L. Tremblay and T. Zhang, *Front. Microbiol.*, 2015, **6**, 201.

8 T. Zhang, *Science*, 2015, **350**, 738–739.

9 D. R. Lovley and K. P. Nevin, *Curr. Opin. Biotechnol.*, 2011, **22**, 441–448.

10 P.-L. Tremblay, D. Höglund, A. Koza, I. Bonde and T. Zhang, *Sci. Rep.*, 2015, **5**, 16168.

11 F. Ammam, P.-L. Tremblay, D. M. Lizak and T. Zhang, *Biotechnol. Biofuels*, 2016, **9**, 163.

12 L. Jourdin, S. Freguia, B. C. Donose, J. Chen, G. G. Wallace, J. Keller and V. Flexer, *J. Mater. Chem. A*, 2014, **2**, 13093–13102.

13 S. Bajracharya, A. ter Heijne, X. Dominguez Benetton, K. Vanbroekhoven, C. J. N. Buisman, D. P. B. T. B. Strik and D. Pant, *Bioresour. Technol.*, 2015, **195**, 14–24.

14 S. A. Patil, J. B. A. Arends, I. Vanwonterghem, J. van Meerbergen, K. Guo, G. W. Tyson and K. Rabaey, *Environ. Sci. Technol.*, 2015, **49**, 8833–8843.

15 L. Chen, P.-L. Tremblay, S. Mohanty, K. Xu and T. Zhang, *J. Mater. Chem. A*, 2016, **4**, 8395–8401.

16 N. Aryal, A. Halder, P.-L. Tremblay, Q. Chi and T. Zhang, *Electrochim. Acta*, 2016, **217**, 117–122.

17 T. Zhang, H. Nie, T. S. Bain, H. Lu, M. Cui, O. L. Snoeyenbos-West, A. E. Franks, K. P. Nevin, T. P. Russell and D. R. Lovley, *Energy Environ. Sci.*, 2013, **6**, 217–224.

18 H. Nie, T. Zhang, M. Cui, H. Lu, D. R. Lovley and T. P. Russell, *Phys. Chem. Chem. Phys. PCCP*, 2013, **15**, 14290–14294.

19 L. Jourdin, T. Grieger, J. Monetti, V. Flexer, S. Freguia, Y. Lu, J. Chen, M. Romano, G. G. Wallace and J. Keller, *Environ. Sci. Technol.*, 2015, **49**, 13566–13574.

20 A. Baudler, I. Schmidt, M. Langner, A. Greiner and U. Schröder, *Energy Environ. Sci.*, 2015, **8**, 2048–2055.

21 H. D. May, P. J. Evans and E. V. LaBelle, *Curr. Opin. Biotechnol.*, 2016, **42**, 225–233.

22 J. O. Bockris and N. Pentland, *Trans. Faraday Soc.*, 1952, **48**, 833–839.

23 K. Ngamlerdpokin and N. Tantavichet, *Int. J. Hydrog. Energy*, 2014, **39**, 2505–2515.

24 A. Paracchino, V. Laporte, K. Sivula, M. Grätzel and E. Thimsen, *Nat. Mater.*, 2011, **10**, 456–461.

25 J. A. Lemire, J. J. Harrison and R. J. Turner, *Nat. Rev. Microbiol.*, 2013, **11**, 371–384.

26 G. Grass, C. Rensing and M. Solioz, *Appl. Environ. Microbiol.*, 2011, **77**, 1541–1547.

27 B. G. Choi, M. Yang, W. H. Hong, J. W. Choi and Y. S. Huh, *ACS Nano*, 2012, **6**, 4020–4028.

28 J. Hou, Z. Liu and P. Zhang, *J. Power Sources*, 2013, **224**, 139–144.

29 H. Yuan and Z. He, *Nanoscale*, 2015, **7**, 7022–7029.

30 M. Segal, *Nat. Nanotechnol.*, 2009, **4**, 612–614.

31 U. Sim, T.-Y. Yang, J. Moon, J. An, J. Hwang, J.-H. Seo, J. Lee, K. Y. Kim, J. Lee, S. Han, B. H. Hong and K. T. Nam, *Energy Environ. Sci.*, 2013, **6**, 3658–3664.

32 U. Sim, J. Moon, J. An, J. H. Kang, S. E. Jerng, J. Moon, S.-P. Cho, B. H. Hong and K. T. Nam, *Energy Environ. Sci.*, 2015, **8**, 1329–1338.

33 Z. Huang, P. Zhong, C. Wang, X. Zhang and C. Zhang, *ACS Appl. Mater. Interfaces*, 2013, **5**, 1961–1966.

34 H. Fei, J. Dong, M. J. Arellano-Jiménez, G. Ye, N. D. Kim, E. L. G. Samuel, Z. Peng, Z. Zhu, F. Qin, J. Bao, M. J. Yacaman, P. M. Ajayan, D. Chen and J. M. Tour, *Nat. Commun.*, 2015, **6**, 8668.

35 A. Xie, N. Xuan, K. Ba and Z. Sun, *ACS Appl. Mater. Interfaces*, 2017, **9**, 4643–4648.

36 S. Muralikrishna, T. n. Ravishankar, T. Ramakrishnappa, D. h. Nagaraju and R. Krishna Pai, *Environ. Prog. Sustain. Energy*, 2016, **35**, 565–573.

37 X.-J. Lv, S.-X. Zhou, C. Zhang, H.-X. Chang, Y. Chen and W.-F. Fu, *J. Mater. Chem.*, 2012, **22**, 18542–18549.

38 B. Möller, R. Oßmer, B. H. Howard, G. Gottschalk and H. Hippe, *Arch. Microbiol.*, 1984, **139**, 388–396.

39 W. S. Hummers and R. E. Offeman, *J. Am. Chem. Soc.*, 1958, **80**, 1339–1339.

40 A. Naumov, F. Grote, M. Overgaard, A. Roth, C. E. Halbig, K. Nørgaard, D. M. Guldi and S. Eigler, *J. Am. Chem. Soc.*, 2016, **138**, 11445–11448.

41 R. Poreddy, C. Engelbrekt and A. Riisager, *Catal. Sci. Technol.*, 2015, **5**, 2467–2477.

42 Y. Deng, A. D. Handoko, Y. Du, S. Xi and B. S. Yeo, *ACS Catal.*, 2016, **6**, 2473–2481.

43 A. Y. W. Sham and S. M. Notley, *Soft Matter*, 2013, **9**, 6645–6653.

44 V. Flexer, J. Chen, B. C. Donose, P. Sherrell, G. G. Wallace and J. Keller, *Energy Environ. Sci.*, 2013, **6**, 1291–1298.

45 S.-E. Oh and B. E. Logan, *Appl. Microbiol. Biotechnol.*, 2006, **70**, 162–169.

46 L. Jourdin, Y. Lu, V. Flexer, J. Keller and S. Freguia, *ChemElectroChem*, 2016, **3**, 581–591.

47 J. S. Deutzmann, M. Sahin and A. M. Spormann, *mBio*, 2015, **6**, e00496-15.

48 K. A. Vincent, A. Parkin and F. A. Armstrong, *Chem. Rev.*, 2007, **107**, 4366–4413.

49 X.-M. Liu, Z. dong Huang, S. woon Oh, B. Zhang, P.-C. Ma, M. M. F. Yuen and J.-K. Kim, *Compos. Sci. Technol.*, 2012, **72**, 121–144.

5 Conclusion and Future prospective

Sporomusa ovata DSMZ 2662, *Sporomusa ovata DSM 2663*, *Sporomusa ovata* DSMZ 3300, *Sporomusa acidovorans*, *Sporomusa malonica*, and *Sporomusa aerivorans* were successfully tested in MES with the objectives of identifying a better acetogenic microbial catalyst. Among the six tested *Sporomusa*, five were capable of drawing current and electrosynthesizing acetate from CO_2 during MES. Only *S. aerivorans* was unable to produce acetate and draw current. Furthermore, *S. ovata* DSM-3300 could form a thin biofilm on the cathode electrode and perform MES, but it was not producing acetate and drawing current as much as most of the other tested *Sporomusa*. Beside *S. aerivorans* and *S. ovata* DSM-3300, the other *Sporomusa* were significantly better at driving MES acetate production and current consumption. More importantly, *S. ovata* DSM-2663 was the best MES microbial catalyst of the tested group regarding acetate production and current consumption. The study also explored growth and acetate production rate under an H_2:CO_2 atmosphere in batch mode to establish if acetogens efficient at coupling H_2 oxidation with CO_2 reduction are automatically productive MES catalysts since H_2 is often considered as the major electron shuttle between the cathode electrode and the microbes during MES. The results showed that fitness on H_2:CO_2 does not necessarily translate into good MES performance.

The work done during this PhD project also focused on the development of novel cathode materials to improve MES performance. In the first strategy, a carbon felt scaffold was coated with reduced graphene oxide *via* solvothermal synthesis method. With this cathode, MES acetate productivity was augmented 6.8 fold. This improvement was due to larger cathode specific surface area, higher electrical conductivity and stronger electrostatic interactions with the microbial catalysts. In the second strategy, free standing flexible graphene paper was synthesized and used in MES system to enhance electron transfer between the cathode and microbe, which in turn facilitates CO_2 reduction and acetate production. MES system equipped with a RGO paper cathode was more performant than MES systems equipped with other types of freestanding carbonaceous cathode such as carbon paper, carbon cloth, graphite stick and carbon felt. In the third strategy, highly-conductive copper foam was modified with rGO and tested in MES. rGO. which is compatible with *S. ovata* was coated on the surface of the copper foam cathode resulting in acetate production rate and current density that were increased dramatically to a level comparable to the most performant MES reactor developed until now by Jourdin et al. [6]. Besides its outstanding physicochemical and electrical properties, rGO and copper foam are cheaper to

produce than other carbon nanomaterials such as MWCN used before in the fabrication of high-performance cathode for MES. Thus, rGO-copper foam cathodes have many features that would be beneficial for the development of productive and cost-effective MES reactors or other bioelectrochemical applications.

5.1 **Potential applications**

MES has the potential to become a key bioprocess technology in the future for the synthesis of biofuels and chemicals. The practical application of MES is the conversion of CO_2 from industrial emissions such as coal power plant, steel industries, and petroleum refineries; with renewable electricity supply to chemicals or gas. One of the features of MES is that it can be used to store excess of electricity in chemicals of interest. It has been reported that Denmark along with other European countries will generate important surplus of electricity from wind power in the immediate future. [1] Hence, power-to-chemicals technologies such as MES would be appropriate for the utilization, storage, and valorization of surplus electricity [2]. Recently, Electrochaea Company established a pilot scale operational plant in Copenhagen for the biological synthesis of methane from electricity by electromethanogenesis In this process, an alkaline electrolyzer was used with an electrical power input of 1 MW to generatehydrogen that is then fed to a methanogenic microbial catalyst for the biological conversion of

CO_2 wastes to methane[1]. As indicated by the European Wind Energy Association (EWEA), onshore wind is the most economical source of energy compared to offshore wind energy, gas, nuclear, coal, and solar photovoltaics energy [3]. Therefore, utilization of onshore wind as a source of energy might be significant for the large scale application of MES technology. With this in mind, electromethanogenesis, has recently been put forward for commercialization[2].Another promising application of MES is artificial bioinorganic photosynthesis for the production of longer carboxylic acids, acetone, and alcohols from CO_2. The integration of highly-efficient photovoltaic (PV) cells and MES technology will increase the efficiency of artificial photosynthesis into a range where industrial applications become economically feasible[4]. The solar energy conversion efficiency into biomass of natural photosynthesis lies between 2.9 to 4.3%[4]. Interestingly, combination of inorganic technologies for sun energy capture with MES could increase significantly solar-to-chemicals efficiency. Furthermore, MES can be combined with anodic processes recovering electrons from wastewater treatment facility that can then be used for the biological reduction of CO_2[5]. This approach could lead to the development of sustainable bioproduction processes converting wastes into commodity chemicals. Recently, a comparative economic evaluation of acetate production was done

for MES and anaerobic fermentation (AF) of syngas ($CO:CO_2$). During AF, bacteria are oxidizing CO to convert CO_2 into chemicals, but because there is not enough reducing equivalents, part of the CO_2 is still released from the reactor. The MES process can be merged to AF to reduce the CO_2 that escapes from the AF reactor. Integrating MES with AF could double production rates from CO_2 while decreasing total investment cost[3]. Optimized acetate production rate will also minimize the reactor size and production facility. Still, an important future research effort for the optimization of MES conversion rates and production yields is necessary for potential commercial application.

Reference

[1] M. Gtz, J. Lefebvre, F. Mrs, A. McDaniel Koch, F. Graf, S. Bajohr, R. Reimert, T. Kolb, Renewable Power-to-Gas: A technological and economic review, Renew. Energy. 85 (2016) 1371–1390. doi:10.1016/j.renene.2015.07.066.

[2] F. Geppert, D. Liu, M. van Eerten-Jansen, E. Weidner, C. Buisman, A. ter Heijne, Bioelectrochemical Power-to-Gas: State of the Art and Future Perspectives, Trends Biotechnol. 34 (2016) 879–894. doi:10.1016/j.tibtech.2016.08.010.

[3] X. Christodoulou, S.B. Velasquez-Orta, Microbial electrosynthesis and anaerobic fermentation: An economic

evaluation for acetic acid production from CO2 and CO, Environ. Sci. Technol. (2016) acs.est.6b02101. doi:10.1021/acs.est.6b02101.

[4] T. Zhang, More efficient together, Science (80-.). 350 (2015) 738–739. doi:10.1126/science.aad6452.

[5] D. Pant, A. Singh, G. Van Bogaert, Y.A. Gallego, L. Diels, K. Vanbroekhoven, An introduction to the life cycle assessment (LCA) of bioelectrochemical systems (BES) for sustainable energy and product generation: Relevance and key aspects, Renew. Sustain. Energy Rev. 15 (2011) 1305–1313. doi:10.1016/j.rser.2010.10.005.

[6] L. Jourdin, T. Grieger, J. Monetti, V. Flexer, S. Freguia, Y. Lu, J. Chen, M. Romano, G.G. Wallace, J. Keller, High Acetic Acid Production Rate Obtained by Microbial Electrosynthesis from Carbon Dioxide, Environ. Sci. Technol. (2015) acs.est.5b03821. doi:10.1021/acs.est.5b03821.